Energy, Mines and Resources Canada

Énergie, Mines et Ressources Canada

CANMET

Canada Centre for Mineral and Energy Technology

Centre canadien de la technologie des minéraux et de l'énergie

Mining Research Laboratories

Laboratoires de recherche minière

Canada

A PRELIMINARY MINE STABILITY ASSESSMENT AT DUMAGAMI MINE, QUEBEC

Y.S. Yu, N.A. Toews, R. Boyle and M. Bétournay

MRL 92-003(TR) January, 1992

This document is ... [illegible] ... report ... [illegible] ... to ... [illegible] ... does not ... [illegible] ... It does not ... [illegible] ... the opinion of the Canada Centre for Mineral and Energy Technology (CANMET)

... [illegible] ... rapport ... [illegible] ... pour ... [illegible] ... de l'opinion du Centre canadien de la technologie des minéraux et de l'énergie (CANMET)

68pp

MICROMEDIA

A PRELIMINARY MINE STABILITY ASSESSMENT AT DUMAGAMI MINE, QUEBEC

by

Y.S. Yu*, N.A. Toews*, R. Boyle** and M. Bétournay**

Abstract

Using the three-dimensional finite element analysis technique, a preliminary mine stability assessment of the Dumagami mine, Quebec, was carried out. As expected the mining of stopes based on the mine plan for the years 1990/2000, will induce very high stresses at the lower level of the mine. The strength of hangingwall and footwall formations are weak and they will not be able to withstand high stresses resulting from stoping. In addition, large areas of tension in both hangingwall and footwall will develop, and subsequently, this would cause ground instability and produce high a degree of dilution.

A coordinated mine plan, if possible, with the neighbouring Bousquet, is considered essential for maintaining the structural integrity of both mines. A strategic field monitoring program should be developed and implemented as soon as possible. Alternative mine plans should be developed with the assistance of model studies, and to establish a favourable mining sequence.

Key Words: Dumagami mine, stability, finite element, three-dimensional, stresses.

* Research Scientists, ** Physical Scientists, Mining Research Laboratories, CANMET, Energy, Mines and Resources Canada, Ottawa.

UNE ÉTUDE PRÉLIMINAIRE DE LA STABILITÉ À LA MINE DUMAGAMI, QUÉBEC.

par

Y.S. Yu*, N.A. Toews*, R. Boyle** and Bétournay**

Résumé

Une étude préliminaire tridimensionnelle sur la stabilité des chantiers de la mine Dumagami au Québec a été complétée en utilisant la technique des éléments finis. Comme prévu, le développement des chantiers planifiés pour les années 1990 à 2000 produira de fortes contraintes aux niveaux inférieurs de la mine. Le roc de l'éponte supérieur et inférieur est faible et ne pourra pas résister aux contraintes élevées dû au développement des chantiers. De plus, des zones étendues de tension se développeront dans l'éponte supérieur et inférieur causant l'instabilité du terrain et entraînant un haut degré de dilution.

Si possible, la planification minière devra être coordonnée avec la mine voisine Bousquet. Cette coordination est essentielle pour assurer l'intégrété structurale des deux mines. Un programme stratégique de surveillance sur le site devra être développé et mis en place le plutôt possible. Des plans miniers alternatifs devraient être développés avec les études de modèles pour établir une séquence minière favorable.

Mots clés: Dumagami, stabilité, éléments finis, tridimensionnel, contraintes.

* Chercheur scientifique, ** Chercheur en sciences physiques, Laboratoires de recherche minière, CANMET, Énergie, Mines et Ressources Canada, Ottawa.

93-00504/

CONTENTS

ABSTRACT i
RÉSUMÉ ii
1. INTRODUCTION 1
2. DUMAGAMI MINE 1
2.1 3-D Dumagami Mine Model 5
2.2 Material Properties of the Mine Rocks 7
2.3 Field Stresses 7
3. RESULTS 7
3.1 Stress Distribution 11
3.2 Potential Failure Areas 42
3.2.1 Hoek and Brown's Empirical Failure Criterion 42
3.2.2 Drucker and Prager Yield Criterion 43
4. CONCLUSIONS AND REMARKS 55
5. ACKNOWLEDGEMENT 61
6. REFERENCES 61

FIGURES

1. Plan view of the Dumagami Mine at 17th level 2
2. A longitudinal section of Dumagami Mine. 3
3. A longitudinal section showing long range mine planning (1991/2000), Dumagami Mine, Quebec. 4
4. Isometric view of the 3-D Dumagami mine model (not in scale) 4
5. A top view of the model showing geological features (not in scale). 6
6(a). Major principal stress contour plot - Mining Stage 1 (Ore zone (H/W), section z = 1045.7m) 12
6(b). Minor principal stress contour plot - Mining Stage 1 (Ore zone (H/W), section z = 1045.7m) 13
7(a). Major principal stress contour plot - Mining Stage 1 (Ore zone (F/W), section z = 1039.2m) 14
7(b). Minor principal stress contour plot - Mining Stage 1 (Ore zone (F/W), section z = 1039.2m) 15
8(a). Major principal stress contour plot - Mining Stage 1 (Footwall, section z = 1032.5m) 16
8(b). Minor principal stress contour plot - Mining Stage 1 (Footwall, section z = 1032.5m) 17
9(a). Major principal stress contour plot - Mining Stage 1 (Hanging wall, section z = 1032.5m) 18

9(b). Minor principal stress contour plot - Mining Stage 1 (Hanging wall, section z = 1032.5m) . . . 19
10(a). Major principal stress contour plot - Mining Stage 1 (North-South section, x = 1762.5m) . . . 20
10(b). Minor principal stress contour plot - Mining Stage 1 (North-south section, x = 1762.5m) . . . 21
11(a). Major principal stress contour plot - Mining Stage 2 (Ore zone (H/W), section z = 1045.7m) . . . 22
11(b). Minor principal stress contour plot - Mining Stage 2 (Ore zone (H/W), section z = 1045.7m) . . . 23
12(a). Major principal stress contour plot - Mining Stage 2 (Ore zone (F/W), section z = 1039.2m) . . . 24
12(b). Minor principal stress contour plot - Mining Stage 2 (Ore zone (F/W), section z = 1039.2m) . . . 25
13(a). Major principal stress contour plot - Mining Stage 2 (Footwall, section z = 1032.5m) . . . 26
13(b). Minor principal stress contour plot - Mining Stage 2 (Footwall, section z = 1032.5m) . . . 27
14(a). Major principal stress contour plot - Mining Stage 2 (Hanging wall, section z = 1032.5m) . . . 28
14(b). Minor principal stress contour plot - Mining Stage 2 (Hanging wall, section z = 1032.5m) . . . 29
15(a). Major principal stress contour plot - Mining Stage 2 (North-South section, x = 1762.5m) . . . 30
15(b). Minor principal stress contour plot - Mining Stage 2 (North-south section, x = 1762.5m) . . . 31
16(a). Major principal stress contour plot - Mining Stage 3 (Ore zone (H/W), section z = 1045.7m) . . . 32
16(b). Minor principal stress contour plot - Mining Stage 3 (Ore zone (H/W), section z = 1045.7m) . . . 33
17(a). Major principal stress contour plot - Mining Stage 3 (Ore zone (F/W), section z = 1039.2m) . . . 34
17(b). Minor principal stress contour plot - Mining Stage 3 (Ore zone (F/W), section z = 1039.2m) . . . 35
18(a). Major principal stress contour plot - Mining Stage 3 (Footwall, section z = 1032.5m) . . . 36
18(b). Minor principal stress contour plot - Mining Stage 3 (Footwall, section z = 1032.5m) . . . 37
19(a). Major principal stress contour plot - Mining Stage 3 (Hanging wall, section z = 1032.5m) . . . 38
19(b). Minor principal stress contour plot - Mining Stage 3

(Hanging wall, section z = 1032.5m) 39
20(a). Major principal stress contour plot - Mining Stage 3 . . . . . .
(North-South section, x = 1762.5m) 40
20(b). Minor principal stress contour plot - Mining Stage 3 . . . . . .
(North-south section, x = 1762.5m) 41
21. Strength/stress ratio - Hoek & Brown's empirical failure criterion . . . . .
(Mining Stage 2, ore zone (H/W), section z = 1045.7m) 44
22. Strength/stress ratio - Hoek & Brown's empirical failure criterion . . . . .
(Mining Stage 2, ore zone (F/W), section z = 1039.2m) 45
23. Strength/stress ratio - Hoek & Brown's empirical failure criterion . . . . .
(Mining Stage 2, footwall, section z = 1032.5m) 46
24. Strength/stress ratio - Hoek & Brown's empirical failure criterion . . . . .
(Mining Stage 2, hanging wall, section z = 1052.5m) 47
25. Strength/stress ratio - Hoek & Brown's empirical failure criterion . . . . .
(Mining Stage 2, north-south section, x = 1762.5m) 48
26. Strength/stress ratio - Hoek & Brown's empirical failure criterion . . . . .
(Mining Stage 3, ore zone (H/W), section z = 1045.7m) 49
27. Strength/stress ratio - Hoek & Brown's empirical failure criterion . . . . .
(Mining Stage 3, ore zone (F/W), section z = 1039.2m) 50
28. Strength/stress ratio - Hoek & Brown's empirical failure criterion . . . . .
(Mining Stage 3, footwall, section z = 1032.5m) 51
29. Strength/stress ratio - Hoek & Brown's empirical failure criterion . . . . .
(Mining Stage 3, hanging wall, section z = 1052.5m) 52
30. Strength/stress ratio - Hoek & Brown's empirical failure criterion . . . . .
(Mining Stage 3, north-south section, x = 1762.5m) 53
31. Strength/stress ratio - Drucker & Prager yield criterion . . . . . .
(Mining Stage 3, ore zone (H/W), section z = 1045.7m) 56
32. Strength/stress ratio - Drucker & Prager yield criterion . . . . . .
(Mining Stage 3, ore zone (F/W), section z = 1039.2m) 57
33. Strength/stress ratio - Drucker & Prager yield criterion criterion . . . . . .
(Mining Stage 3, footwall, section z = 1032.5m) 58
34. Strength/stress ratio - Drucker & Prager yield criterion criterion . . . . . .
(Mining Stage 3, hanging wall, section z = 1052.5m) 59
35. Strength/stress ratio - Drucker & Prager yield criterion criterion . . . . . .
(Mining Stage 3, north-south section, x = 1762.5m) 60

TABLES

1. Physical properties of the mine rocks. 8
2. A list of stress contour plots. 9
3. A list of strength/stress ratio plots. 10

1.0 Introduction

This report is a preliminary mine stability assessment of the Dumagami Mines Ltd., using three-dimensional finite element analysis techniques. In the study, the overall stability of Dumagami Mine, based on a long range mine planning from 1991-2000, was evaluated. The impact of mining activities in the adjacent mining property was only partially taken into account due to lack of detailed information. The overall structural stability based on Drucker-Prager yield criterion and Hoek & Brown's empirical failure criterion, was also examined.

The main objectives of this research project which was initiated in 1991 between Dumagami Mines Ltd., Quebec, and the Mining Research Laboratories (MRL) of CANMET, are mainly concerned with:

(**a**) to contribute to the development of a geomechanical data-base on the physical and mechanical properties of mine rocks;

(**b**) to assess the regional and local stability of the mine structure by means of numerical simulation, based on the determined rock properties and the in-situ stress measurement; and

(**c**) to provide essential design guidelines for making long range mine planning and ground control decisions.

The determination of physical properties of the mine rocks were carried out by the Mining Research Laboratories, CANMET. In situ stress determinations were conducted between 1987 and 1988 at la mine Bousquet and in Bousquet/Dumagami Mines. The pre-mining stress conditions were established based on the in situ stress measurements and used in this analysis. Numerical modelling based on these information forms an essential part of the research project.

2.0 Dumagami Mine

Project background information and the general geological conditions and mine layout of Dumagami Mine have been described in previous reports [1]. For completeness, a plan view of the mine at the 17th level and a longitudinal section are provided in Figures 1 and 2, respectively. A nine-year mine scheduling plan is illustrated in Figure 3.

The Dumagami Mine, a division of Agnico-Eagle Mines Ltd., came into production in 1986, after diamond drilling exploration had delineated a gold bearing ore zone averaging a grade of 0.134 oz per tonne. The mine is located 60 km west of Val d'Or, Quebec.

The orebody consists of gold disseminated in a massive pyrite orebody, oriented east-west with a thickness of 5-15 m.The orebody has a longitudinal extent of about 300 m, an 85° dip to the south and a plunge of 60° west. The upper portion is located in the Dumagami property, the lower portion in Lac Mineral's Bousquet No. 2 property. A boundary separates the two

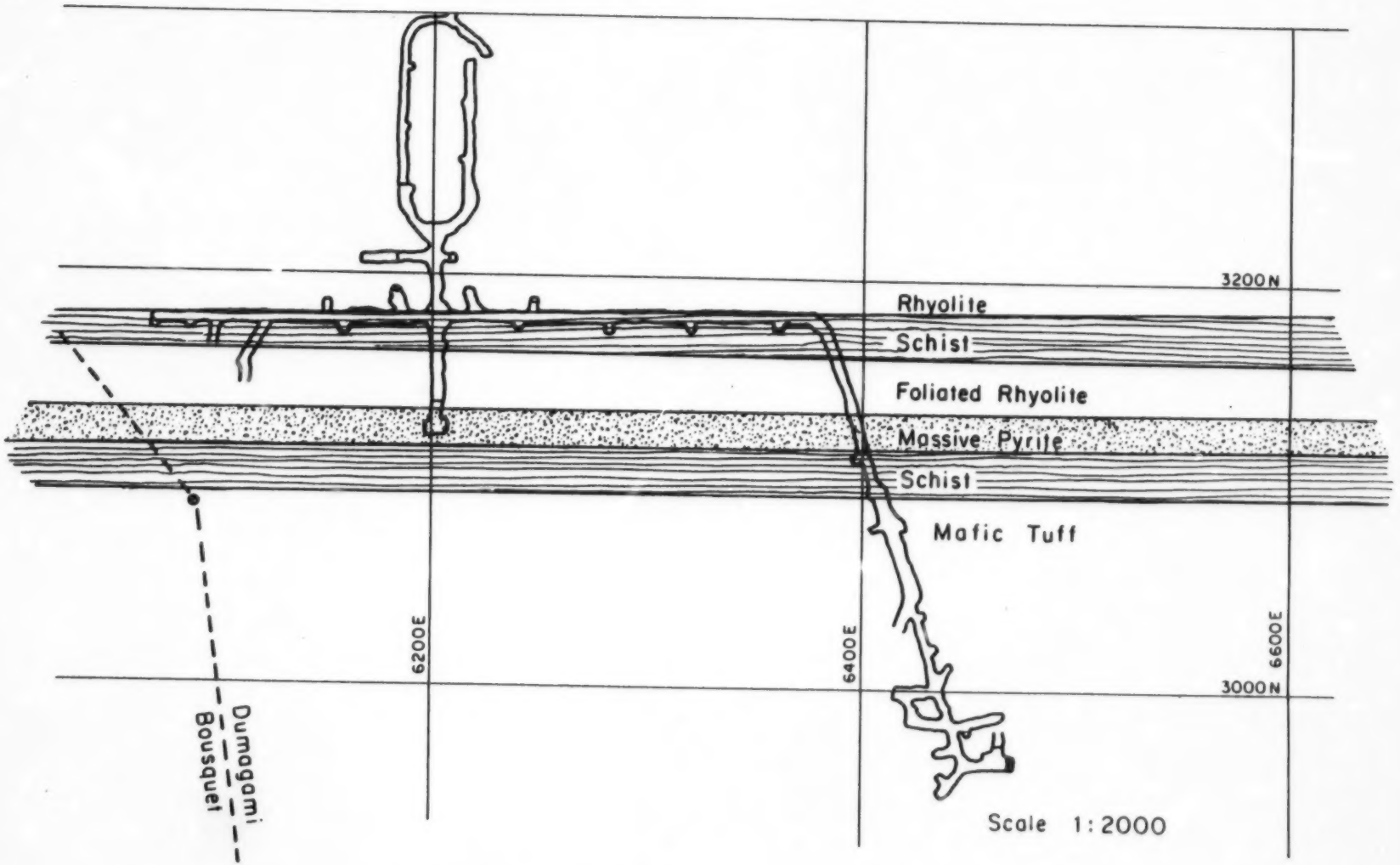

Fig. 1 Plan View of the Dumagami Mine at 17th Level

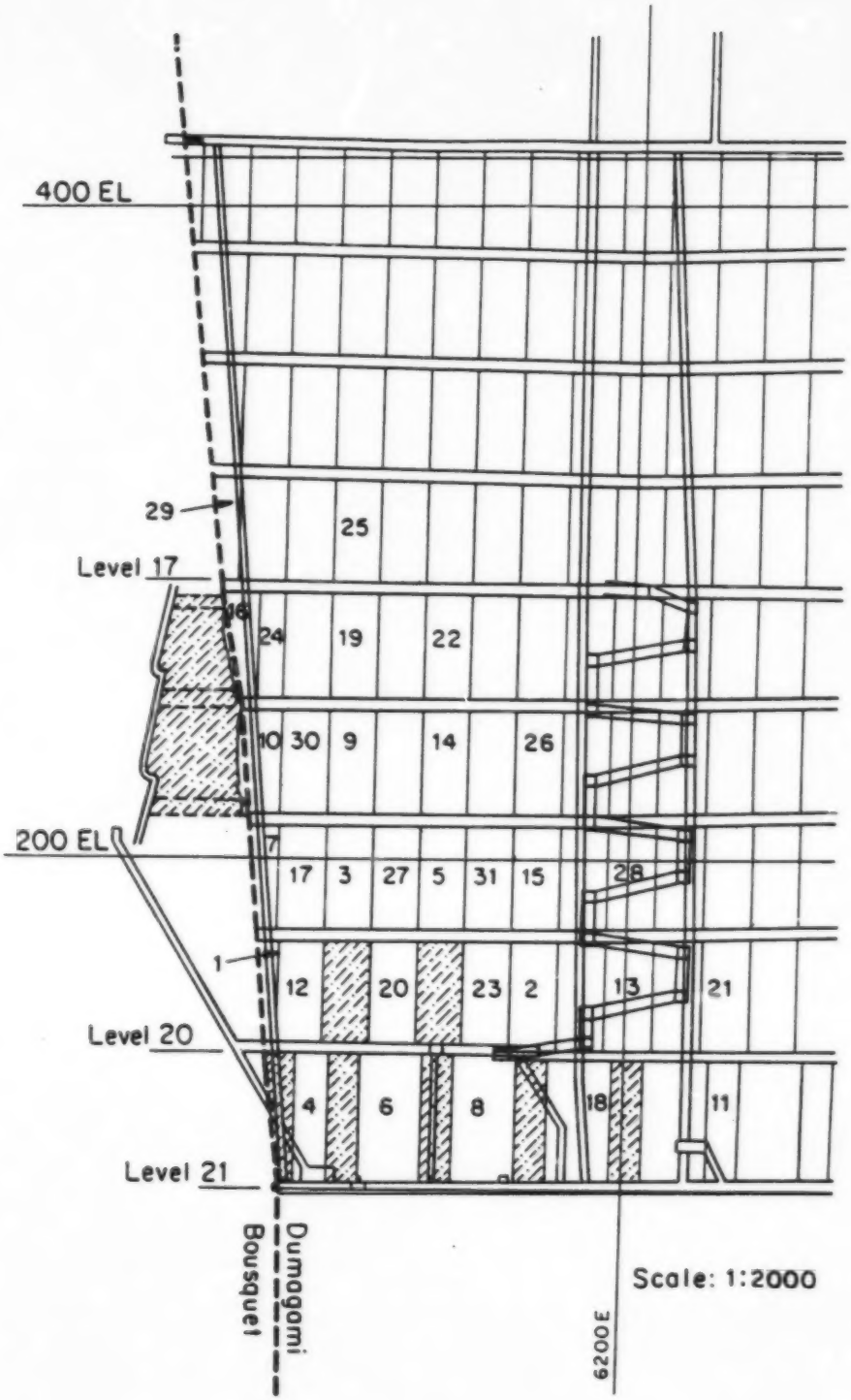

Fig. 2 A longitudinal section of Dumagami Mine

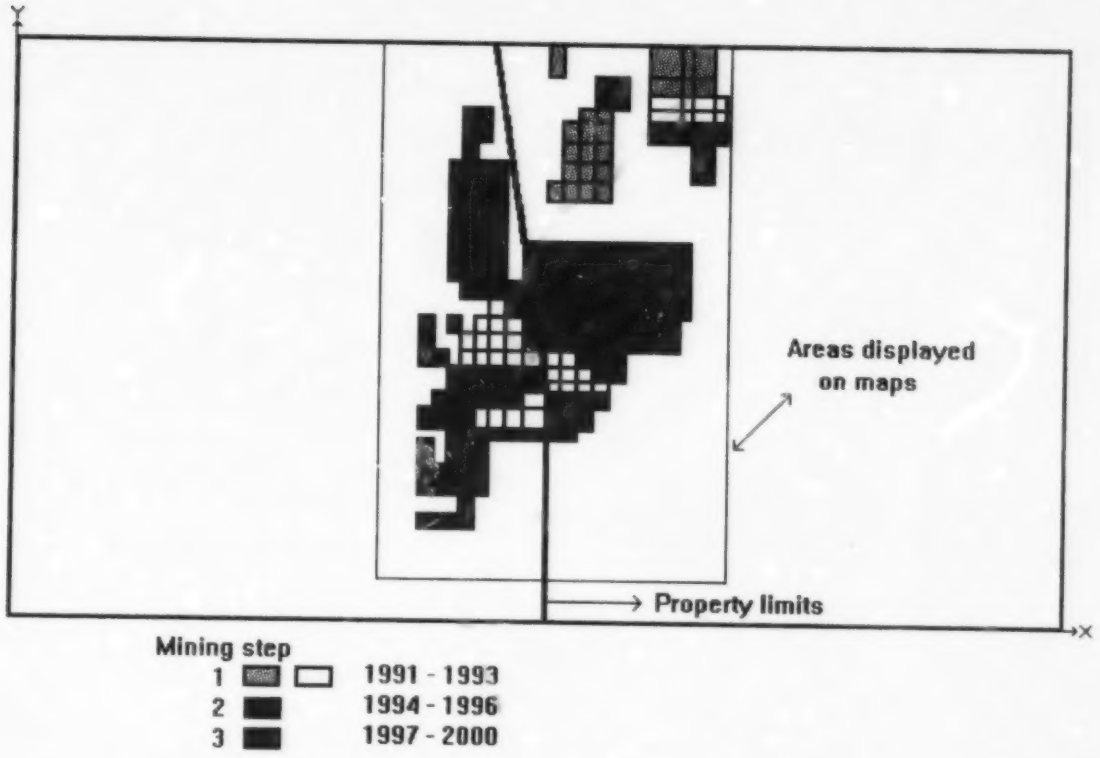

Fig. 3 A longitudinal section showing long range mine planning (1991/2000) Dumagami Mine, Quebec

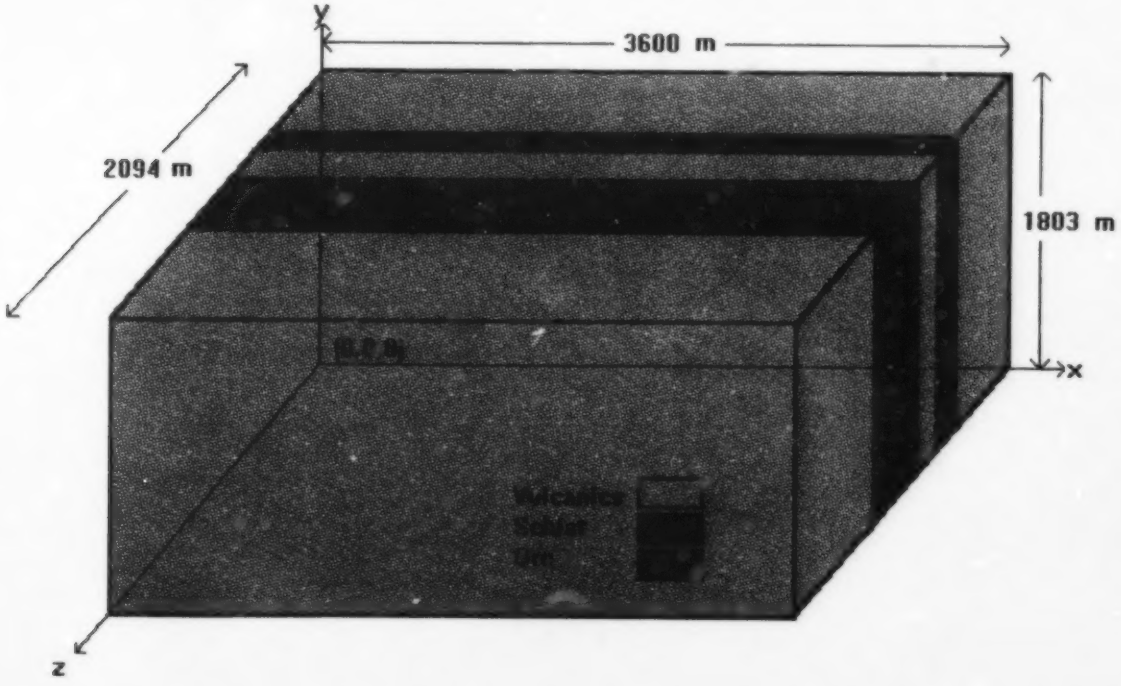

Fig. 4 Isometric View of the 3-D Dumagami Mine Model (not in scale)

properties, although current plans are to mine all of the orebody without leaving a boundary pillar.

The orebody is located in a sequence of fine to medium-grained volcanoclastic rock sequence located within the southern margin of the Abitibi greenstone belt. The sequence of vertical geological units from hangingwall to footwall can be generalized as follows: a mafic tuff, becoming more foliated towards the ore zone, a 15 m wide highly foliated to sericite shistose unit, worse at the contact with the orebody, a massive pyrite orebody; an immediate 20 m wide footwall of poorly to moderately-foliated rhyolite with disseminated or stronger pyrite, a 15 m highly-foliated schistose unite, and rhyolite.

The upper stopes of the mine, now completed, were extracted using a sub level blasthole method, retreating to the centre of the orebody. Some portions of these openings were filled with cemented rockfill.

The lower levels, currently under extraction, use a panel and pillar method, with 20 m side stope and pillars. These stopes and pillars are planned to be retreated from the property boundary in an even vertically upward fashion, as indicated in Figure 2.

2.1 3-D Dumagami Mine Model

A large-sized 3-D mine model including all mining stopes in both lower and upper levels was constructed. The mining sequences in the adjacent mining property - Bousquet, was also taken into account. To simplify the mine geometry for modelling purposes, the boundary between the two mine properties has been assumed to be vertical. This simplification should provide at least a first order approximation on the stress state.

An isometric view of the finite element model used in the study is shown in Fig. 4. It includes the Dumagami mine and its adjacent property - la mine Bousquet. A top view of the model showing the geological features is illustrated in Figure 5. Because of the size of the mines, the finite element discretization were relatively coarse: a total of 8736 8-noded elements and 10179 nodes were used for a preliminary assessment. Later, a more refined mesh, with 11,648 elements and 13311 nodes were used. The results presented in this report was based on the refined mesh.

In the simulation, the mining sequence consists of three stages, namely:

- Stage 1 - Mining of stopes scheduled for 1991 to 1993 including open pit and stoping development at the upper level.
- Stage 2 - Mining of stopes scheduled for 1994 to 1996.
- Stage 3 - Mining of stopes scheduled for 1997 to 2000.

The mine plan for the period of 1991-2000 is shown in Fig. 3.

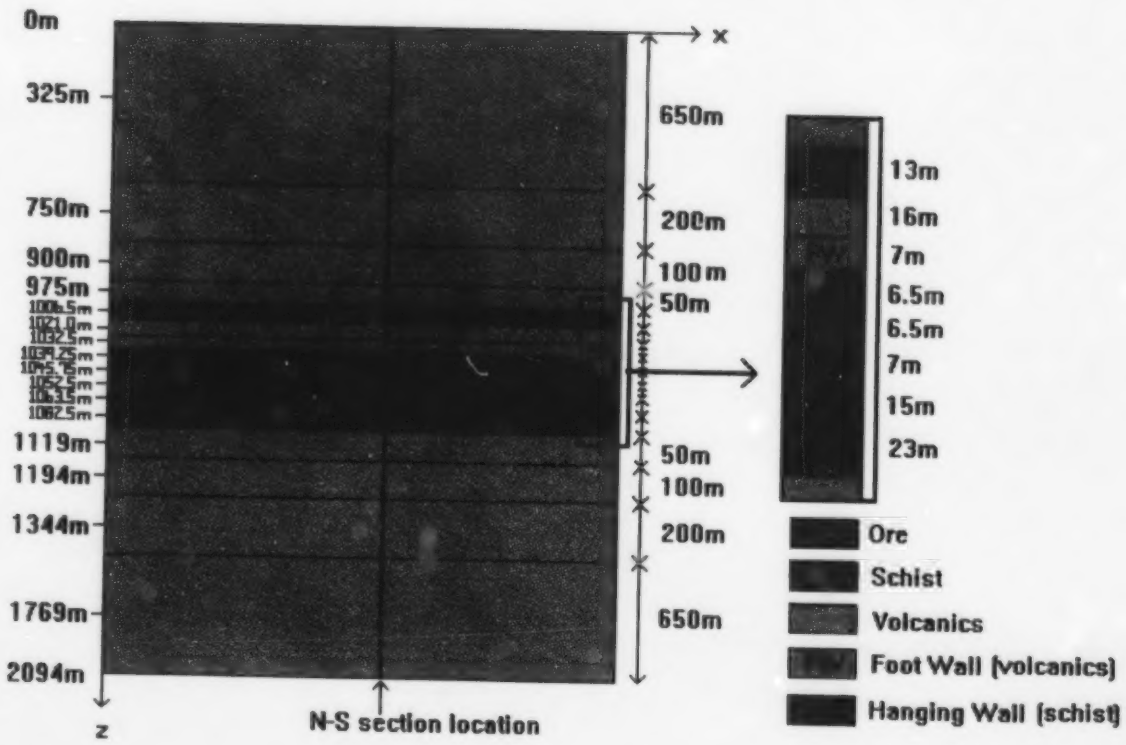

Fig. 5 A top view of the model showing geological features (not in scale)

The computer program, BMINES, was used for this study. BMINES was originally developed by the U.S. Bureau of Mines [2] and has been extensively modified to run on a Sun Sparcstation under Unix operating system at the Mining Research Laboratories. The program has a good collection of element library including eight-node or 20-node brick elements. The basic 8-node elements with three degrees of freedom at each node was used for this study. The program has capabilities for static, linear elastic analysis, or for non-linear elastic analysis. In this preliminary study, a linear elastic analysis was performed. Material properties are assumed to be isotropic.

The program is capable of handling gravitational and distributed surface loads. Initial residual stresses, if known, can also be used as input.

2.2 Material Properties of the Mine Rocks

The material properties including modulus of deformation, uniaxial compressive strength, and shear strength parameters of the mine rocks were determined in laboratory tests [3]. The mechanical properties of mine rocks used for this study were similar to those used in the two-dimensional finite element studies [1], and are shown in Table 1.

Table 1 - Physical Properties of Mine Rocks

Rock Types and Properties	Volcanics (H/W)	Schist (H/W)	pyrite (ore zone)	Schist (F/W)	Vocanics (F/W)
Young's Modulus (GPa)	23.0	15.0	23.50	23.0	23.0
Density (MN/m^3)	0.027	0.027	0.027	0.027	0.027
Poisson's Ratio	0.25	0.38	0.028	0.038	0.25
Cohesion (MPa)	4.0	0.50	6.00	0.50	4.00
Friction Angle (degrees)	20.0	35.0	30.0	35.0	20.0
Compressive Strength (MPa)	60.0	98.0	85.0	60.0	60.0
Constant m	2.50	0.30	4.50	0.70	2.50
Constant s	0.075	0.001	0.035	0.002	0.075

2.3 Field Stresses

In situ stress determinations were carried out in la mine Bousquet and in Bousquet- Dumagami Mines during 1987-88 [4,5].

In the Canadian Shield, it is known that the horizontal stress is greater than the vertical stress. Based on the limited stress data at the Bousquet and Dumagami mines, the following far field stress conditions are suggested:

$$\sigma_y = \gamma Y \tag{1}$$

$$\sigma_x = 1.49\sigma_y \tag{2}$$

$$\sigma_z = 2.38\sigma_y \tag{3}$$

Where σ_y is the vertical stress at a depth Y, σ_x and σ_z are the horizontal stresses parallel and perpendicular to the strike directions (EW and NS) respectively; γ is the unit weight of rock material.

3.0 Results

Even with the refined mesh (11,648 elements and 13311 nodes) the finite element discretization was still considered relatively coarse. However, this model should provide a first order approximation to the stress distribution around various stopes and its adjacent areas.

Results from the numerical analyses indicate that the stresses induced in the ore zone from the first stage of mining (1991 - 1993), under the assumed conditions, are not high enough to cause any serious stability problems in the orebody. However, tensile stresses developed in areas of hanging and footwalls might cause localized failure. The subsequent mining schedules (stages 2 and 3) will certainly induce large compressive stresses around some areas of the stopes at lower levels. In addition, tensile zones will penetrate into the hangingwall and footwall, which would cause structural instability and hence produce serious dilution problems.

At the present, the interaction between the two mining properties, i.e., Dumagami and Bousquet, was not clear, and additional modelling, incorporating different mining strategies is required.

Note that the sign convention of stresses presented in the report are compressive stress negative, and tensile stress positive.

3.1 Stress Distribution

Table 2 - A List of Stress Contour Plots

Locations	Stress Contours	Mining Steps	Fig. No.
Ore Zone (H/W, z= 1045.7m)	σ_1	1	6(a)
Ore Zone (F/W, z= 1039.2m)	σ_1	1	7(a)
Footwall (z= 1032.5m)	σ_1	1	8(a)
Hangingwall (z= 1052.5m)	σ_1	1	9(a)
N-S Section (x= 1762.5m)	σ_1	1	10(a)
Ore Zone (H/W, z= 1045.7m)	σ_3	1	6(b)
Ore Zone (F/W, z= 1039.2m)	σ_3	1	7(b)
Footwall (z= 1032.5m)	σ_3	1	8(b)
Hangingwall (z = 1052.5m)	σ_3	1	9(b)
N-S Section (x = 1762.5m)	σ_3	1	10(b)
Ore Zone (H/W, z= 1045.7m)	σ_1	2	11(a)
Ore Zone (F/W, z= 1039.2m)	σ_1	2	12(a)
Footwall (z= 1032.5m)	σ_1	2	13(a)
Hangingwall (z= 1052.5m)	σ_1	2	14(a)
N-S Section (x = 1762.5m)	σ_1	2	15a(a)
Ore Zone (H/W, Z= 1054.7m)	σ_3	2	11(b)
Ore Zone (F/W, z= 1039.2m)	σ_3	2	12(b)
Footwall (z= 1032.5m)	σ_3	2	13(b)
Hangingwall (z = 1052.5m)	σ_3	2	14(b)
N-S Section (x = 1762.5m)	σ_3	2	15(b)
Ore Zone (H/W, z= 1045.7m)	σ_1	3	16(a)
Ore Zone (F/W, z= 1039.2m)	σ_1	3	17(a)
Footwall (z= 1032.5m)	σ_1	3	18(a)
Hangingwall (z= 1052.5m)	σ_1	3	19(a)
N-S Section (x = 1762.5m)	σ_1	3	20(a)
Ore Zone (H/W, Z= 1054.7m)	σ_3	3	16(b)
Ore Zone (F/W, z= 1039.2m)	σ_3	3	17(b)
Footwall (z= 1032.5m)	σ_3	3	18(b)
Hangingwall (z = 1052.5m)	σ_3	3	19(b)
N-S Section (x = 1762.5m)	σ_3	3	20(b)

Table 3 - A List of Strength/Stress Ratio Plots

Locations	Stress Contours	Mining Steps	Fig. No.
Ore Zone (H/W, z=1045.7m)	SF (Hoek-Brown)	2	21
Ore Zone (F/W, z=1039.2m)	SF (Hoek-Brown)	2	22
Footwall (z= 1032.5m)	SF (Hoek-Brown)	2	23
Hangingwall (z= 1052.5m)	SF (Hoek-Brown)	2	24
N-S Section (x= 1762.5m)	SF (Hoek-Brown)	2	25
Ore Zone (H/W, z=1045.7m)	SF (Hoek-Brown)	3	26
Ore Zone (F/W, z=1039.2m)	SF (Hoek-Brown)	3	27
Footwall (z= 1032.5m)	SF (Hoek-Brown)	3	28
Hangingwall (z= 1052.5m)	SF (Hoek-Brown)	3	29
N-S Section (x= 1762.5m)	SF (Hoek-Brown)	3	30
Ore Zone (H/W, z= 1045.7)	SF (Drucker-Prager)	3	31
Ore Zone (F/W, z=1039.2)	SF (Drucker-Prager)	3	32
Footwal (z= 1032.5m)	SF (Drucker-Prager)	3	33
Hangingwall (z= 1052.5m)	SF (Drucker-Prager)	3	34
N-S Section (x= 1762.5m)	SF (Drucker-Prager)	3	35

Any three-dimensional finite element analysis will produce a large amount of information, thus programs have been developed to represent graphically the stress in a contour form for easy visual inspection.

In this report, only the principal stresses (major and minor) and the strength/stress ratio or 'local factor of safety', based on the selected failure criteria, are presented in a contour form for various sections of the mine model. The sections include: longitudinal sections passing through the orebody, hangingwall, footwall and a vertical N-S section cutting through all these formations. Lists of the stress contour plots and the factor of safety contour plots or the plots of strength/stress ratio are given, respectively, in Tables 2 and 3.

Figures 6 to 20 show the principal stress contours resulting from the three mining stages (stages 1, 2 and 3). They were plotted only for the longitudinal sections z = 1045.7m, 1039.2m, 1032.5m, 1052.5m and the N-S section x = 1762.5m. The sections with z = 1045.7m and z = 1039.2m, are located in the ore zone and approximately 3.25m in from either the hangingwall or the footwall formations. Sections z = 1052.5m and 1032.5m are located at about 3.5m into the hangingwall and footwall, respectively. The N-S section is located at x = 1762.5m and is approximately 100 m east from the boundary of the two properties. Those figures provide a quick and direct comparison between different sections and between different stages of mining.

The development of tensile zones, in shaded areas, at different stages, is shown in Figures 8a, 9a, 10a, 13a, 14a, 15a, 18a, 19a and 20a. As illustrated in some of the Figures, large areas of tensile stresses were observed in the footwall and hangingwall. Tensile zones penetrate into the stope walls approximately 10-30m deep, in the N-S direction as shown in Figures 15a and 20a.

As expected, the mining of stages 2 and 3 (1994-1996, 1997-2000), under existing stresses, induced much higher compressive stresses around the stopes at lower level. These compressive stresses are high enough to initiate some forms of shear failure. Tensile stresses occur in both hangingwall and footwall. These tensile stresses, approximately $20MPa$ or larger, occurred in some area of the footwall and hangingwall. This certainly exceeds the tensile strength of the schist material.

The results can be summarized as follows:

(a) Under existing stress conditions, the effect of excavating stopes in the first stage of mining, on the overall stability of the mine and its adjacent areas will be minimal. The largest compressive stresses, with magnitude of more than $100MPa$ occur only in a small area around the stopes. These are sufficiently high to cause minor localized stability problems in terms of shear failure in the orebody. Tensile stresses induced in the hangingwall and footwall may cause localized structural instability.

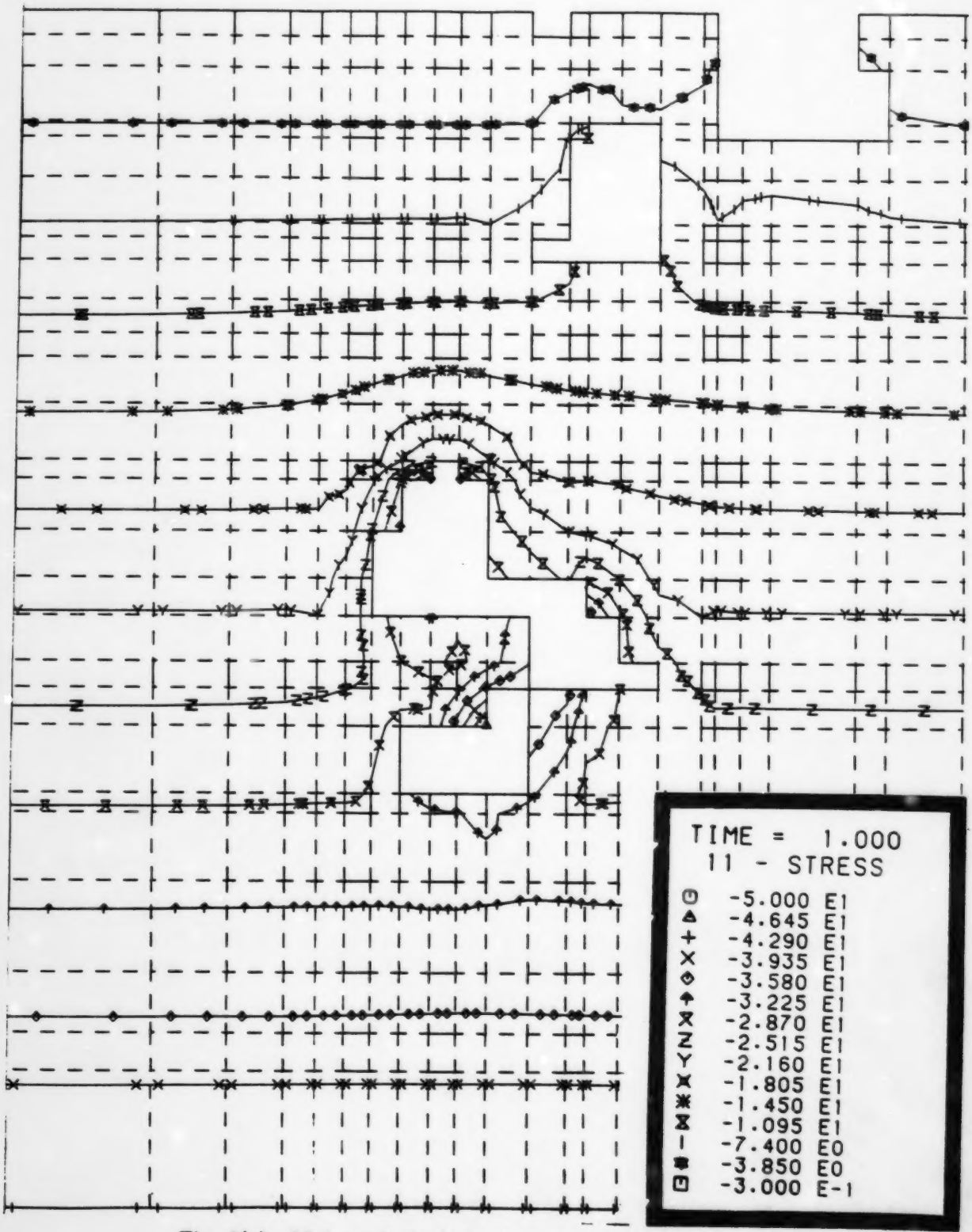

Fig. 6(a) Major principal stress contour plot - Mining Stage 1
(Ore zone (H/W), section z = 1045.7m)

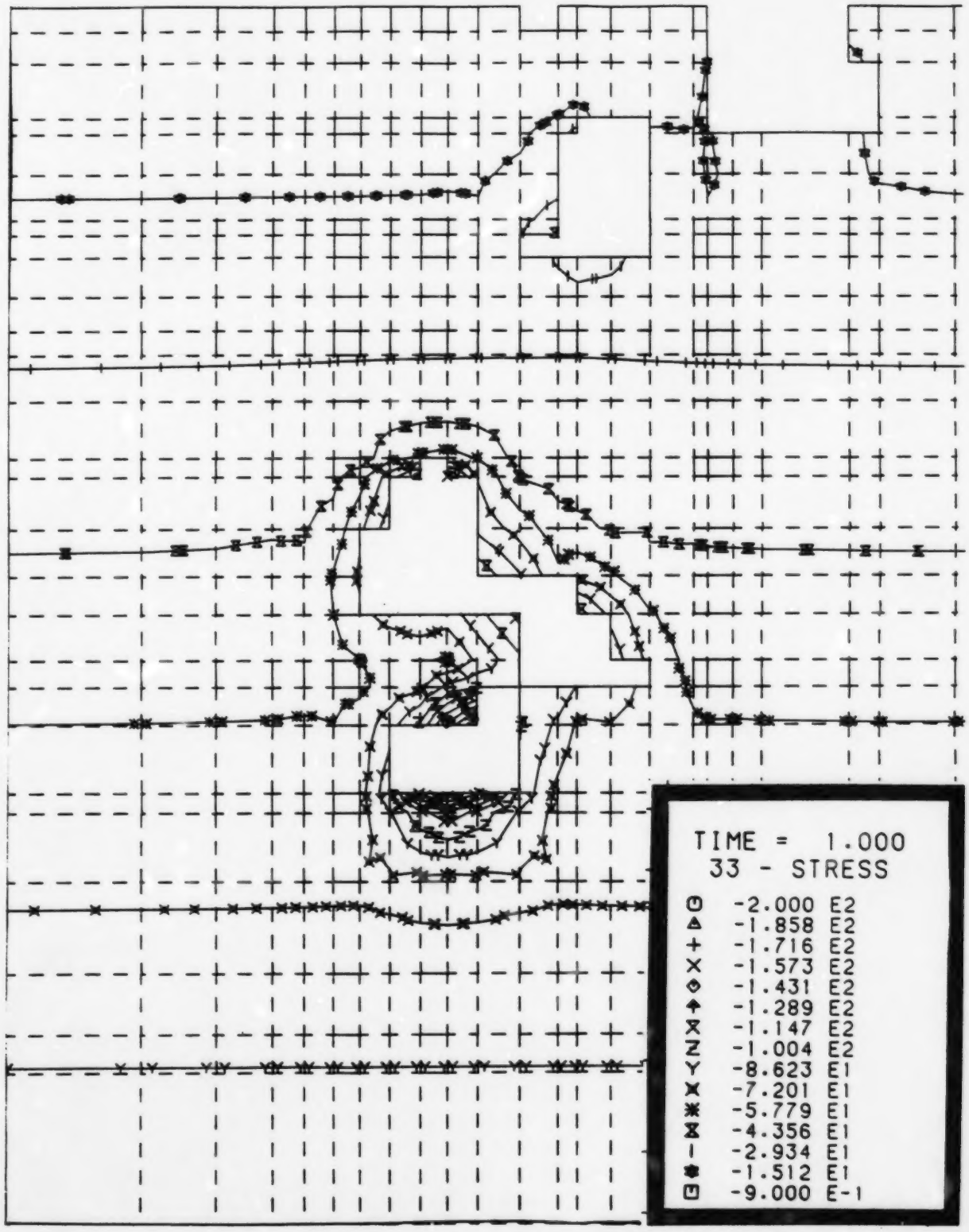

Fig. 6(b) Minor principal stress contour plot - Mining Stage 1
(Ore zone (H/W), section z = 1045.7m)

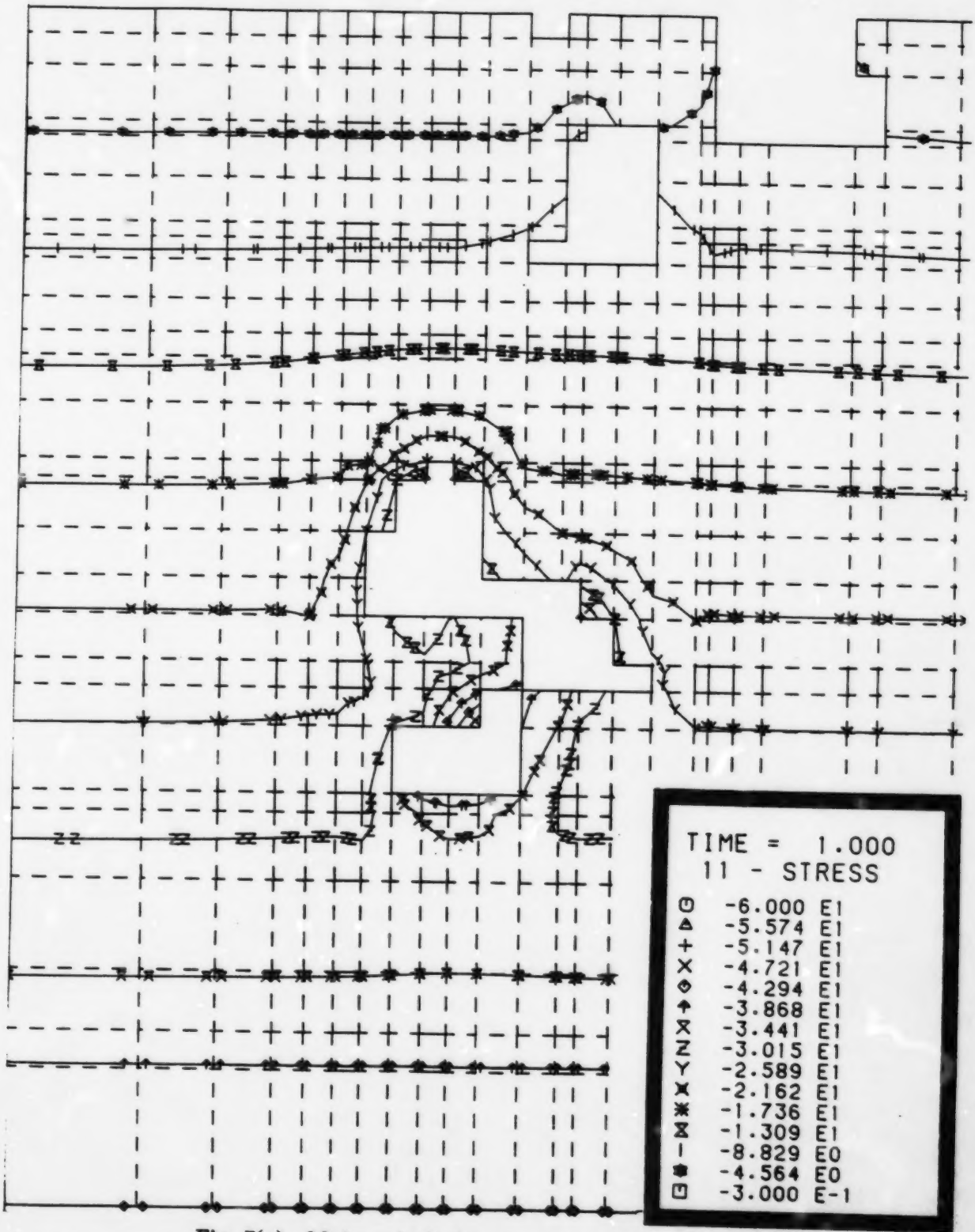

Fig. 7(a) Major principal stress contour plot - Mining Stage 1
(Ore zone (F/W), section z = 1039.2m)

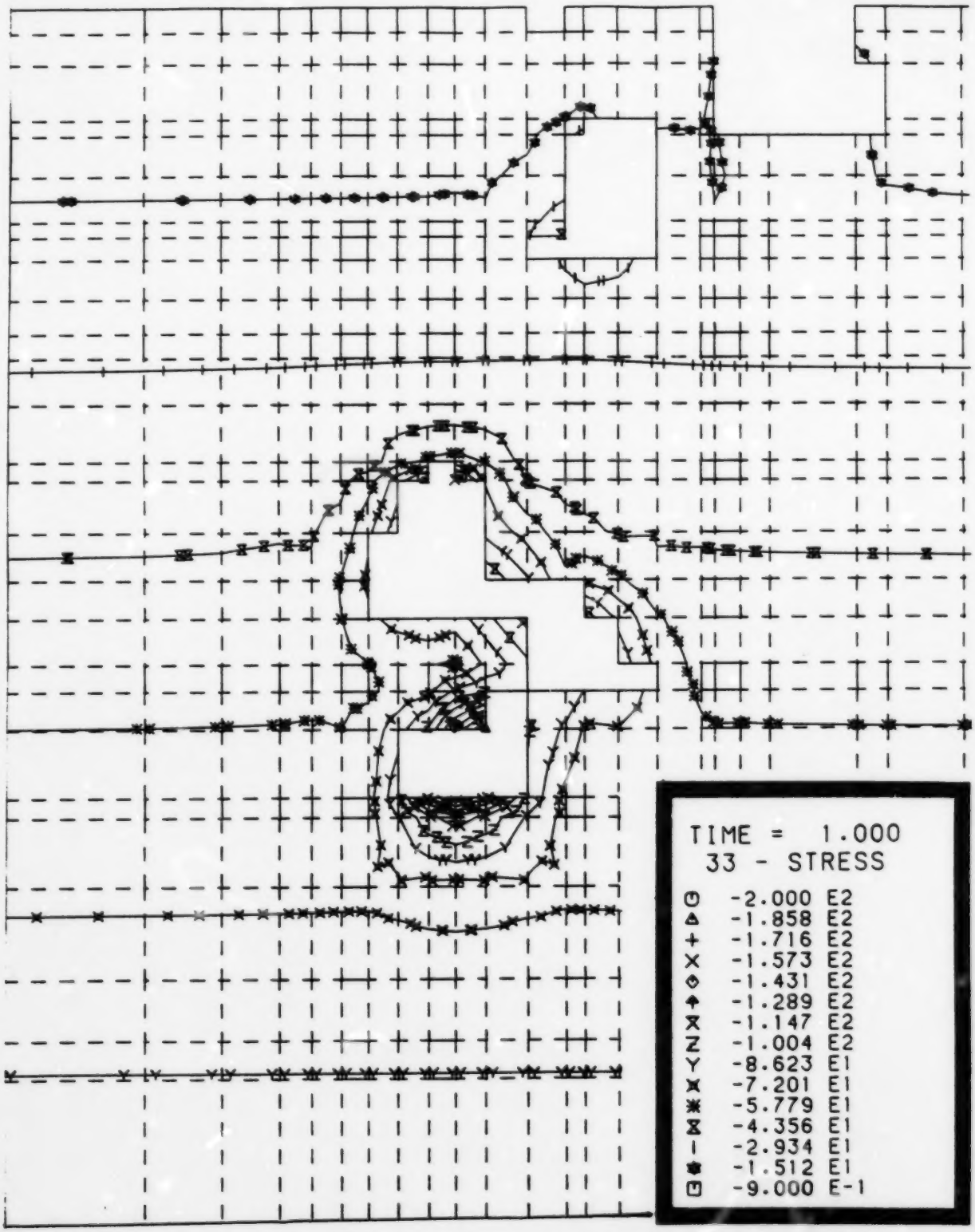

Fig. 7(b) Minor principal stress contour plot - Mining Stage 1
(Ore zone (F/W), section z = 1039.2m)

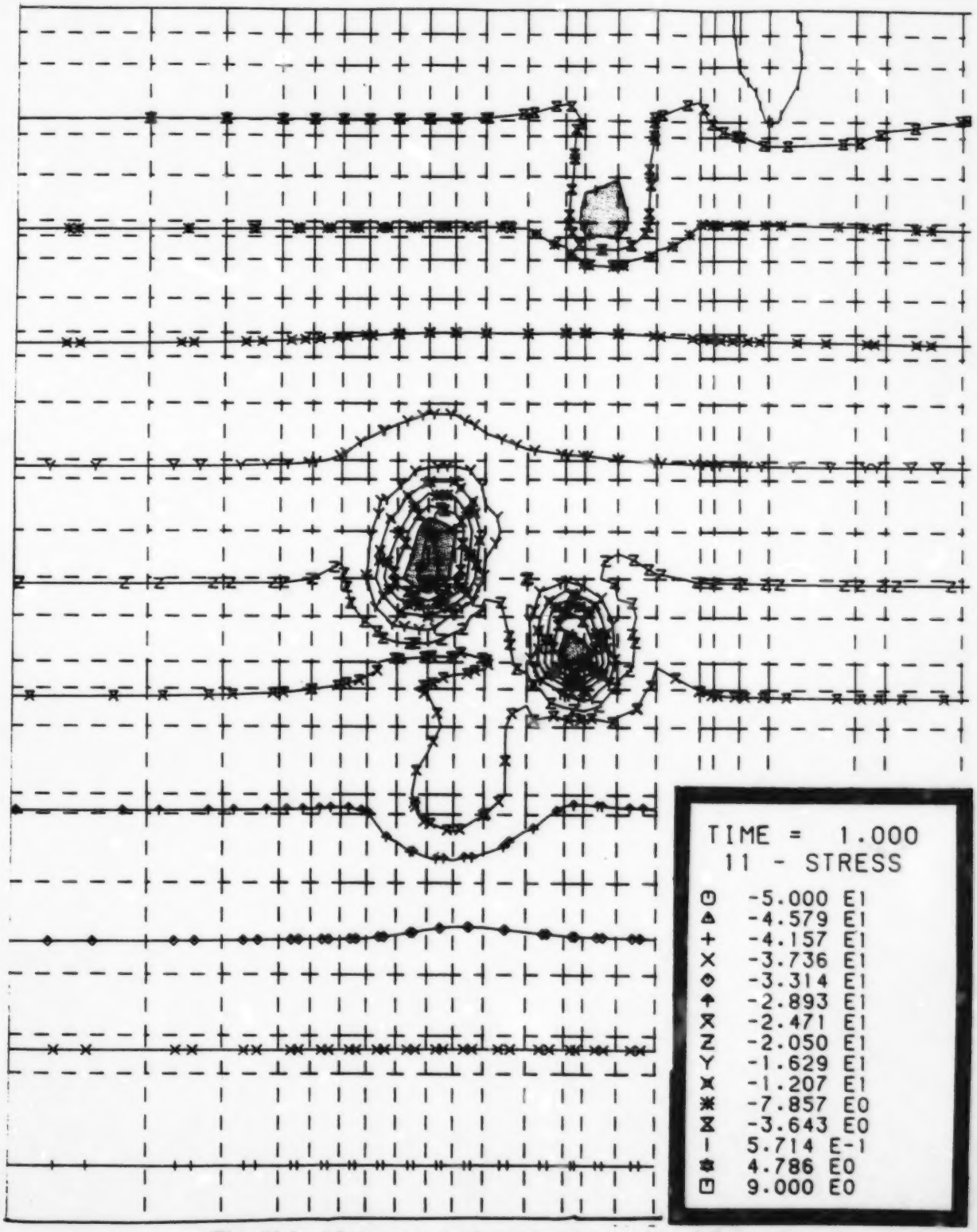

Fig. 8(a) Major principal stress contour plot - Mining Stage 1
(Footwall, section z = 1032.5m)

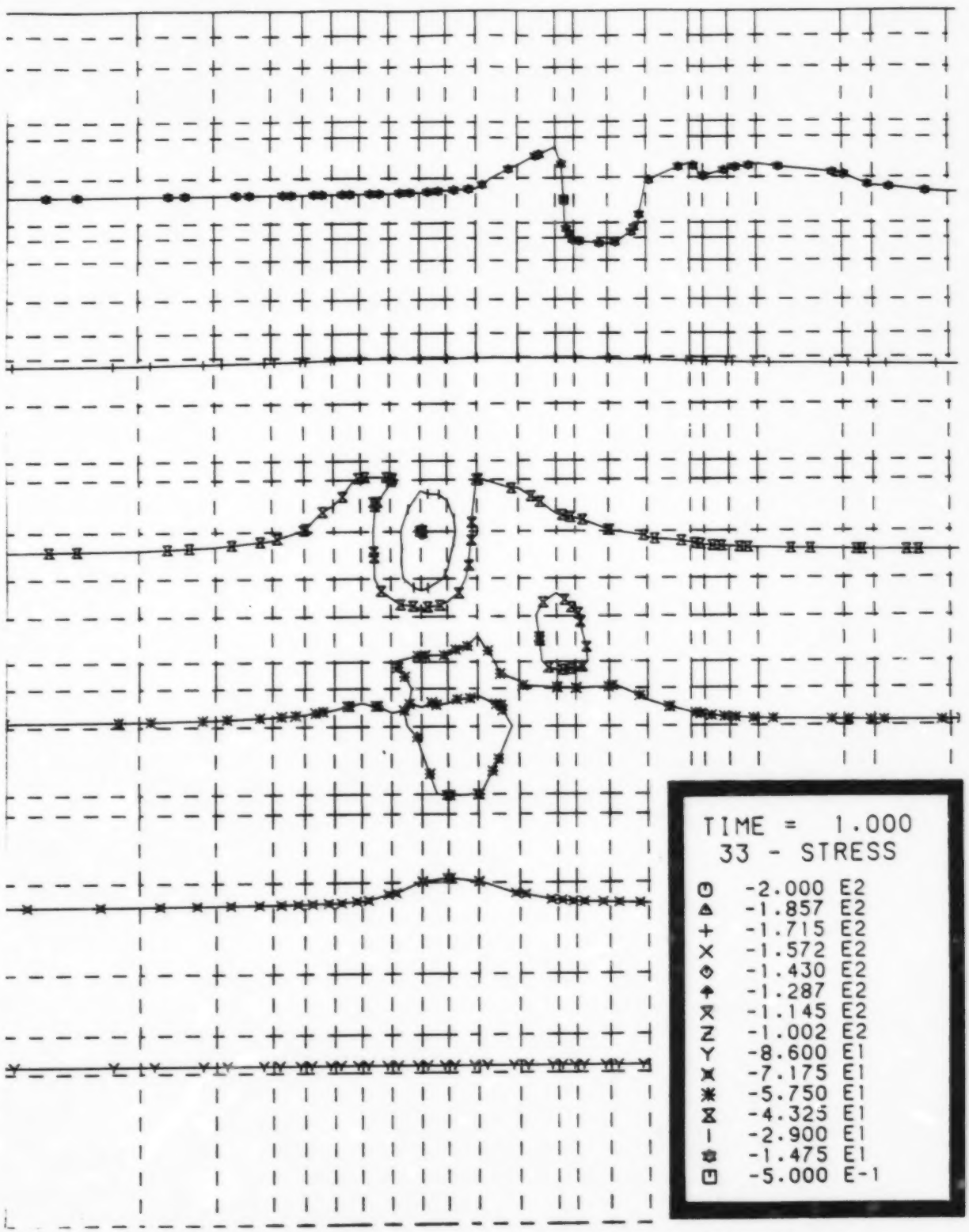

Fig. 8(b) Minor principal stress contour plot - Mining Stage 1
(Footwall, section z = 1032.5m)

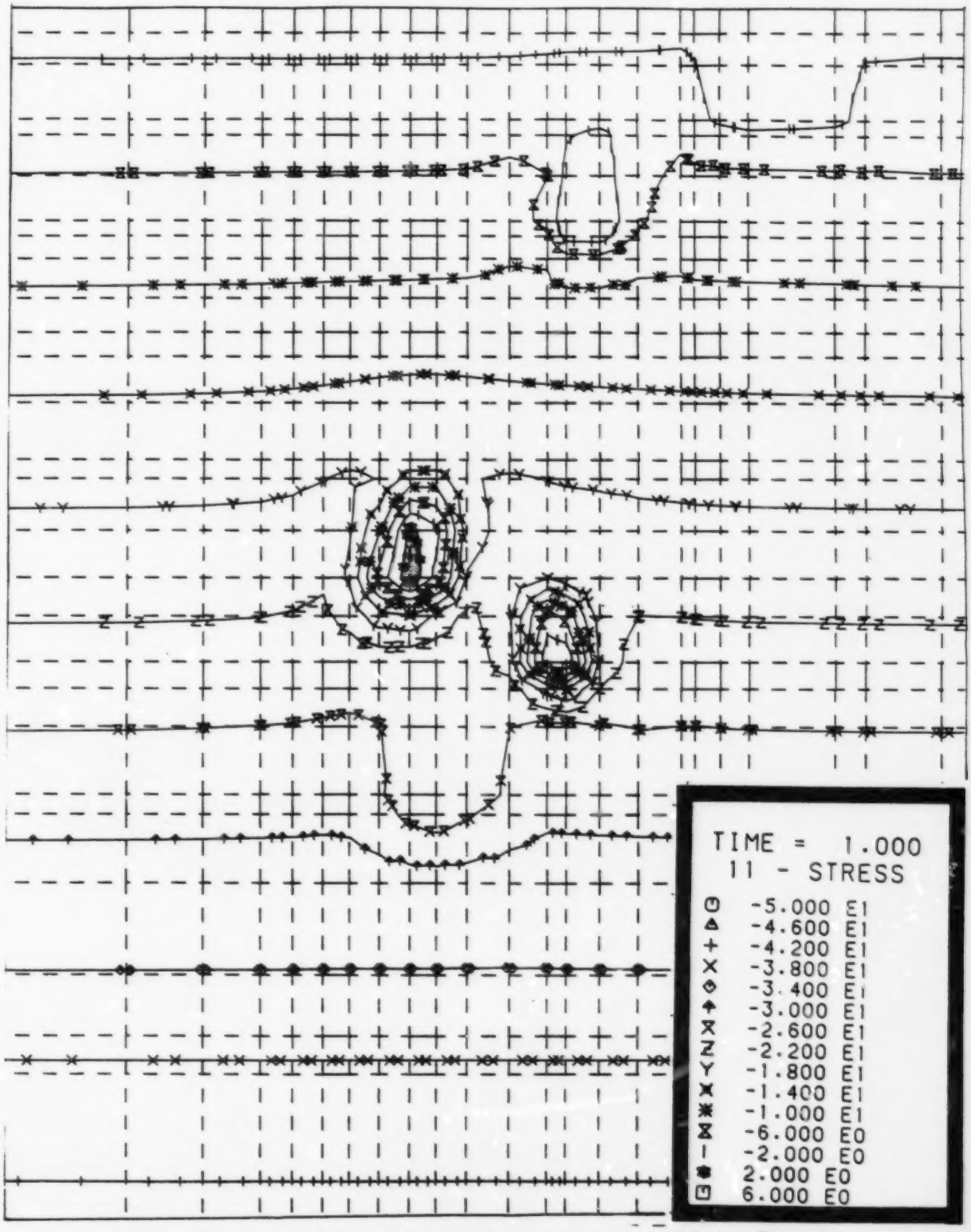

Fig. 9(a) Major principal stress contour plot - Mining Stage 1
(Hanging wall, section z = 1052.5m)

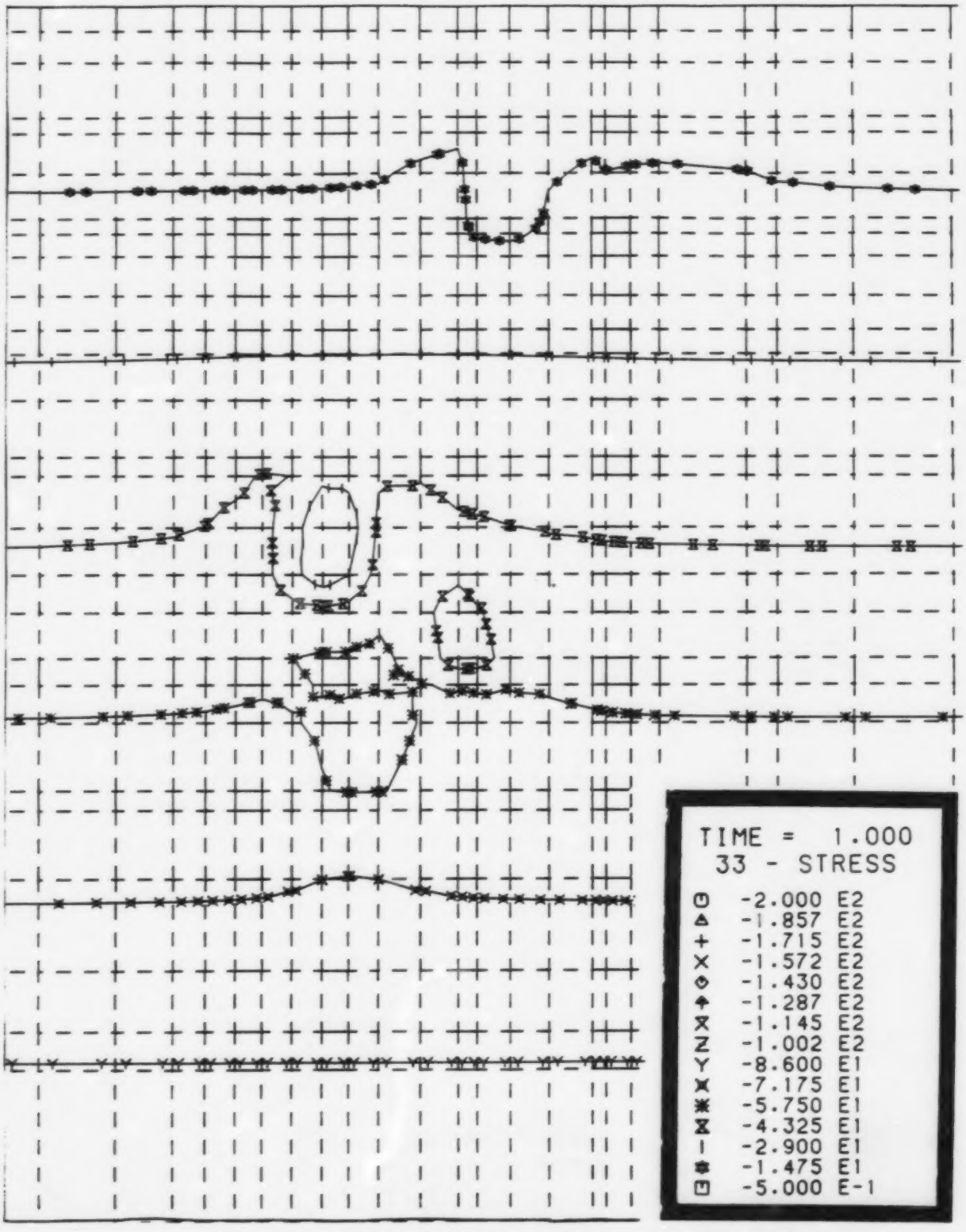

Fig. 9(b) Minor principal stress contour plot - Mining Stage 1
(Hanging wall, section z = 1052.5m)

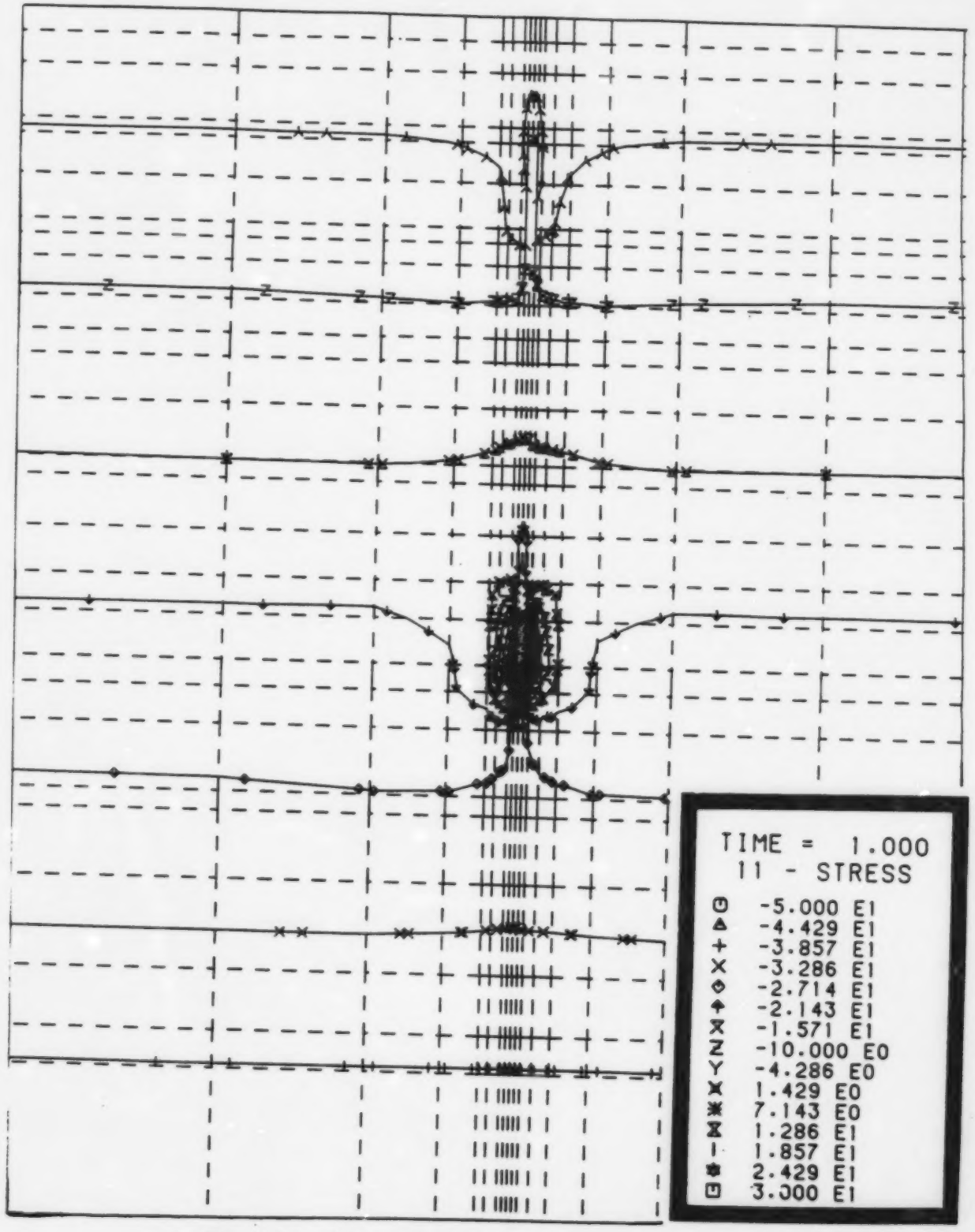

Fig. 10(a) Major principal stress contour plot - Mining Stage 1
(North-South section x= 1762.5m)

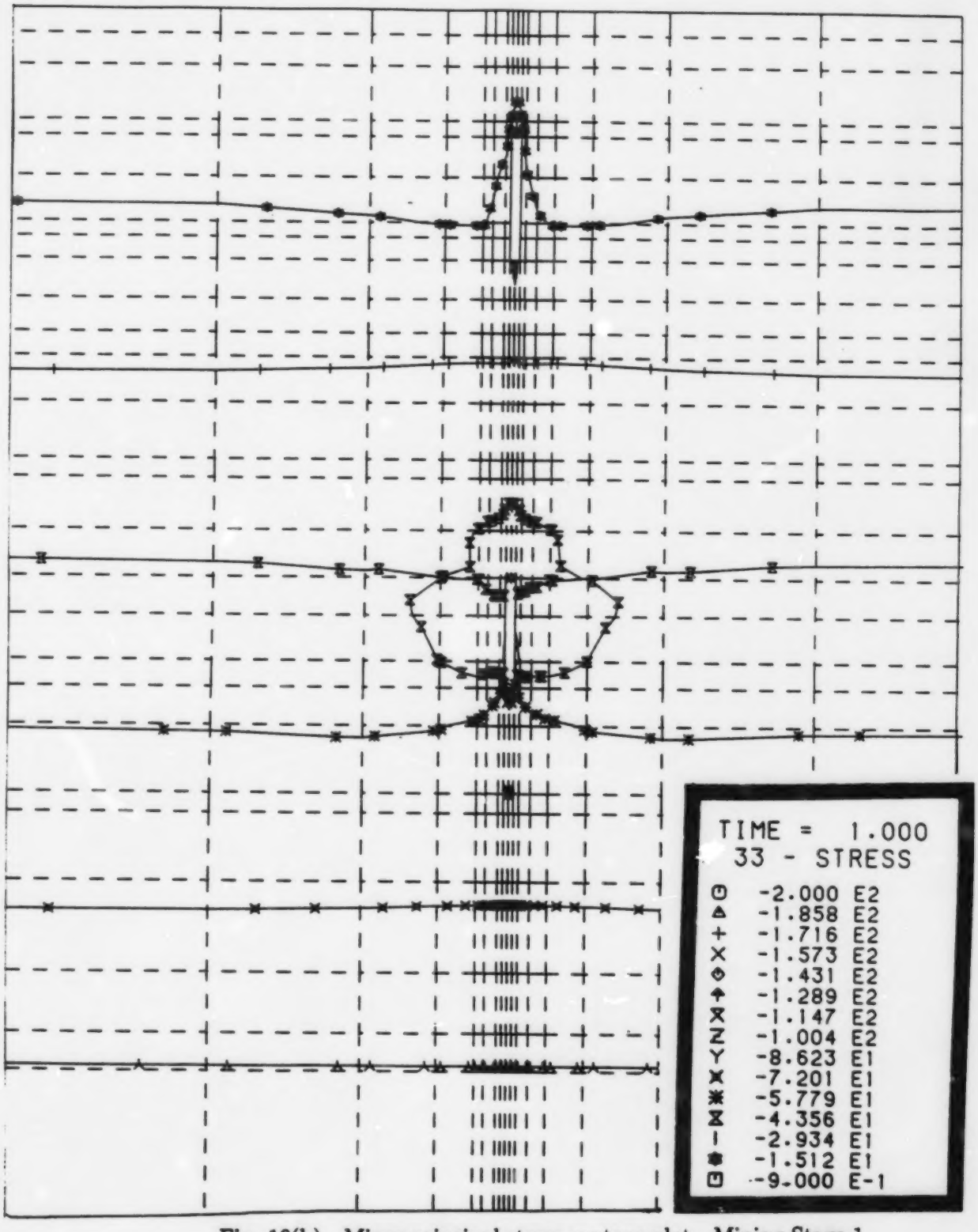

Fig. 10(b) Minor principal stress contour plot - Mining Stage 1
(N-S section x = 1762.5m)

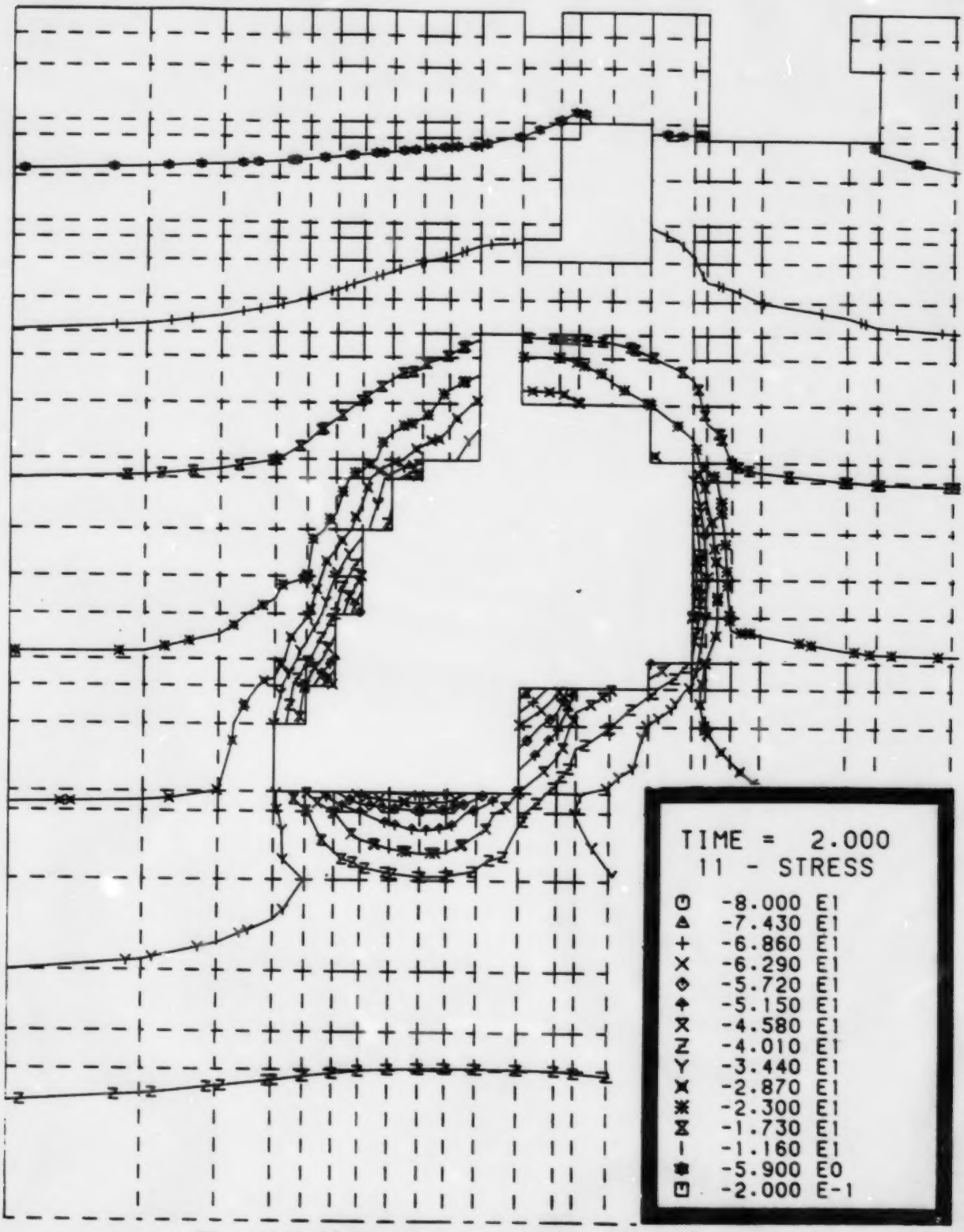

Fig. 11(a) Major principal stress contour plot - Mining Stage 2
(Ore zone (H/W), section z = 1045.7m)

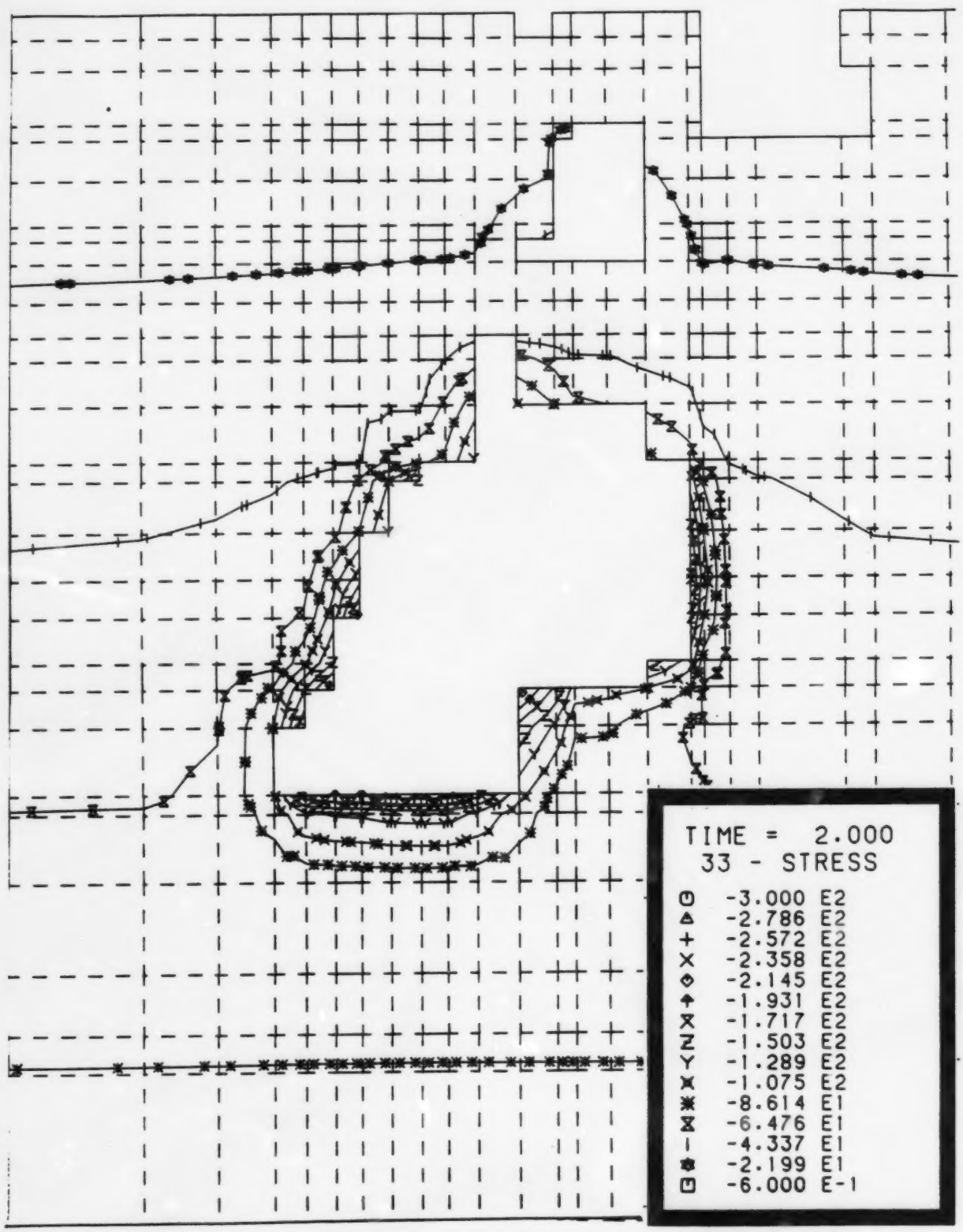

Fig.11(b) Minor principal stress contour plot - Mining Stage 2
(Ore zone (H/W), section z = 1045.7m)

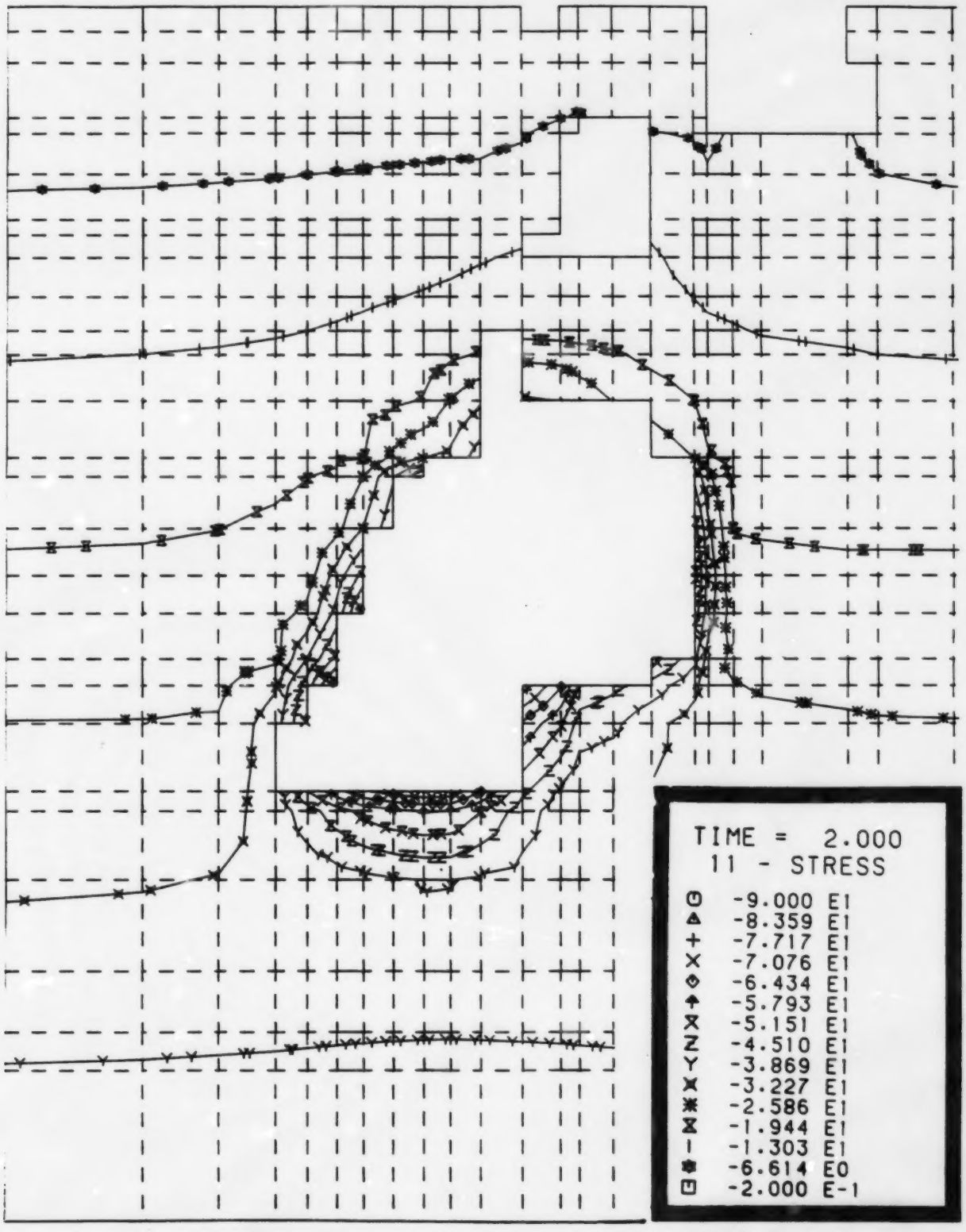

Fig.12(a) Major principal stress contour plot - Mining Stage 2
(Ore zone (F/W), section z = 1039.2m)

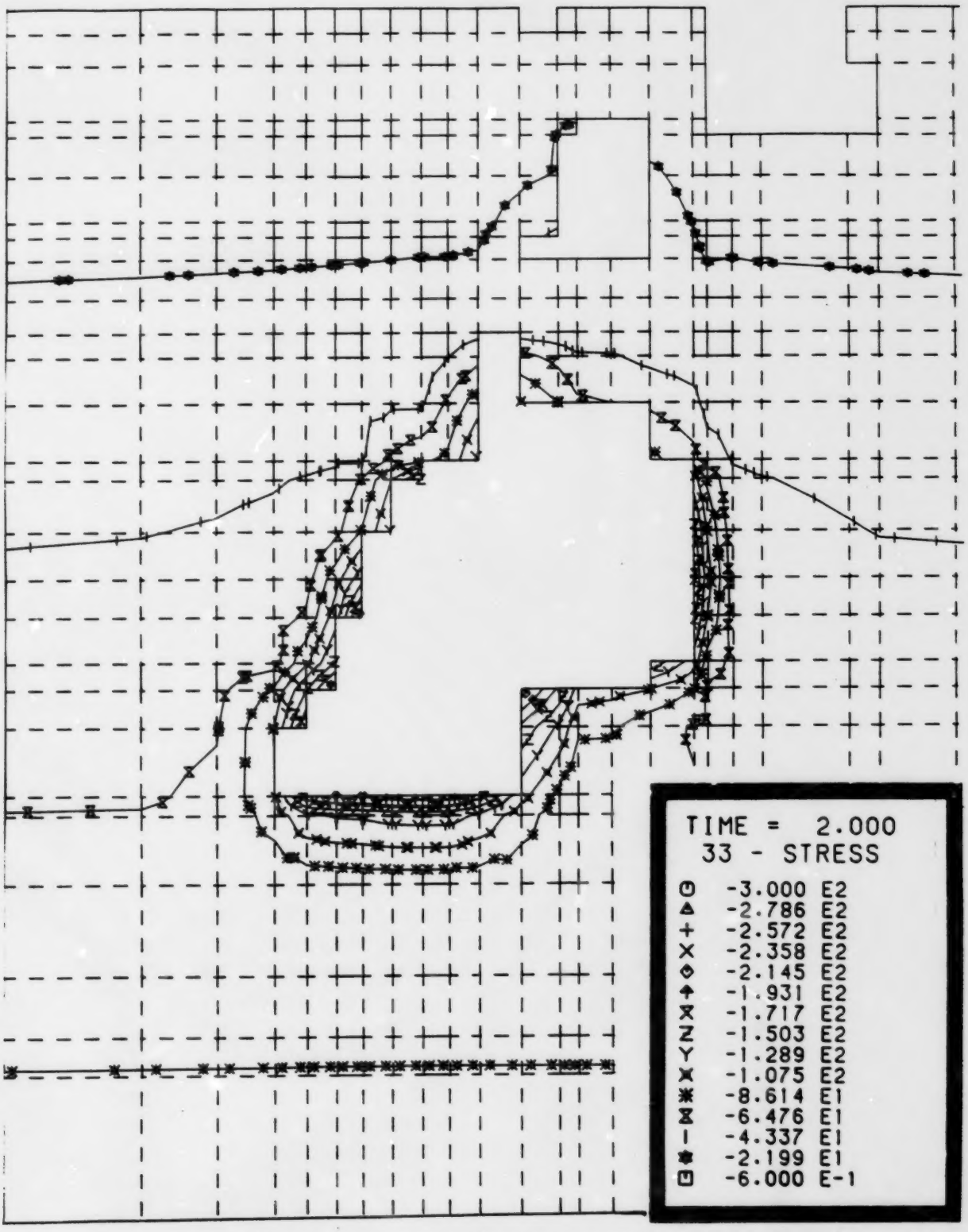

Fig.12(b) Minor principal stress contour plot - Mining Stage 2
(Ore zone (F/W), section z = 1039.2m)

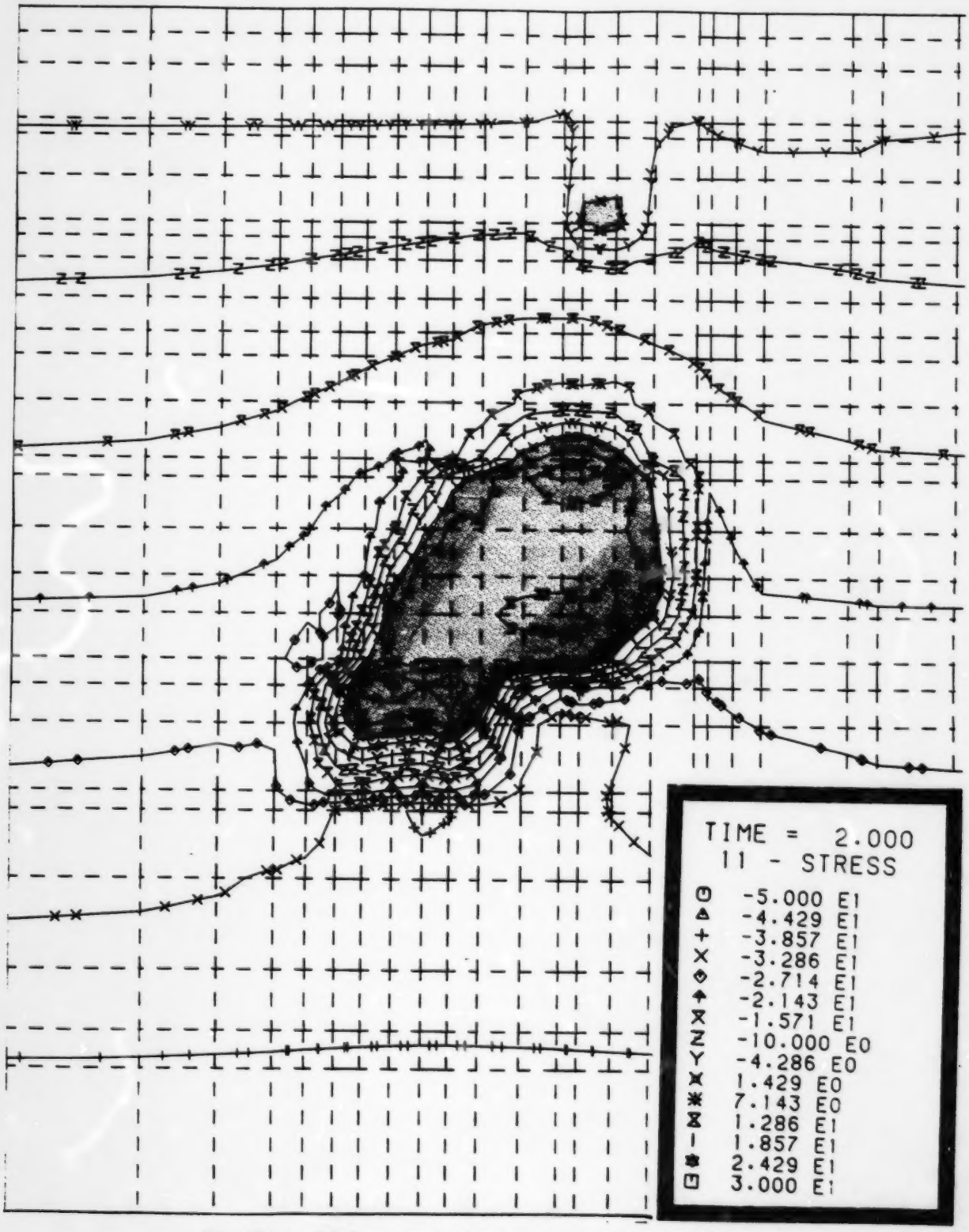

Fig.13(a) Major principal stress contour plot - Mining Stage 2
(Footwall, section z = 1032.5m)

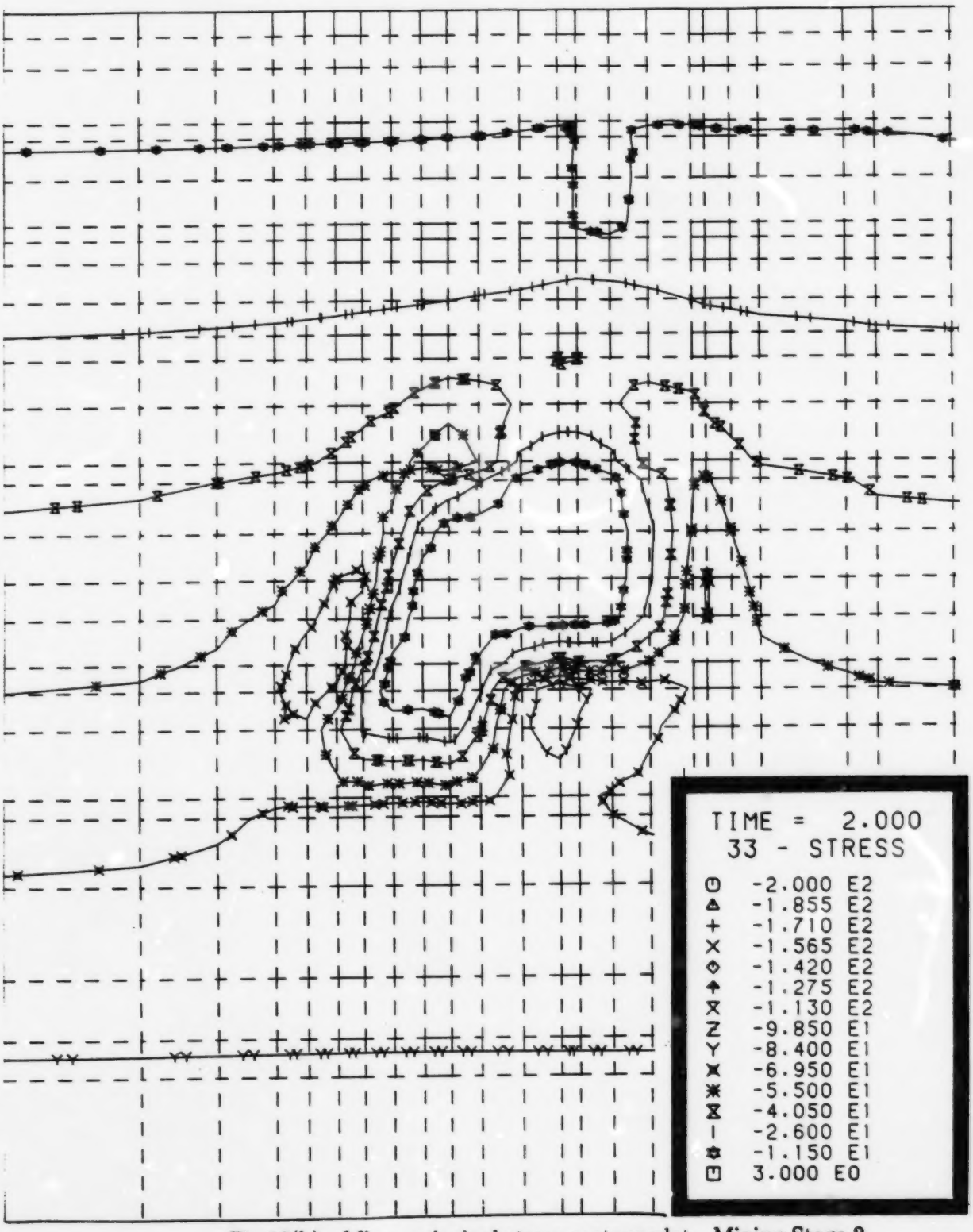

Fig.13(b) Minor principal stress contour plot - Mining Stage 2
(Footwall, section z = 1032.5m)

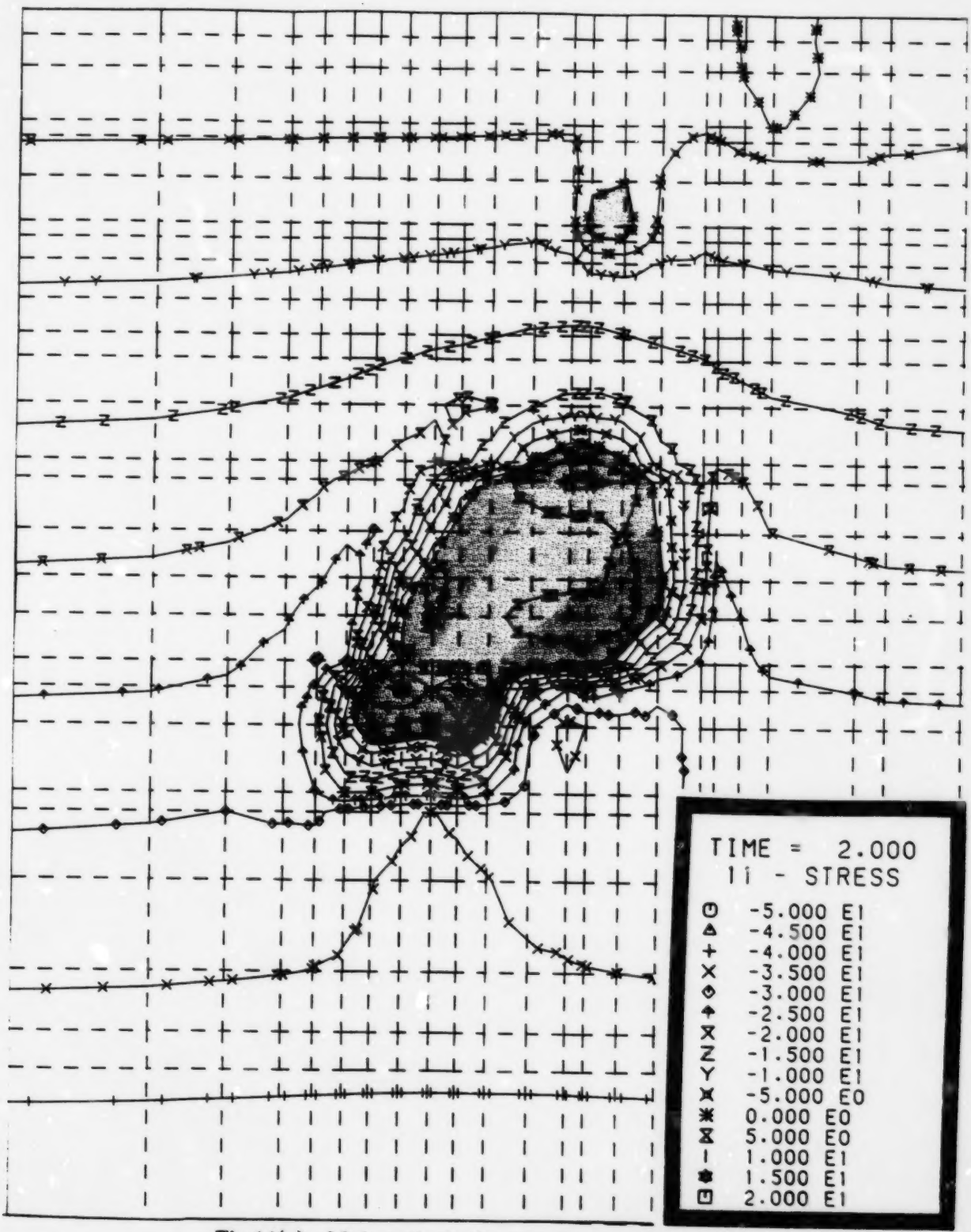

Fig.14(a) Major principal stress contour plot - Mining Stage 2
(Hanging wall, section z = 1052.5m)

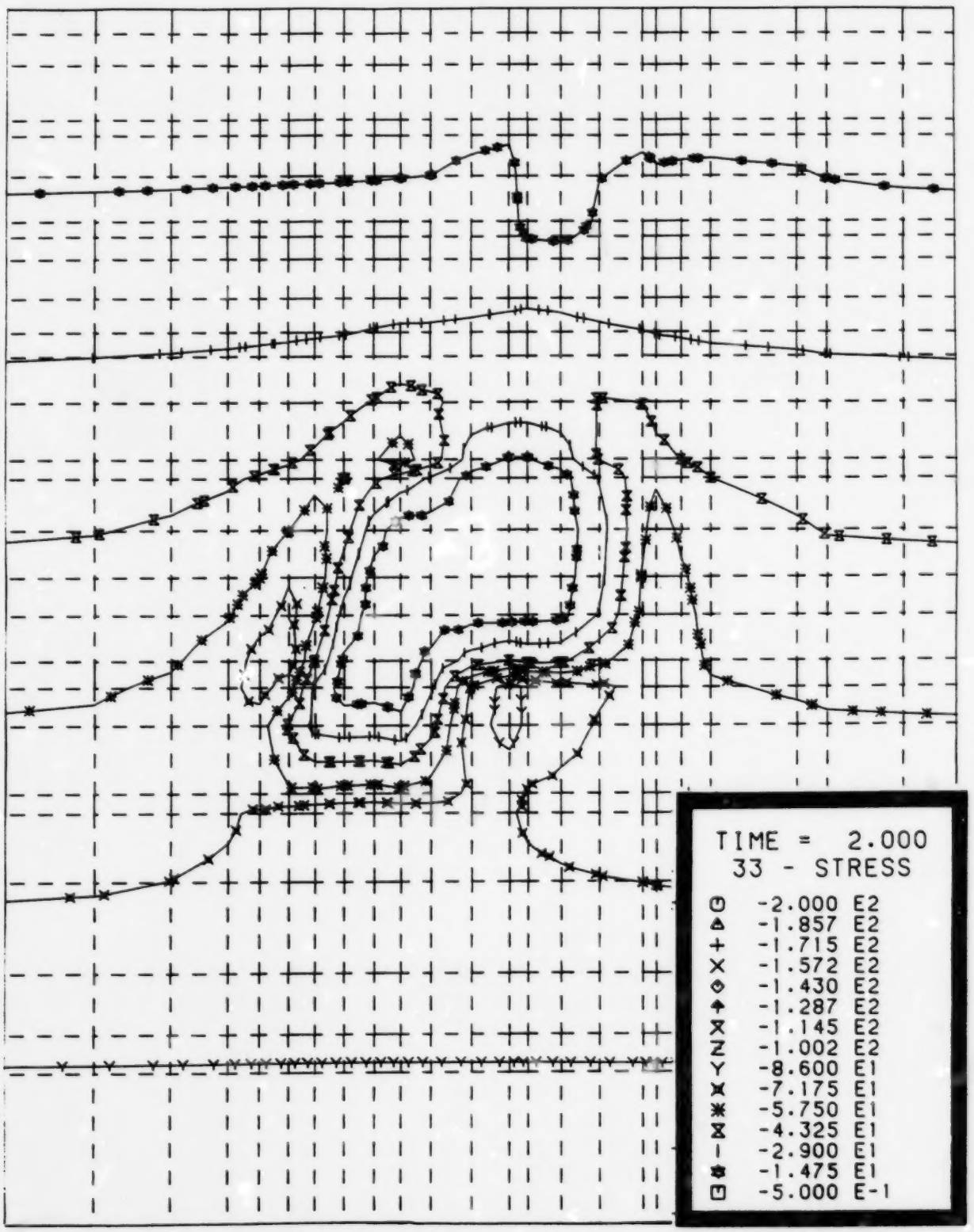

Fig.14(b) Minor principal stress contour plot - Mining Stage 2
(Hanging wall, section z = 1052.5m)

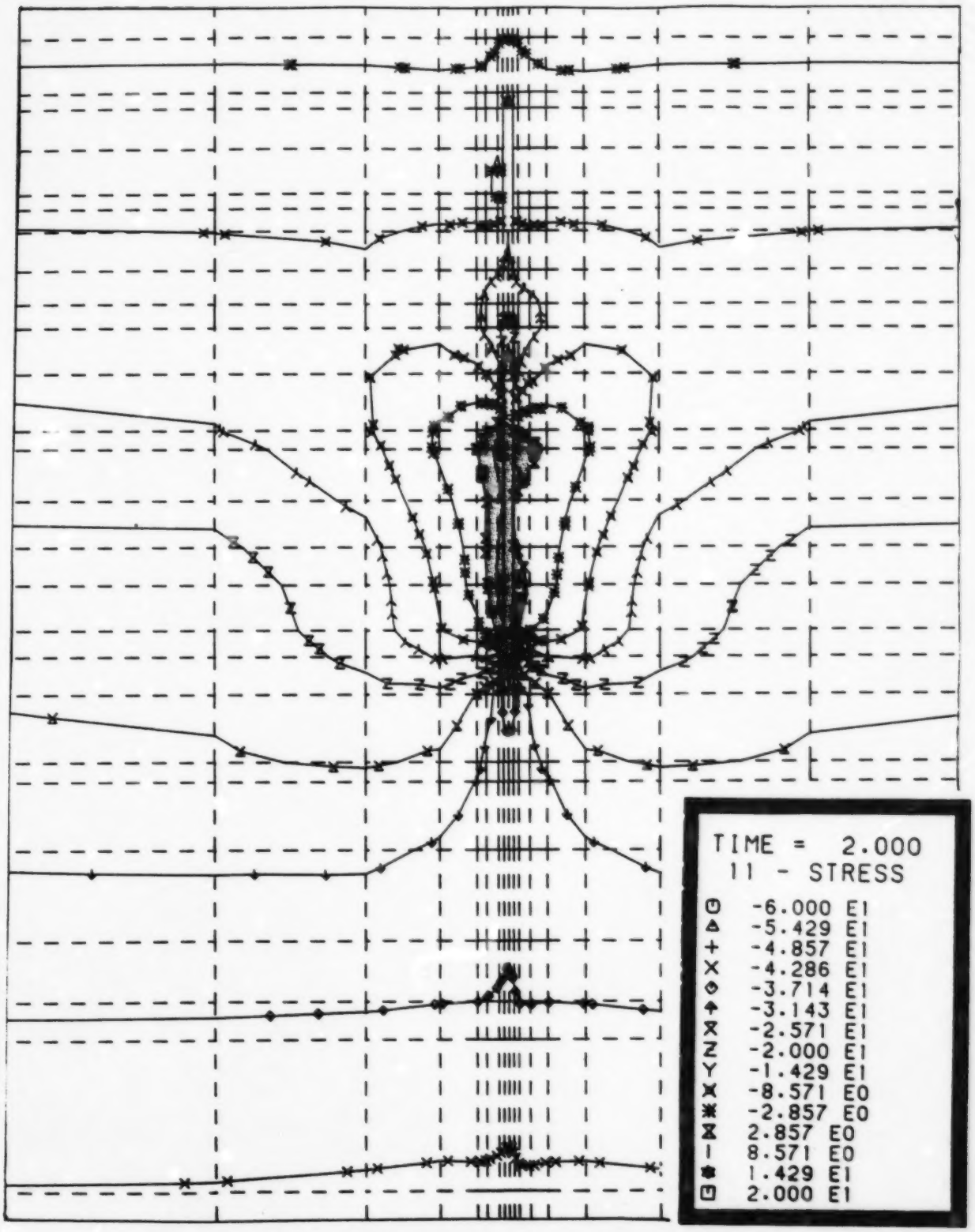

Fig. 15(a) Major principal stress contour plot - Mining Stage 2
(N-S section, x = 1762.5m)

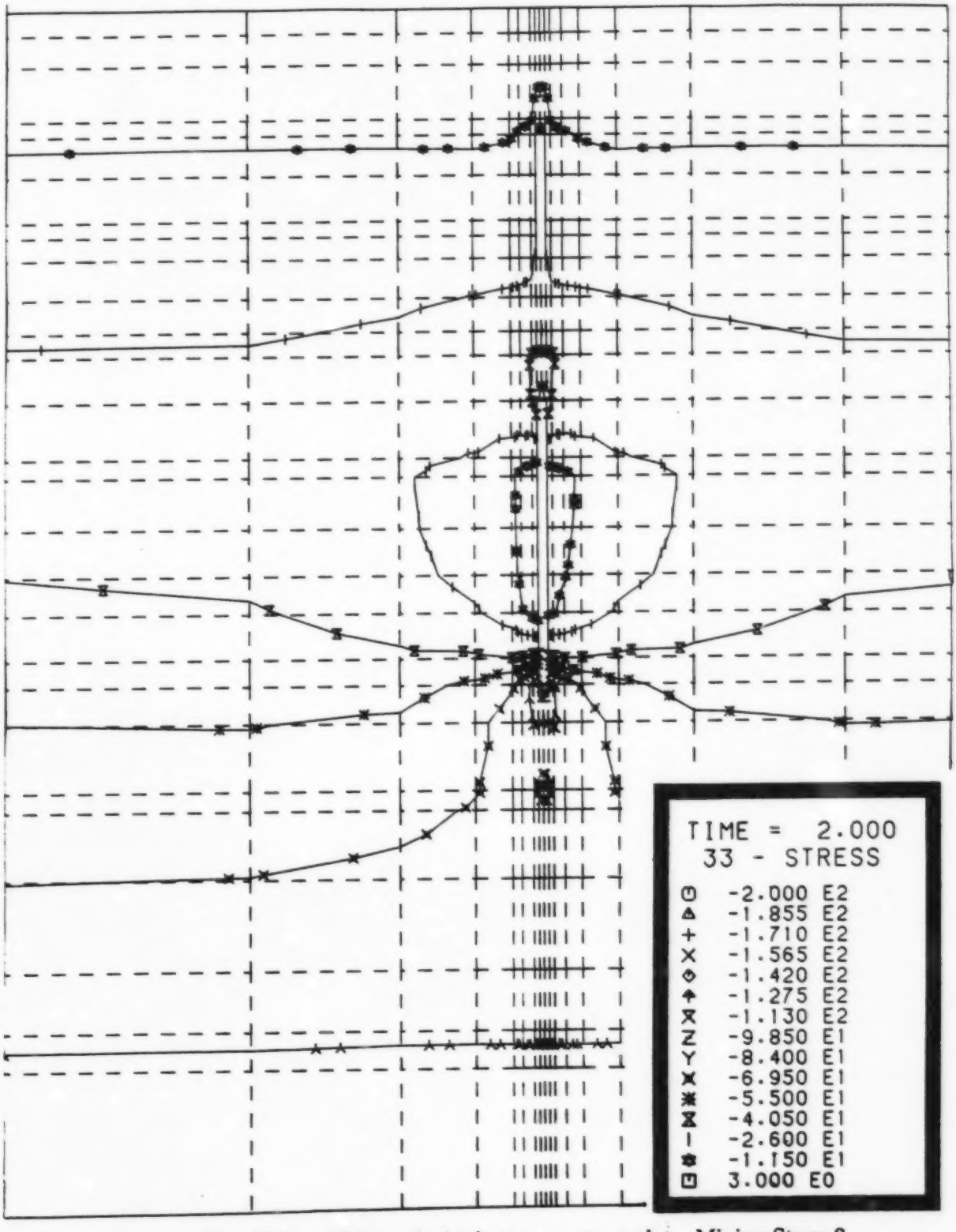

Fig. 15(b) Minor principal stress contour plot - Mining Stage 2
(N-S section, x = 1762.5m)

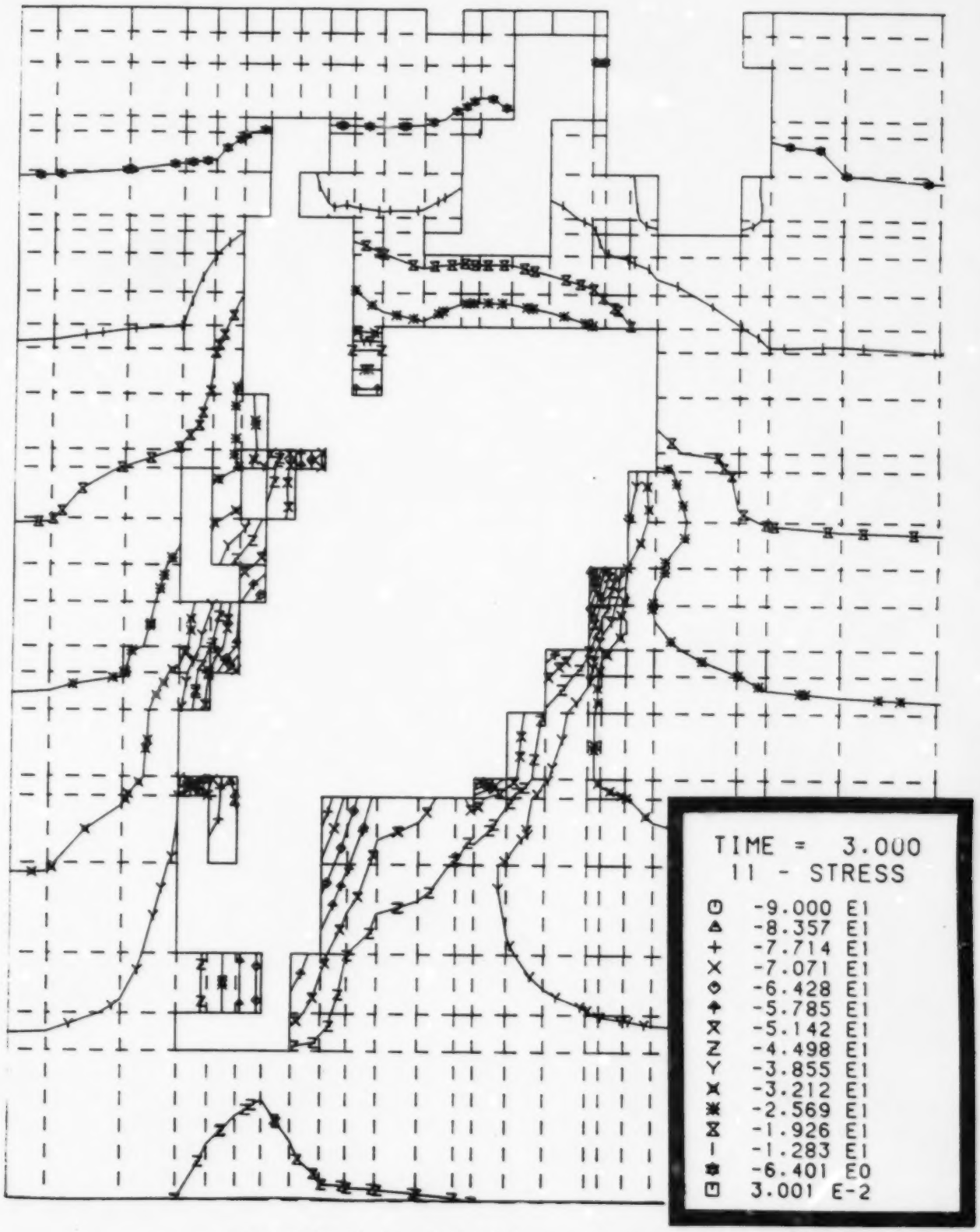

Fig. 16(a) Major principal stress contour plot - Mining Stage 3
(Ore zone (H/W), section z = 1045.7m)

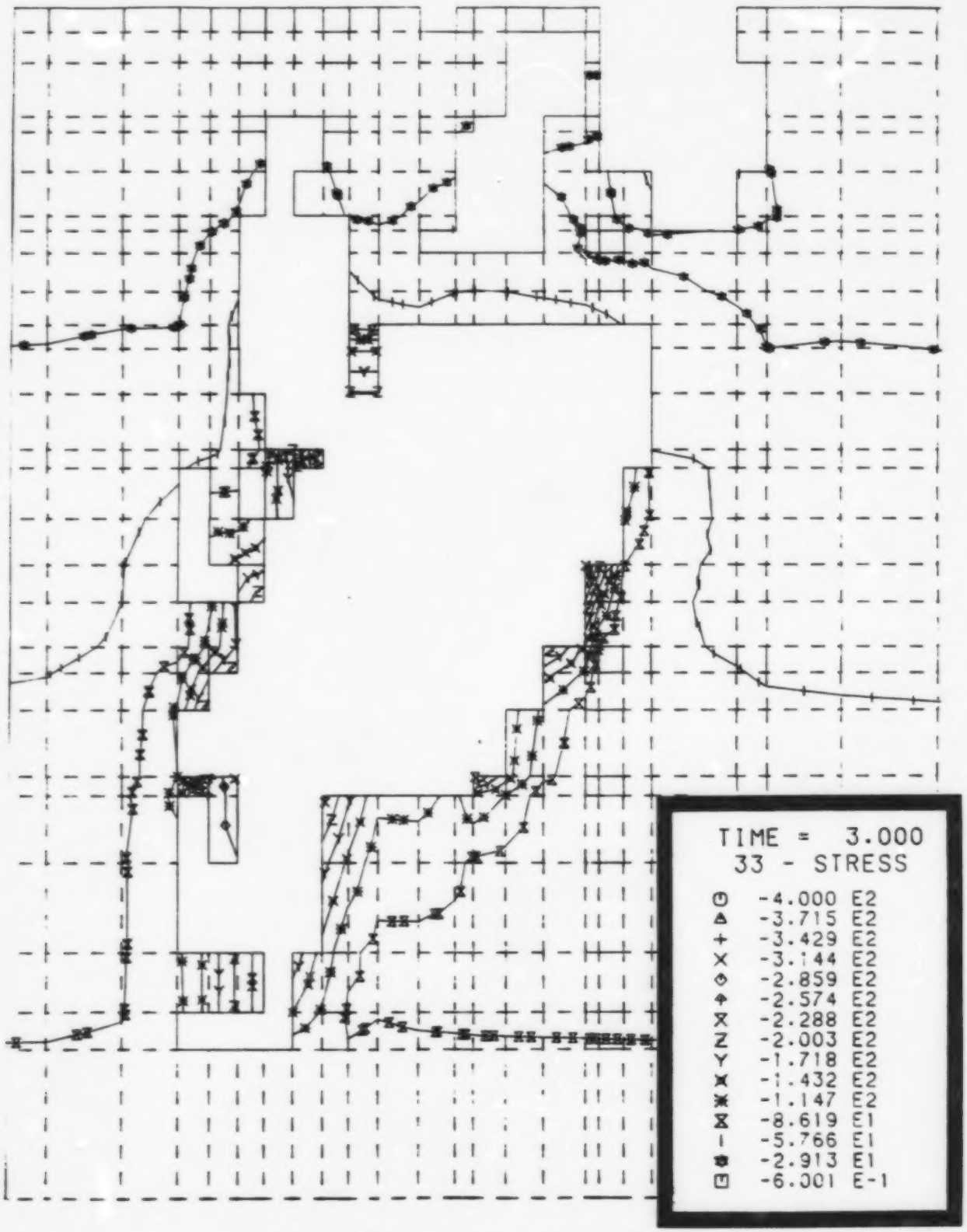

Fig. 16(b) Minor principal stress contour plot - Mining Stage 3
(Ore zone (H/W), section z = 1045.7m)

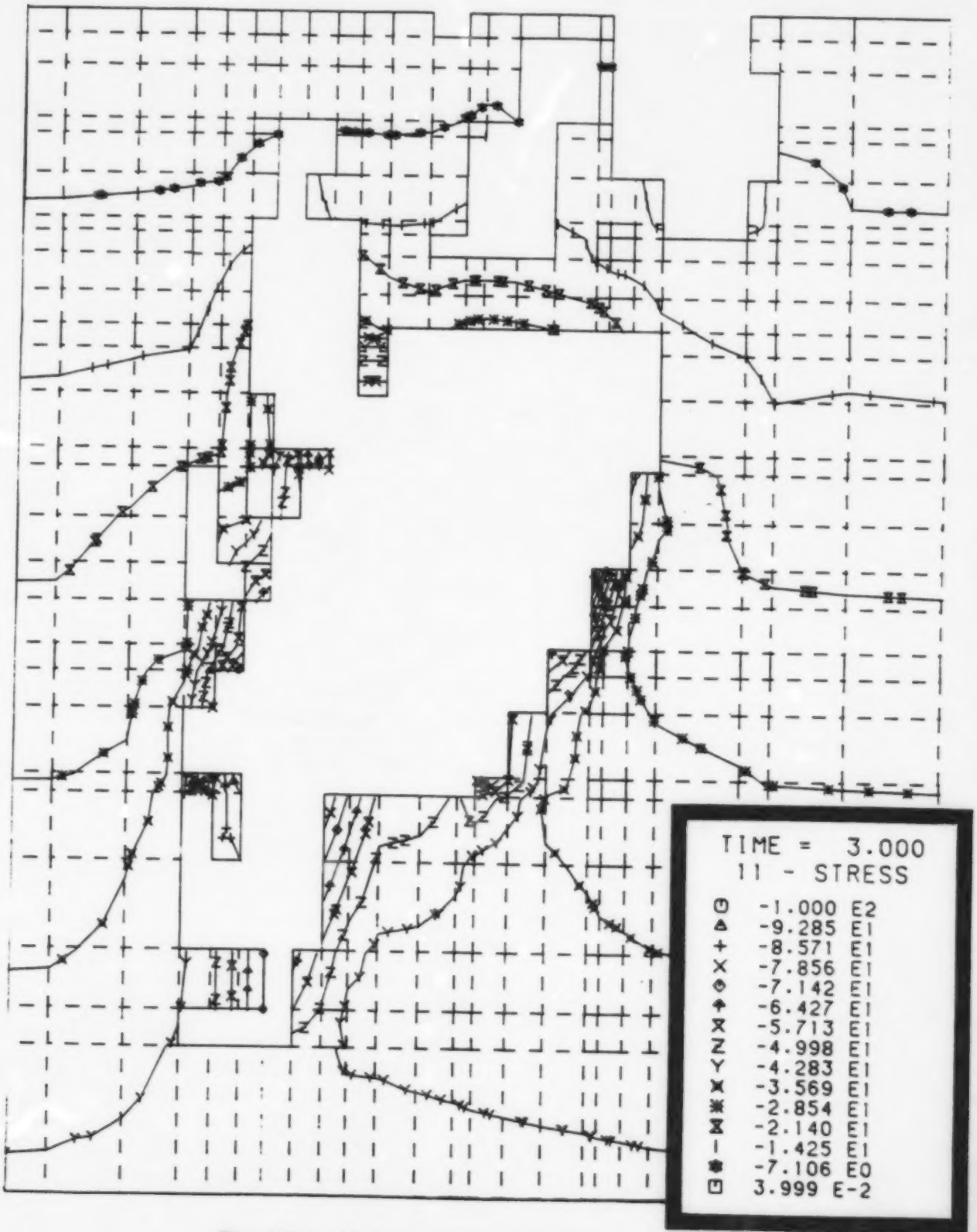

Fig. 17(a) Major principal stress contour plot - Mining Stage 3
(Ore zone (F/W), section z = 1039.2m)

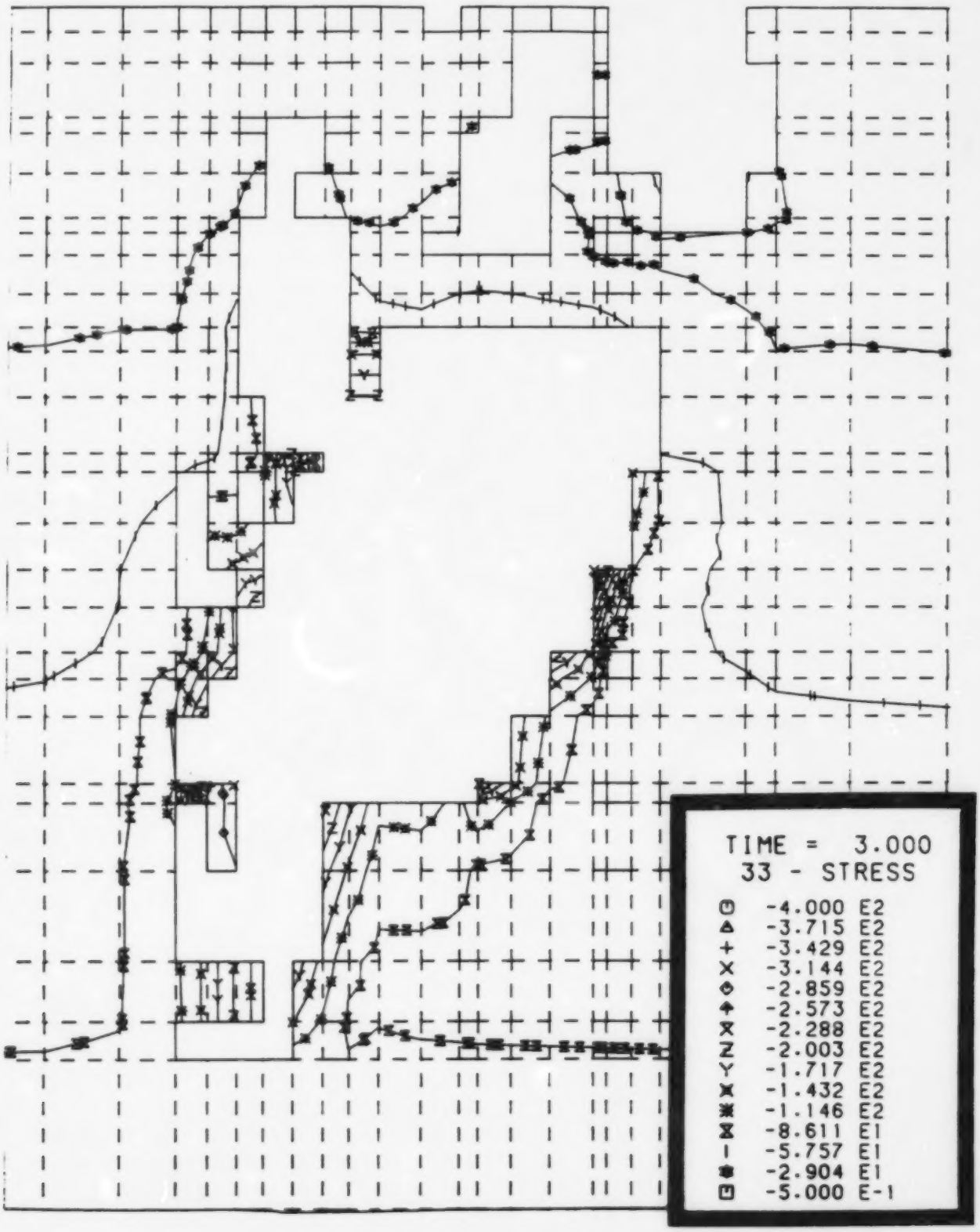

Fig. 17(b) Minor principal stress contour plot - Mining Stage 3
(Ore zone (F/W), section z = 1039.2m)

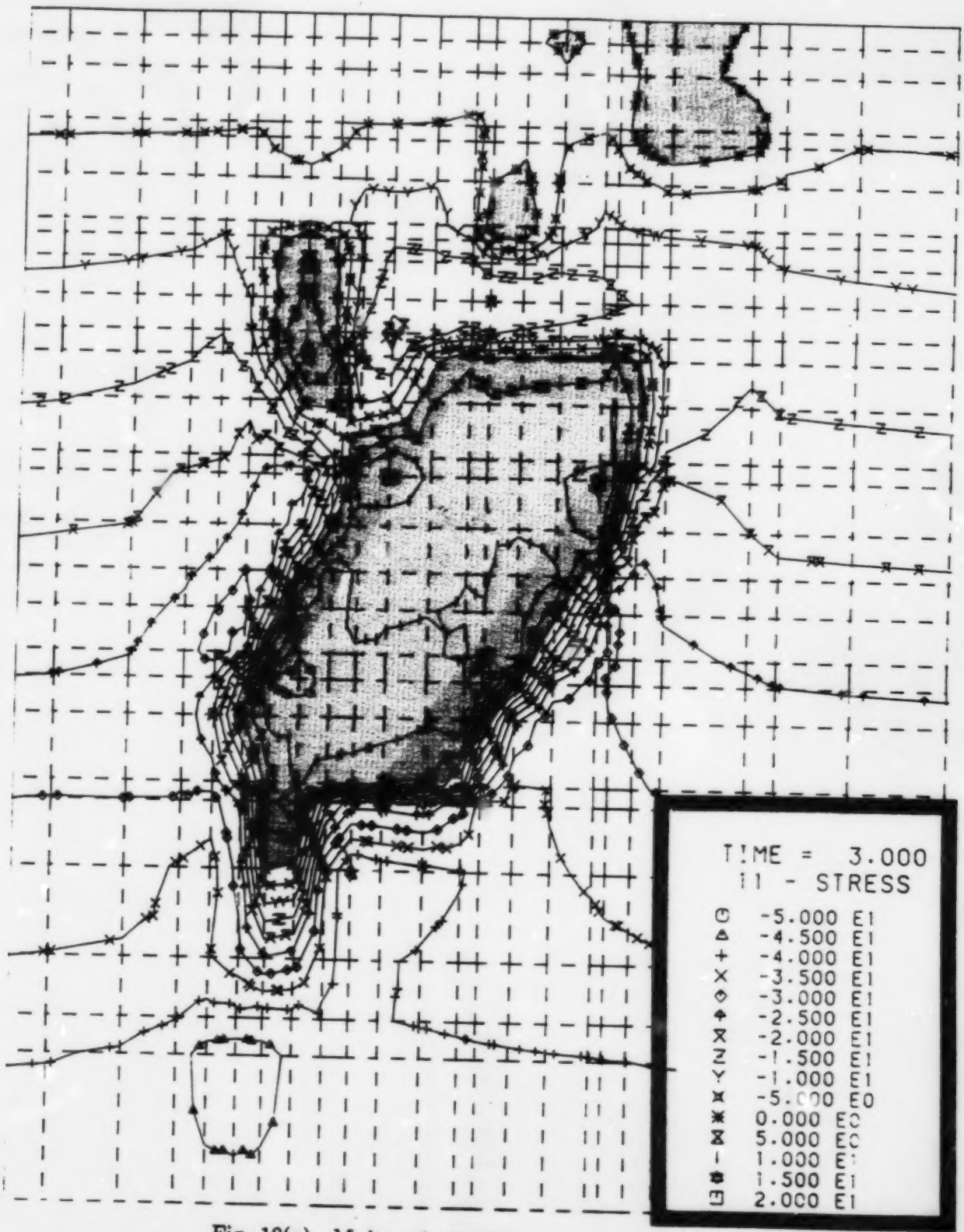

Fig. 18(a) Major principal stress contour plot - Mining Stage 3
(Footwall, section z = 1032.5m)

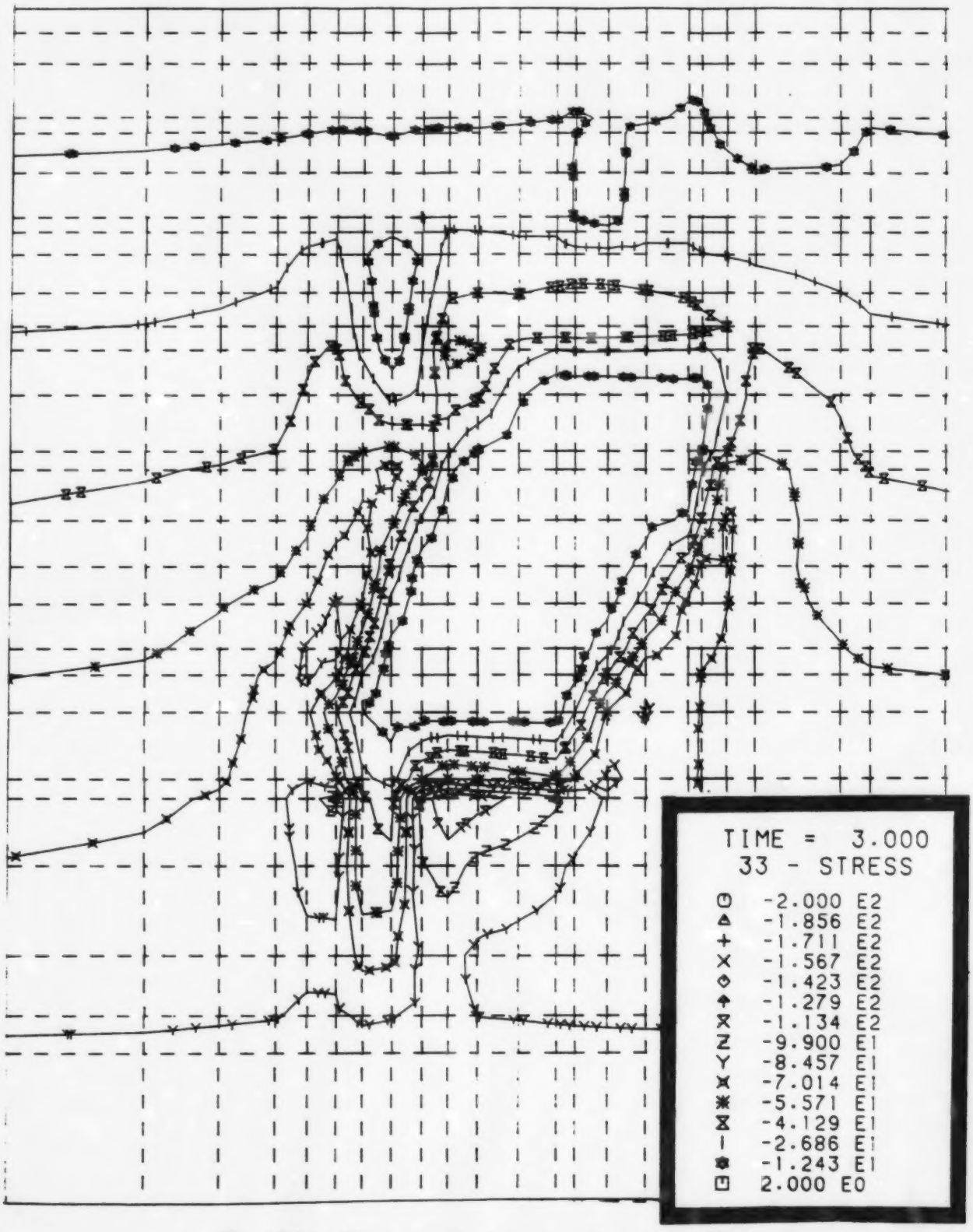

Fig. 18(b) Minor principal stress contour plot - Mining Stage 3
(Footwall, section z = 1032.5m)

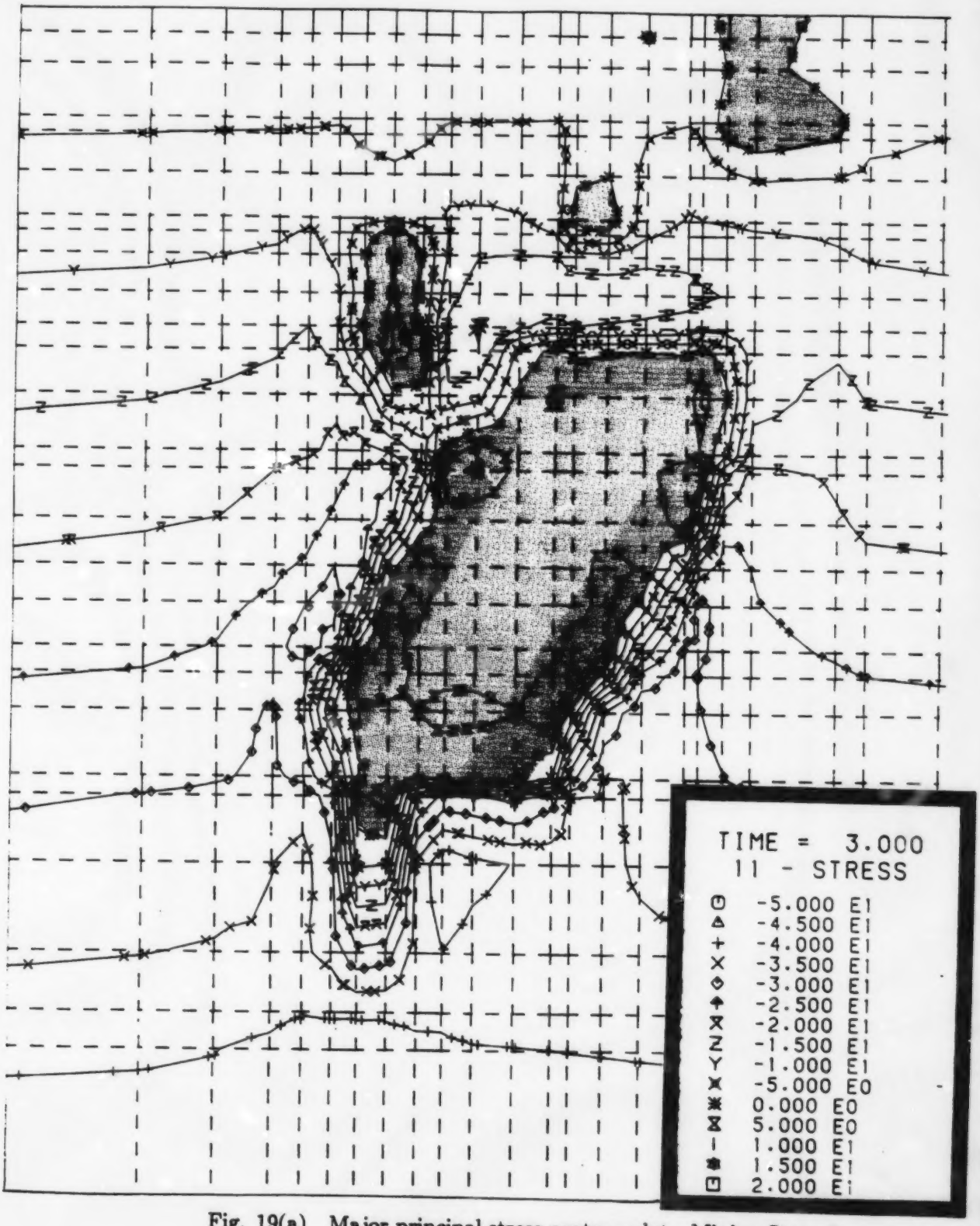

Fig. 19(a) Major principal stress contour plot - Mining Stage 3
(Hanging wall, section z = 1052.5m)

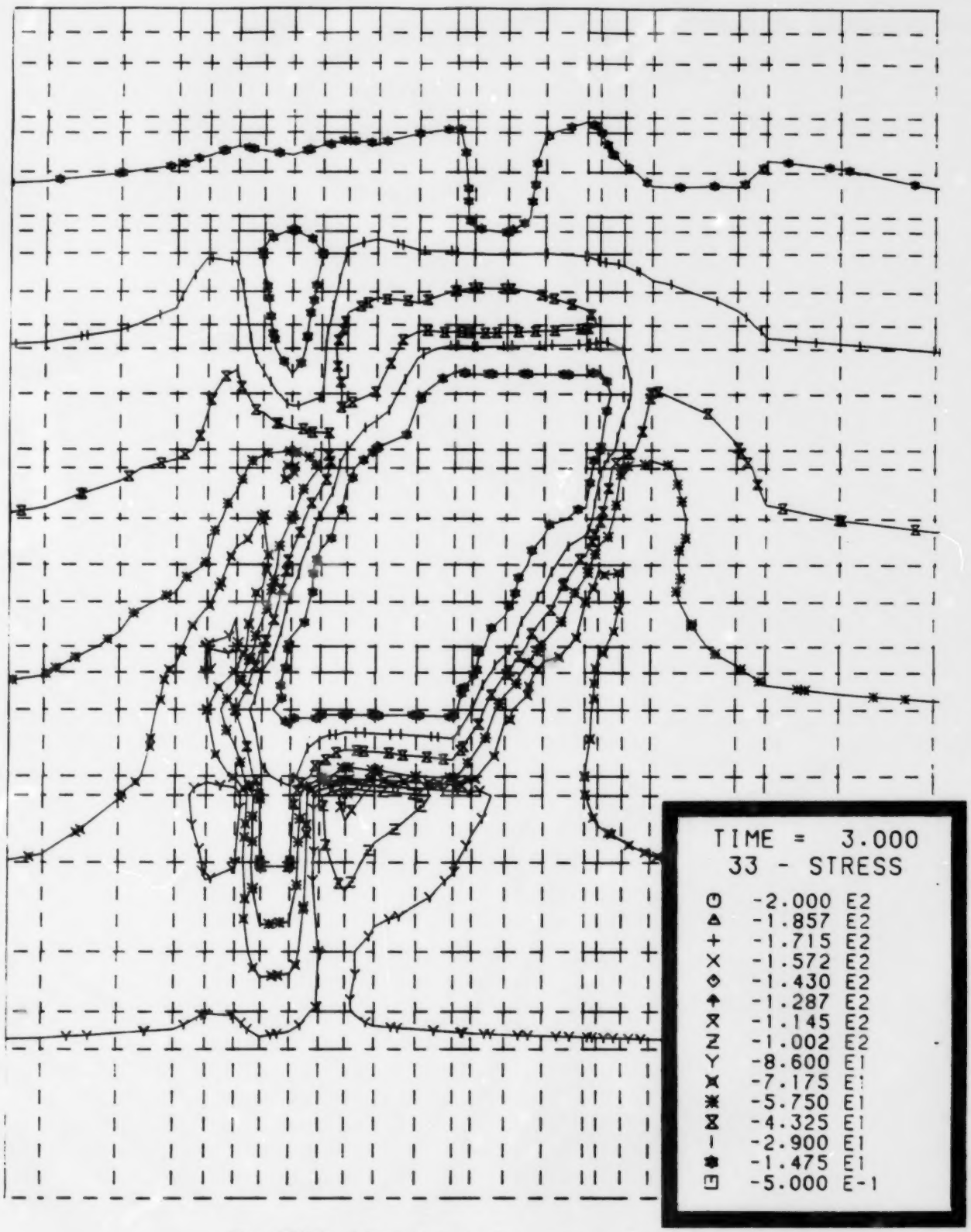

Fig. 19(b) Minor principal stress contour plot - Mining Stage 3
(Hanging wall, section z = 1052.5m)

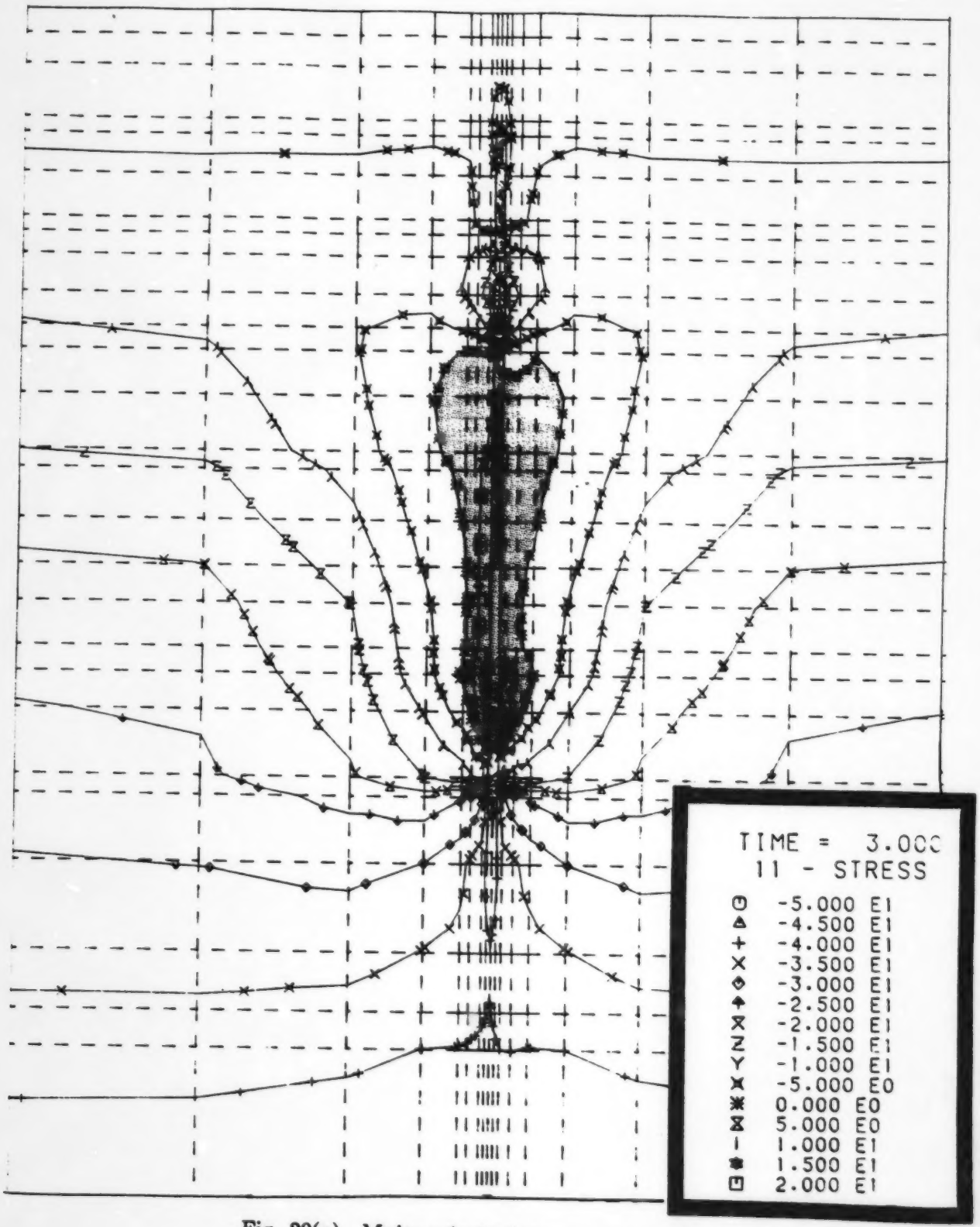

Fig. 20(a) Major principal stress contour plot - Mining Stage 3
(North-South section, x= 1762.5m)

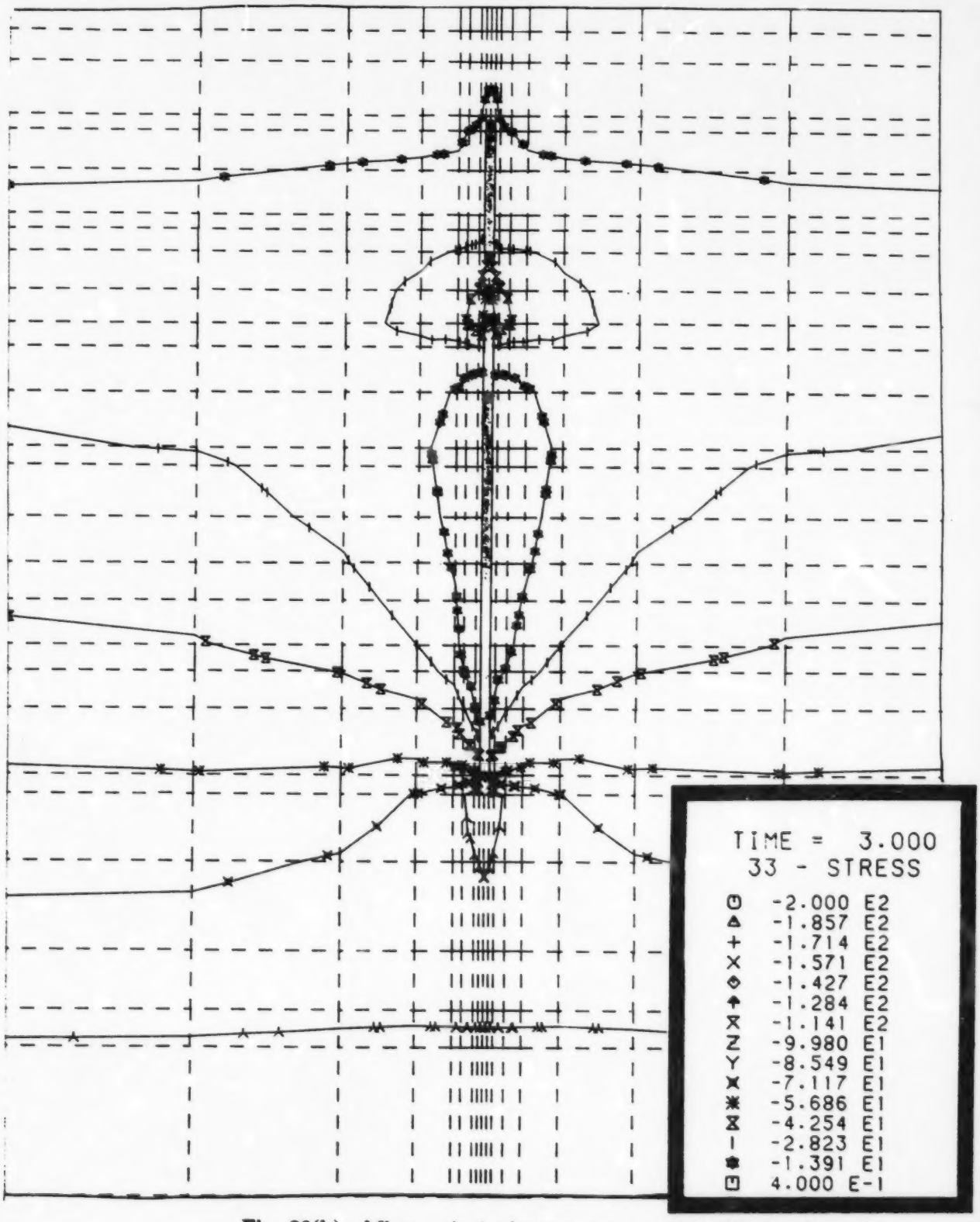

Fig. 20(b) Minor principal stress contour plot - Mining Stage 3
(N-S section, x = 1762.5m)

(b) The orebody is a relatively competent and intact material. It will be able to withstand larger compressive stresses. However, large areas of tension, with magnitudes of approximately 20 MPa or greater, were observed in both footwall and hangingwall. Both hangingwall and footwall schists are relatively soft and weak materials, they would not be able to withstand these high tensile stresses. Localized tensile failure could eventually progress to a large scale failure. Subsequently, this could produce serious dilution and pose a threat to maintaining the overall structural integrity.

3.2 Potential Failure Areas

Frequently, there is an interest in defining a local factor of safety or a strength/stress ratio. This is some scalar function of stress that is assumed to determine stability. It is difficult to find a realistic failure criterion for rock mass surrounding an underground excavation, since the stability of the rock in the immediate vicinity of underground openings is related to the existing discontinuities and fractures induced in the rock by blasting, and drilling process, etc. For the purpose of underground excavation design, the failure criterion should describe the response of an intact rock sample in different stress conditions (from uniaxial tensile to triaxial compression), and it should be capable of predicting the influence of discontinuities on the behaviour of rock mass.

No one criterion is capable of predicting potential ground failure for all types of rock. The Drucker-Prager yielding criterion takes into account the triaxial stress conditions but it fails to predict any tensile failure. Hoek and Brown's empirical failure criterion seems to be gaining popularity for rock mechanics applications in recent years. Although it ignores the intermediate principal stress, it does take into account rock mass quality, which is influenced by discontinuities, for both shear and tensile failures.

In this study, a normalized Drucker-Prager yield function and an empirical Hoek-Brown's failure criterion were selected.

3.2.1 Hoek and Brown's Empirical Failure Criterion

Hoek and Brown's empirical failure criterion assumes that the intermediate principal stresses has no influence on failure, the equation relating the principal stresses at failure is given by [5]:

$$\sigma_1 = \sigma_3 + \sqrt{m\sigma_c\sigma_3 + s\sigma_c^2} \tag{4}$$

where σ_1, σ_3 = *the major and minor principal stresses at failure*

σ_c = *the uniaxial compressive strength of the intact rock material in the specimen*

m, s = *constants depend upon the properties of the rock and upon the extent to which it has been broken before being subjected to the stresses* σ_1 *and* σ_3. *For intact rock* $s = 1$,

for previously over stressed $s < 1$, and for jointed and broken rock sample s decreases to a limiting value of zero.

The uniaxial compressive strength, σ_u, and the uniaxial tensile strength, σ_t, of the rock specimen (rock mass) can be related to the uniaxial compressive strength of the intact rock material in the specimen [5]:

$$\sigma_u = \sqrt{s\sigma_c^2} \tag{5}$$

$$\sigma_t = \frac{1}{2}\sigma_c(m - \sqrt{m^2 + 4s}) \tag{6}$$

When considering shear failure, the strength/stress ratio can be calculated as follows:

$$SF = \frac{\sigma_1 - \sigma_3}{\sqrt{m\sigma_c\sigma_3 + s\sigma_c^2}} \tag{7}$$

A series of analyses based on the values of m and s as given in Table 1, were carried out. The strength/stress ratio maps for the five sections under consideration (i.e., the planes z = 1045.7 m, 1039.2 m, 1032.5 m and 1052.5 m, and x= 1762.5 m) were calculated and are shown in Figures 21 to 30. All analyses indicated that only minor failure zones around the stopes in the orebody, except the vertical section x = 1762.5 m, were observed. As expected, large potential failure zones in both hangingwall and footwall were observed. The tensile zone in the hanginwall extends a great distance to the lower lever. This is due to the fact that the m and s values for the hangingwall schist is much lower as compared to those for the footwall schist.

Areas with factor of safety or strength/stress ratio > 1.5 were considered stable. Areas with factor of safety lies between 1.0 - 1.50 were considered potential failure zones; area with $FS \leq 1.0$ was considered already yielded region, as shown in Figure 23, 24, and 25. These areas were mainly located at the footwall and hangingwall.

3.2.2 Drucker-Prager Yield Criterion

Another indicator for failure is based on Drucker-Prager yield function. Drucker-Prager yield criterion takes all three principal stresses into account, and the calculation for LFS or strength/stress ratio in terms of Drucker-Prager yield function is briefly described below:

The Drucker-Prager yield criterion may be written as :

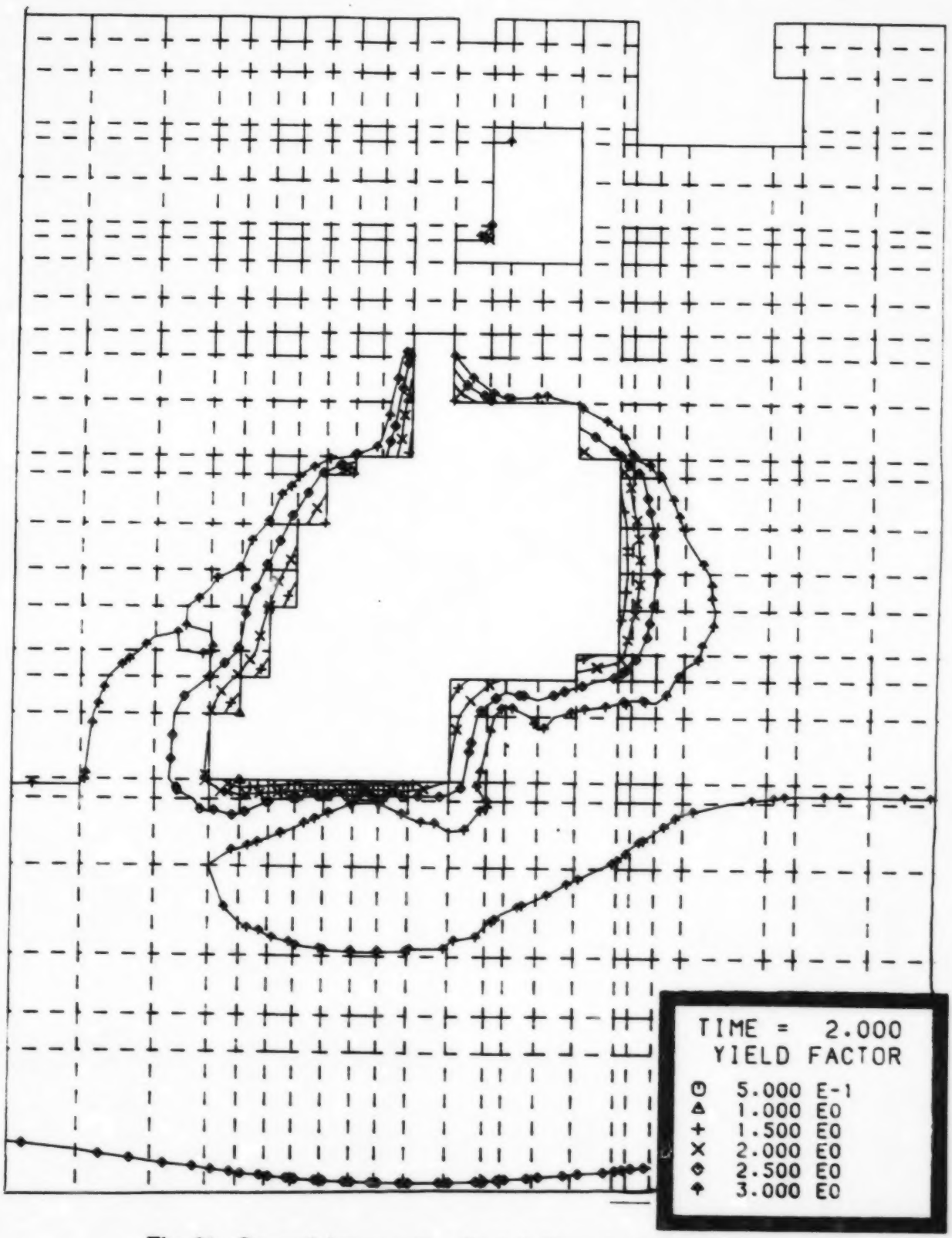

Fig. 21 Strength/stress ratio - Hoek & Brown's empirical failure criterion (Mining Stage 2, ore zone (H/W), section z = 1045.7m)

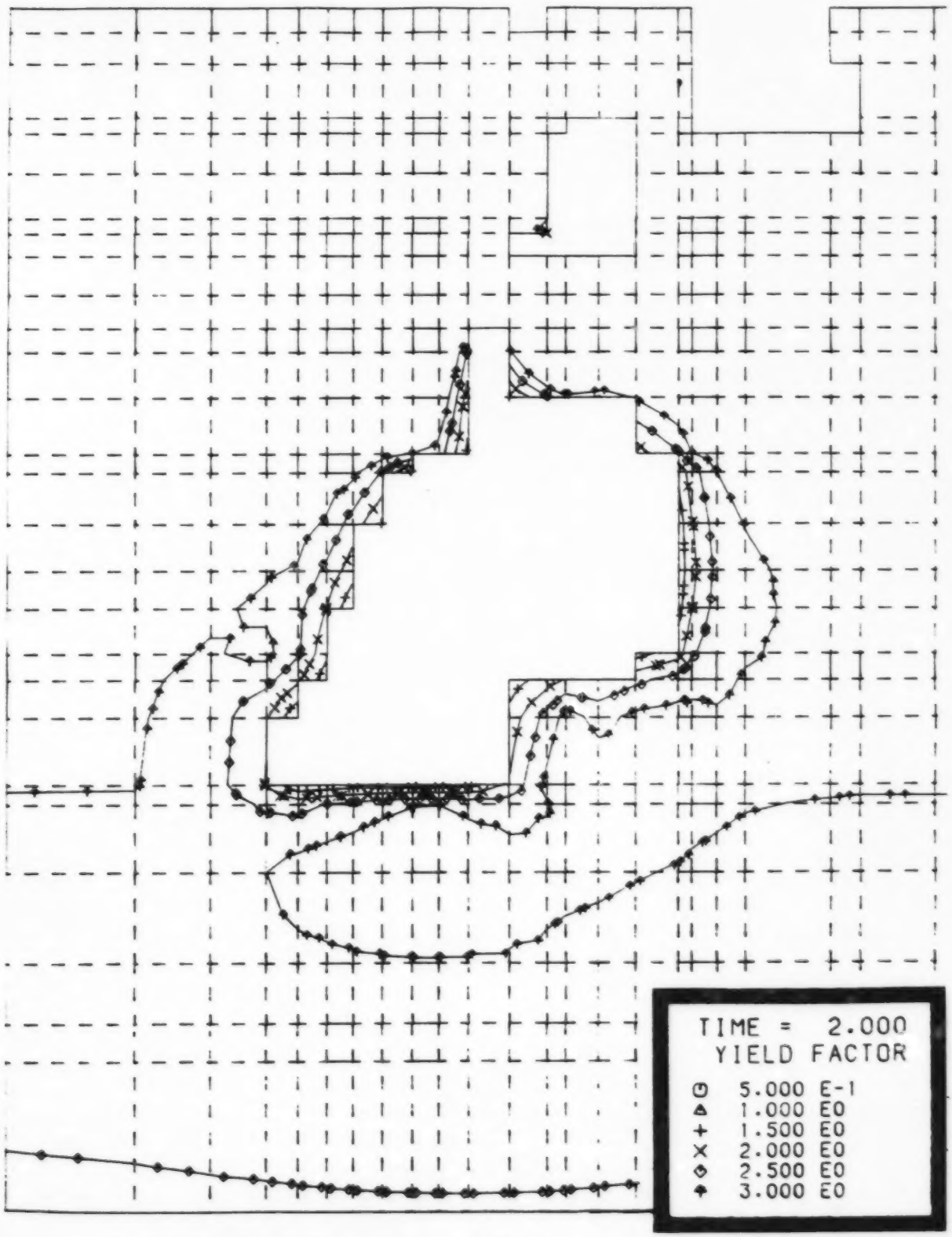

Fig. 22 Strength/stress ratio - Hoek & Brown's empirical failure criterion
(Mining Stage 2, ore zone (F/W), section z = 1039.2m)

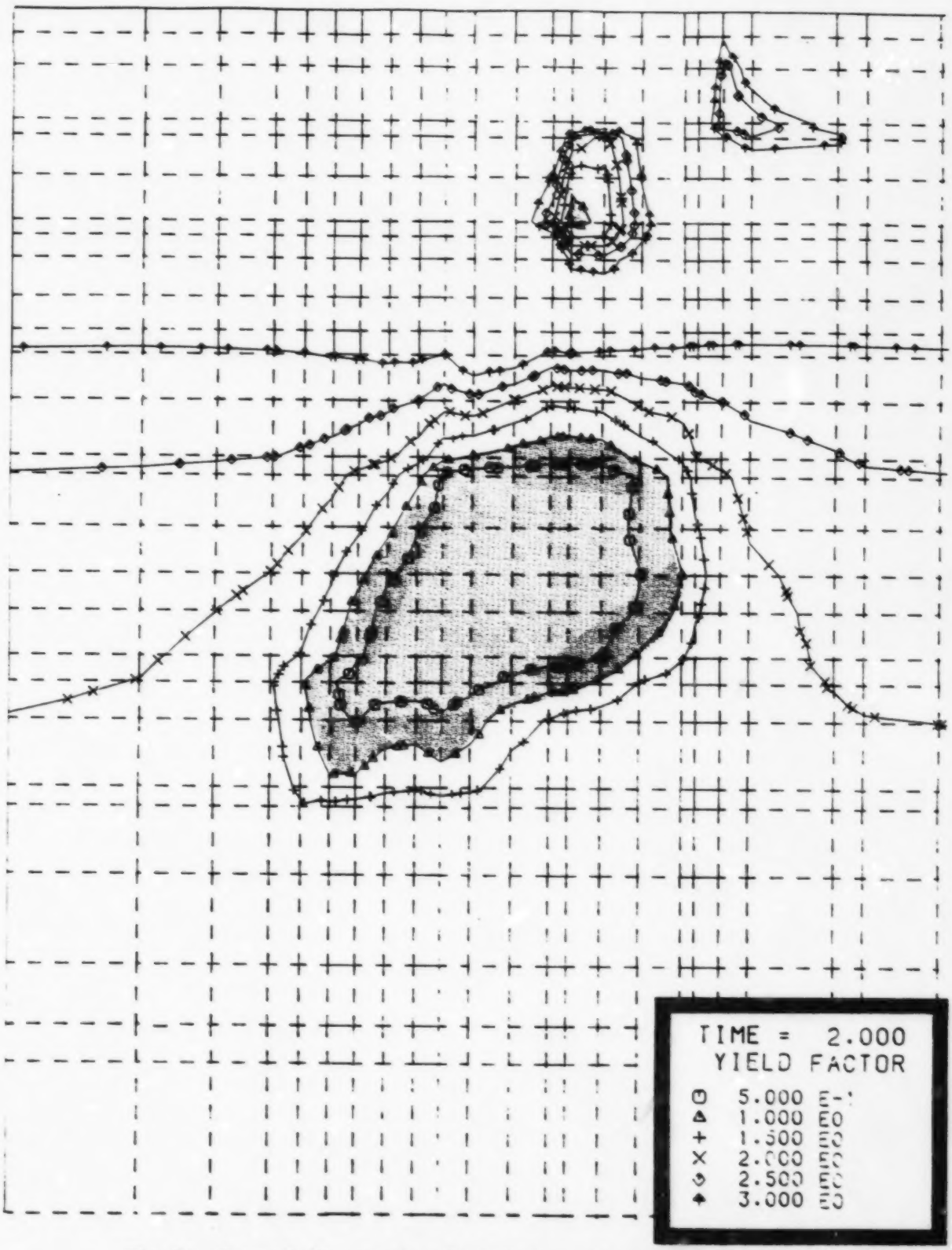

Fig. 23 Strength/stress ratio - Hoek & Brown's empirical failure criterion
(Mining Stage 2, footwall, section z = 1032.5m)

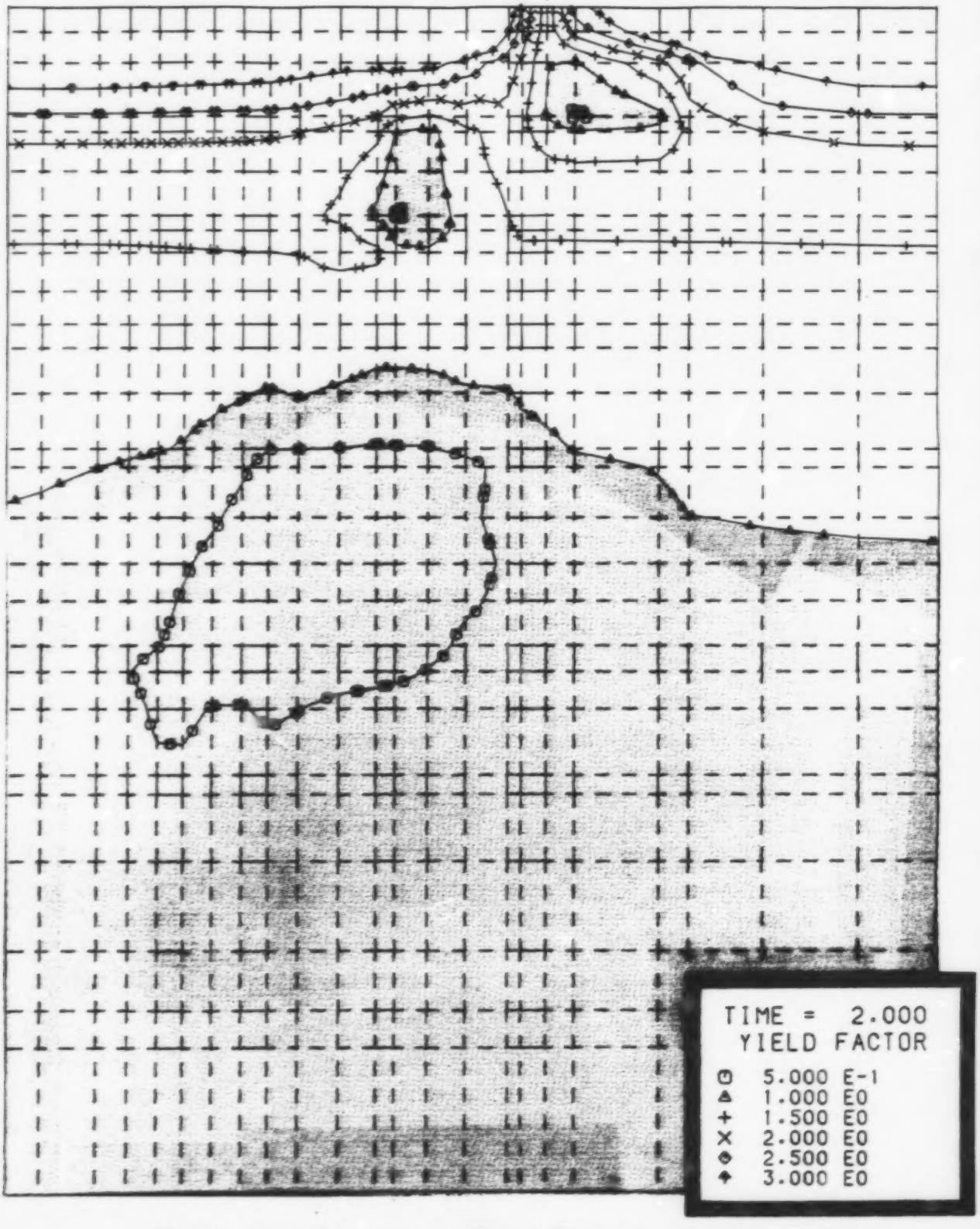

Fig. 24 Strength/stress ratio - Hoek & Brown's empirical failure criterion
(Mining Stage 2, hanging wall, section z = 1052.5m)

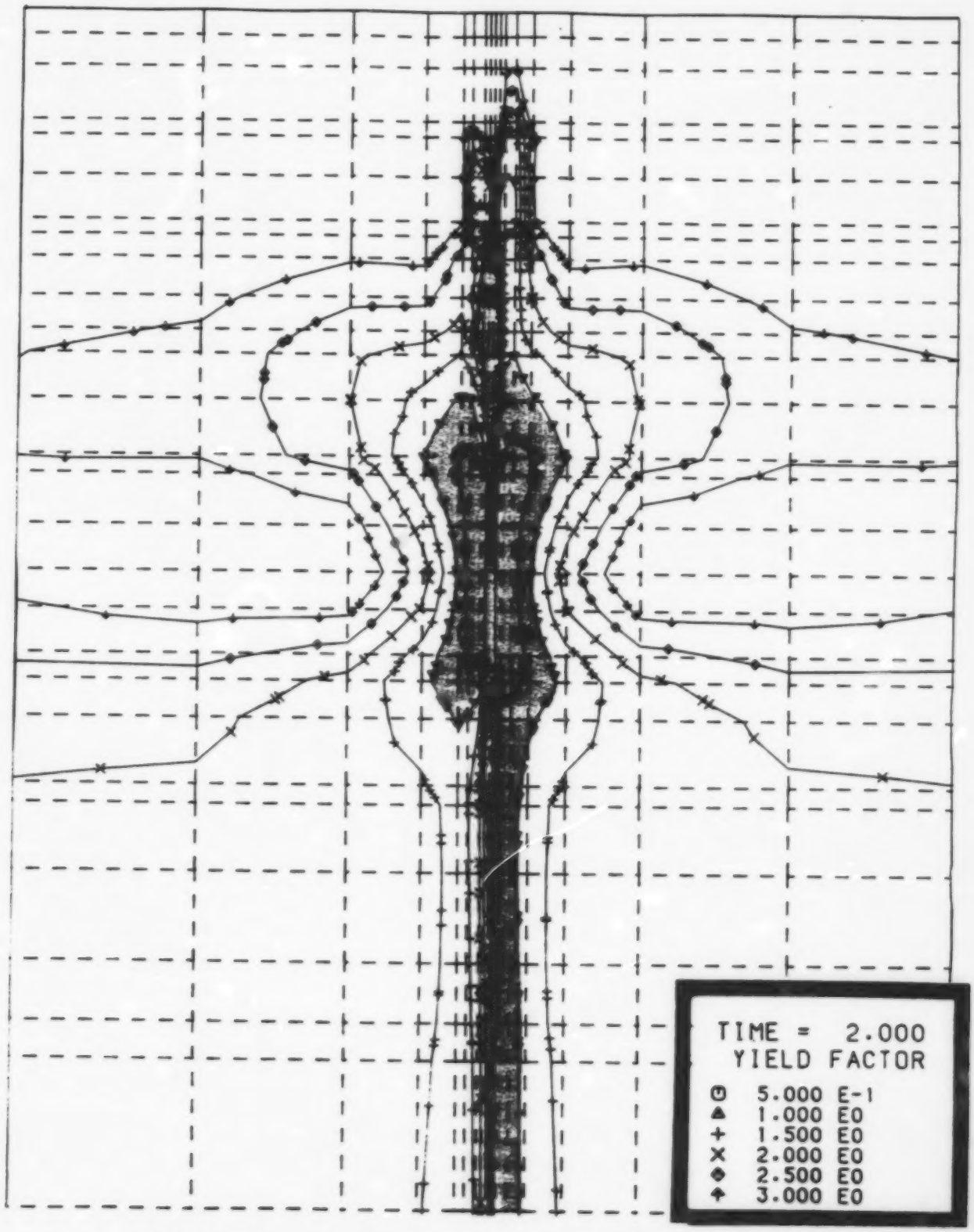

Fig. 25 Strength/stress ratio - Hoek & Brown's empirical failure criterion
(Mining Stage 2, N-S section x = 1762.5m)

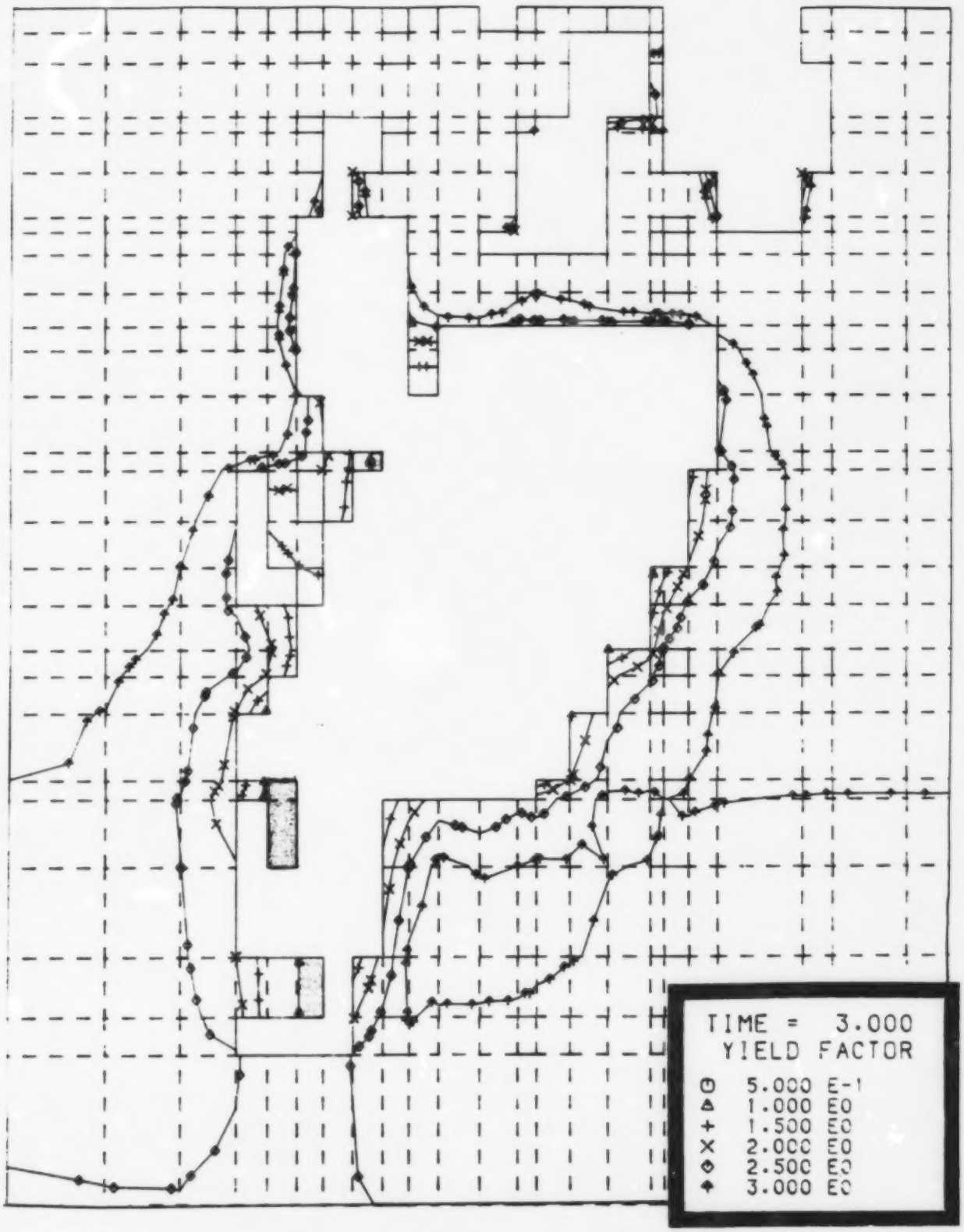

Fig. 26 Strength/stress ratio - Hoek & Brown's empirical failure criterion
(Mining Stage 3, ore zone (H/W), section z = 1045.7m)

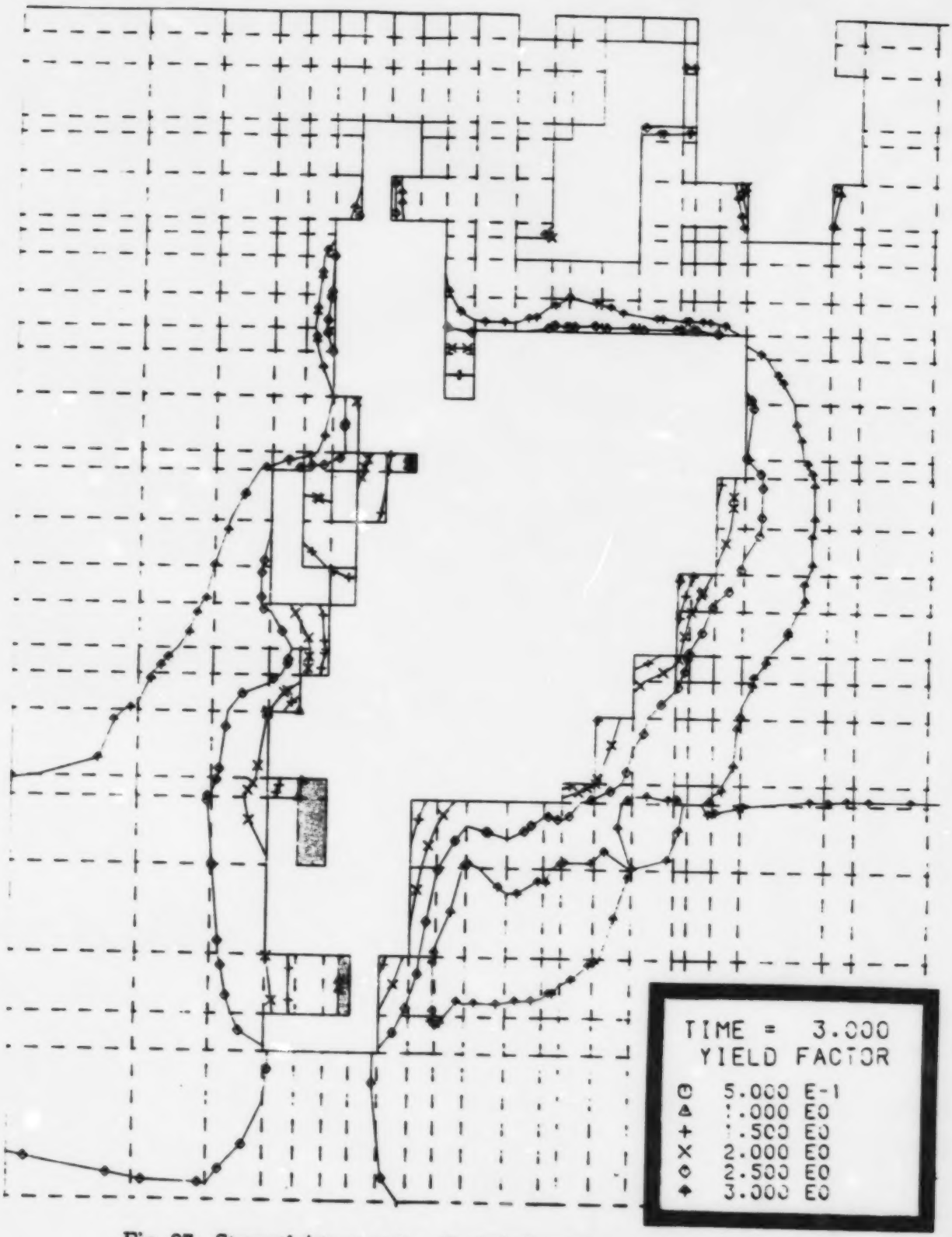

Fig. 27 Strength/stress ratio - Hoek & Brown's empirical failure criterion
(Mining Stage 3, ore zone (F/W), section z = 1039.2m)

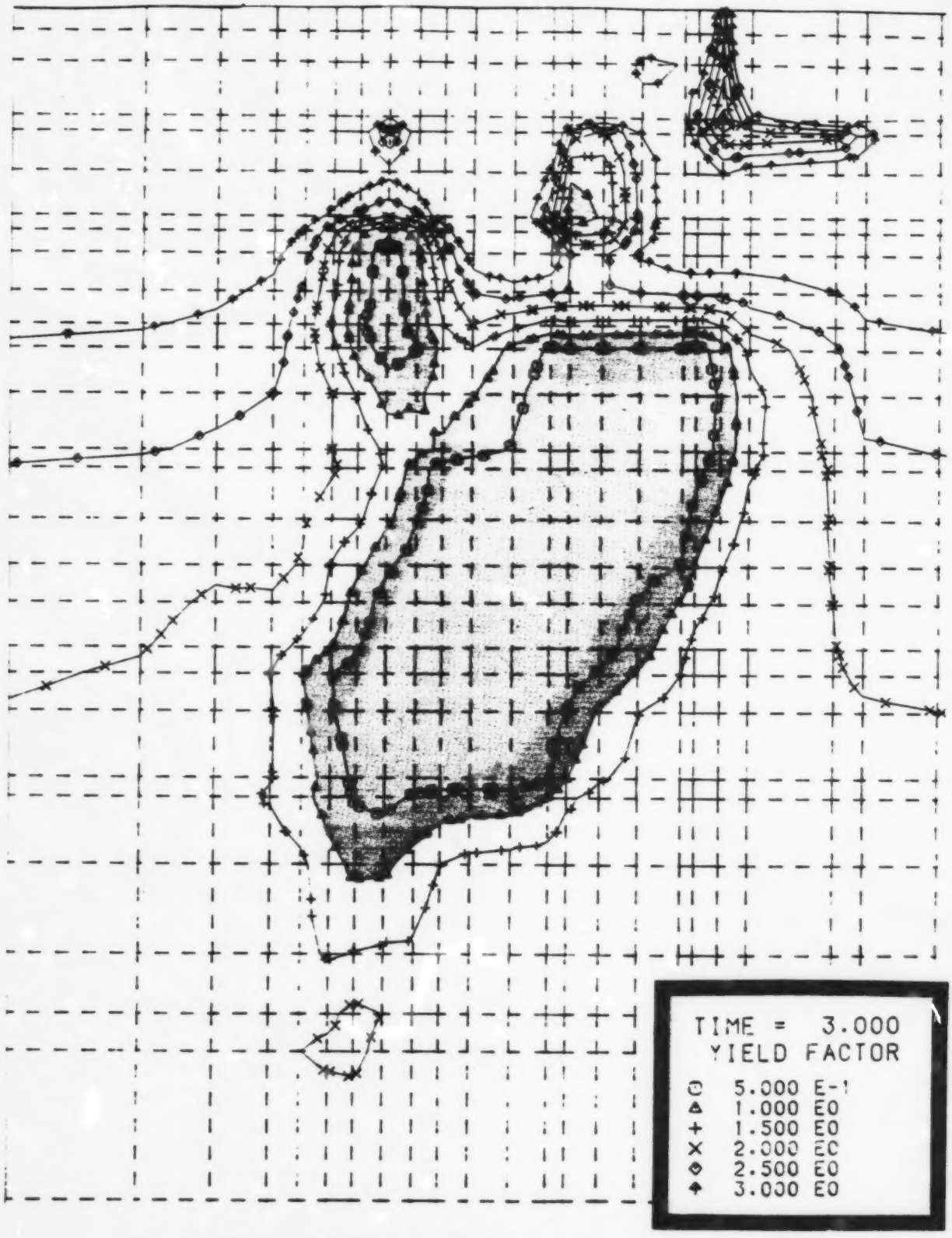

Fig. 28 Strength/stress ratio - Hoek & Brown's empirical failure criterion
(Mining Stage 3, Footwall, section z = 1032.5m)

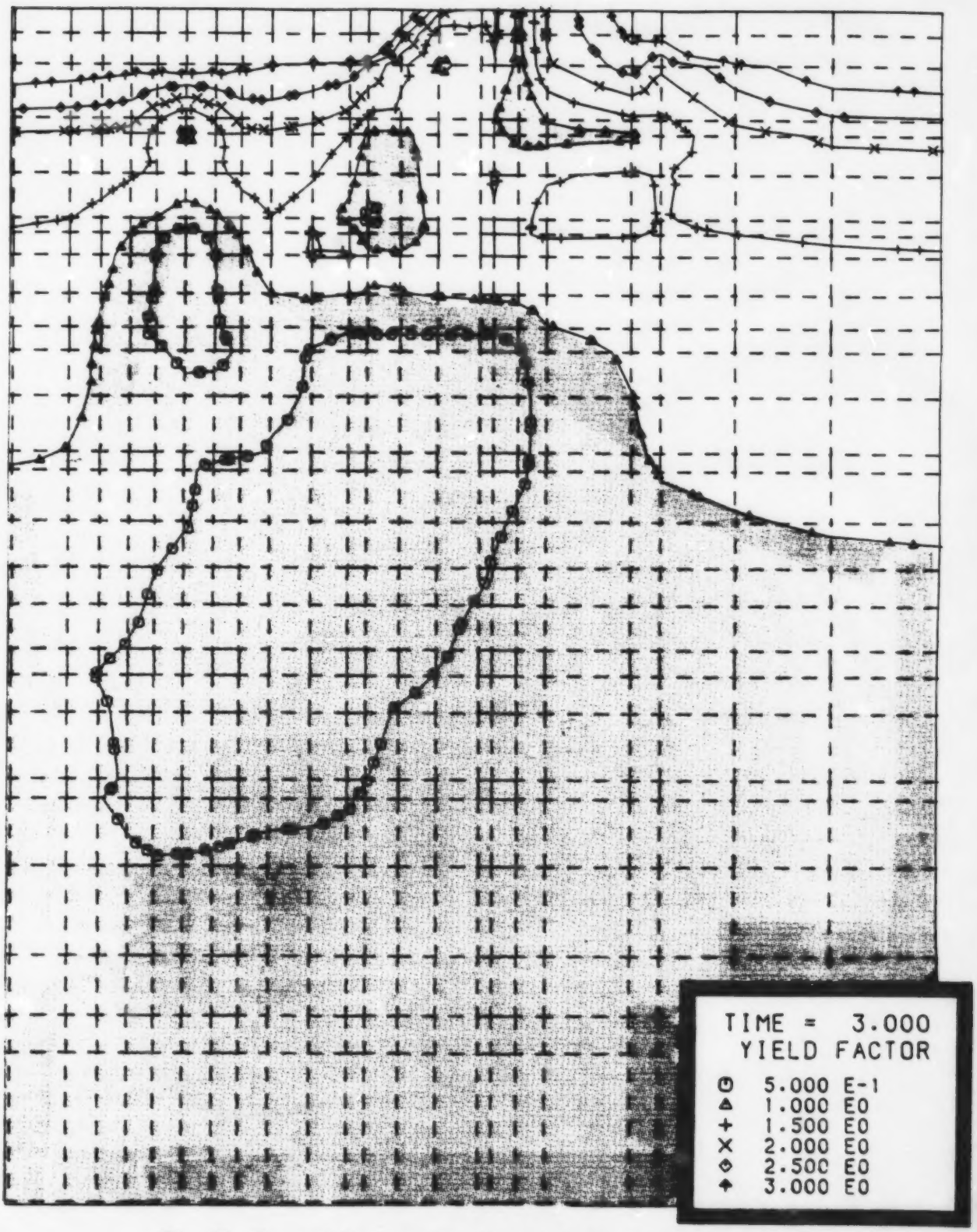

Fig. 29 Strength/stress ratio - Hoek & Brown's empirical failure criterion
(Mining Stage 3, Hanging wall, section z = 1052.5m)

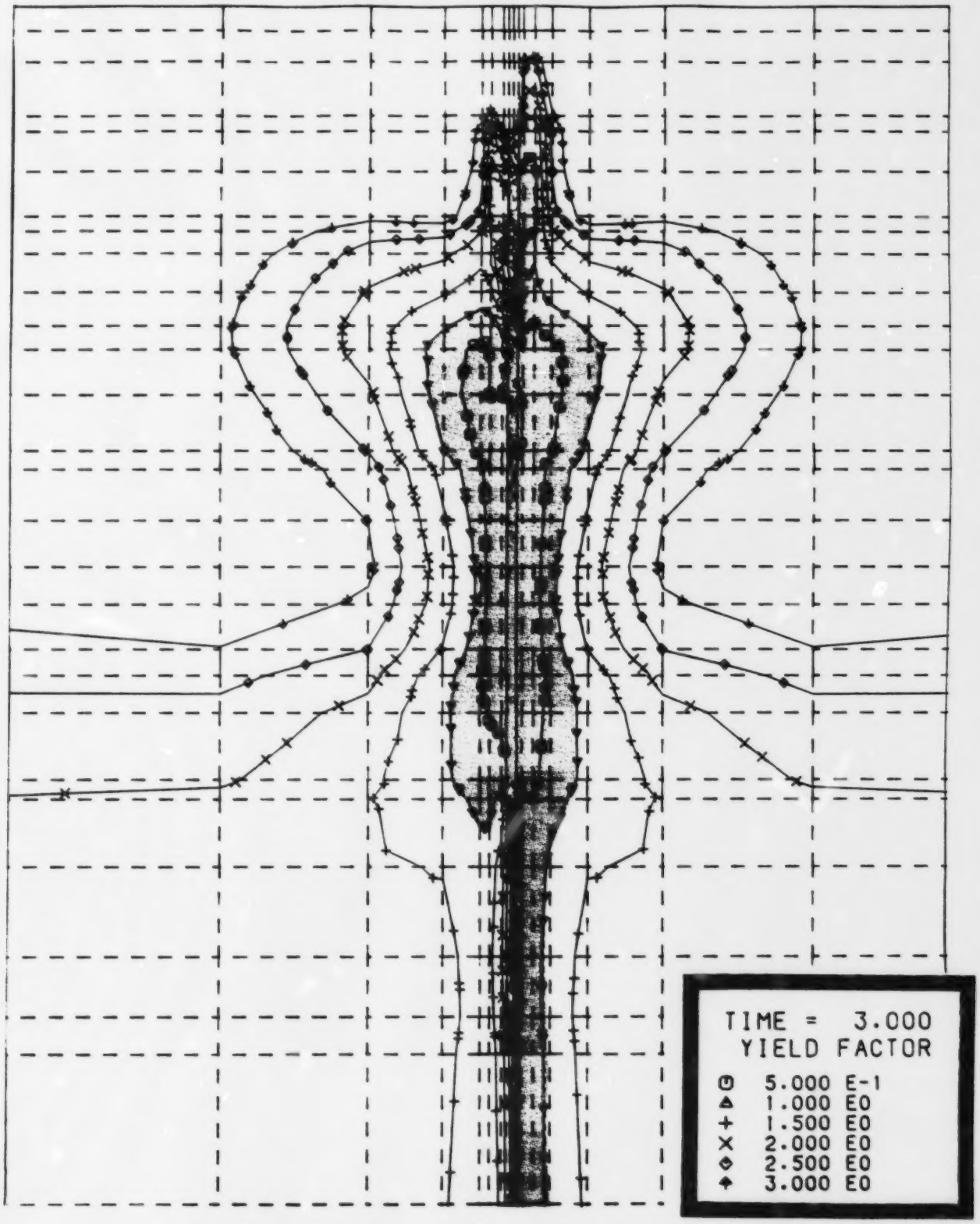

Fig. 30 Strength/stress ratio - Hoek & Brown's empirical failure criterion
(Mining Stage 3, N-S section x = 1762.5m)

$$F = \left(\frac{6sin\phi}{3 - sin\phi}\right)\sigma_m + \sqrt{3}\sqrt{J_2} - \left(\frac{6cos\phi}{3 - sin\phi}\right) = 0 \tag{8}$$

where ϕ is the angle of internal friction, σ_m is the mean stress and

$$\sigma_m = \frac{1}{3}\sigma_{ii} \tag{9}$$

where $\sigma_{ii} = \sigma_{xx} + \sigma_{yy} + \sigma_{zz}$

and J_2 is the second invariant of the deviatoric stress tensor.

$$J_2 = \frac{1}{2}S_{ij}S_{ij} \tag{10}$$

$$S_{ij} = \sigma_{ij} - \delta_{ij}\sigma_m \tag{11}$$

and δ_{ij} is the Kronecker delta.

$J_2 = \frac{1}{2}\left\{(\sigma_{xx} - \sigma_m)^2 + (\sigma_{yy} - \sigma_m)^2 + (\sigma_{zz} - \sigma_m)^2\right\} + (\sigma_{xy})^2 + (\sigma_{xz})^2 + (\sigma_{yz})^2$

The factor of safety is defined as:

$$SF = \frac{\sqrt{J_{2f}}}{\sqrt{J_2}} \tag{12}$$

Where J_{2f} is the second invariant of the deviatoric stress tensor at failure on a $\sigma_m vs \sqrt{J_2}$ failure envelope. J_{2f} is defined as:

$$J_{2f} = \frac{1}{\sqrt{3}}\left(\frac{6cos\phi}{3 - sin\phi}\right) - \left(\frac{6sin\phi}{\sqrt{3}(3 - sin\phi)}\right)\sigma_m$$

In case either of the principal stresses > 0.50 C, a tension failure is assumed, and, SF is set equal to 0.5.

A series of analyses based on the Drucker-Prager yield criterion was carried out. The strength/stress ratio or safety-factor-contour maps for various sections, for mining stage 3, were plotted as

shown in Figures 31 to 35. The material constants used for this analysis are given in Table 1. Similarly, areas with factor of safety > 1.5 were considered stable. Areas with factor of safety lies between 1.0 - 1.50 were considered potential failure zones, area with $FS \leq 1.0$ was considered already yielded region, as shown in Figsure 33, 34 and 35. These areas were mainly located at the footwall and hangingwall. The failure zones or potential failure zones are fairly comparable with those determined by the Hoek-Brown empirical failure criterion, except that these zones determined from the Drucker-Prager yield criterion are more confined. Therefore, the safety-factor-contour maps for other mining stages were not analyzed.

4.0 Conclusions and Remarks

(a) As expected, the mining operation based on the current mine plan scheduled for the year 1991/2000, will induce very higher compressive stresses around the stopes at the lower level of the mine. Compressive stress levels of about 100 MPa or larger, will be developed around the stope floor; these are sufficiently high to cause a ground stability problem. even though the compressive strength of pyrite (ore zone) is considered strong.

The strength of the hangingwall and footwall formation are much weaker; they will not be able to withstand the high stresses resulting from stoping. In addition, large areas of tension in both the hangingwall and footwall were observed, and subsequently, this certainly would cause ground instability and produce high degree of dilution.

(b) The analyses based on either Mohr-Coulomb yield criterion or Hoek & Brown's empirical failure criterion indicate that large failure zones or potential failure zones will occur in both hangingwall and footwall. Therefore, either shear failure or tensile failure should be anticipated in both hangingwall and footwall.

Tensile stresses, with magnitudes of 20 MPa or larger occur in the hanging wall and footwall. Structural stability of the H/W and F/W walls could be greatly influenced by the tensile stresses.

(c) Under these stress conditions, the current mining plan - open stoping without backfill, retreating from bottom up and no barrier pillars left between the two operations, will create serious problems before reaching the final stage of mining on both properties. The problem might be complicated even further by the Bousquet operation if the mining operations are not coordinated between the companies. To maintain the overall structural integrity of both mines, it is strongly suggested that a coordinated mining plan from both operations should be envisaged. In view of this, alternative mine plans should be examined with the assistance of model studies and a favorable mining sequence should be determined. In addition, a strategic field monitoring program should be developed and implemented as soon as possible.

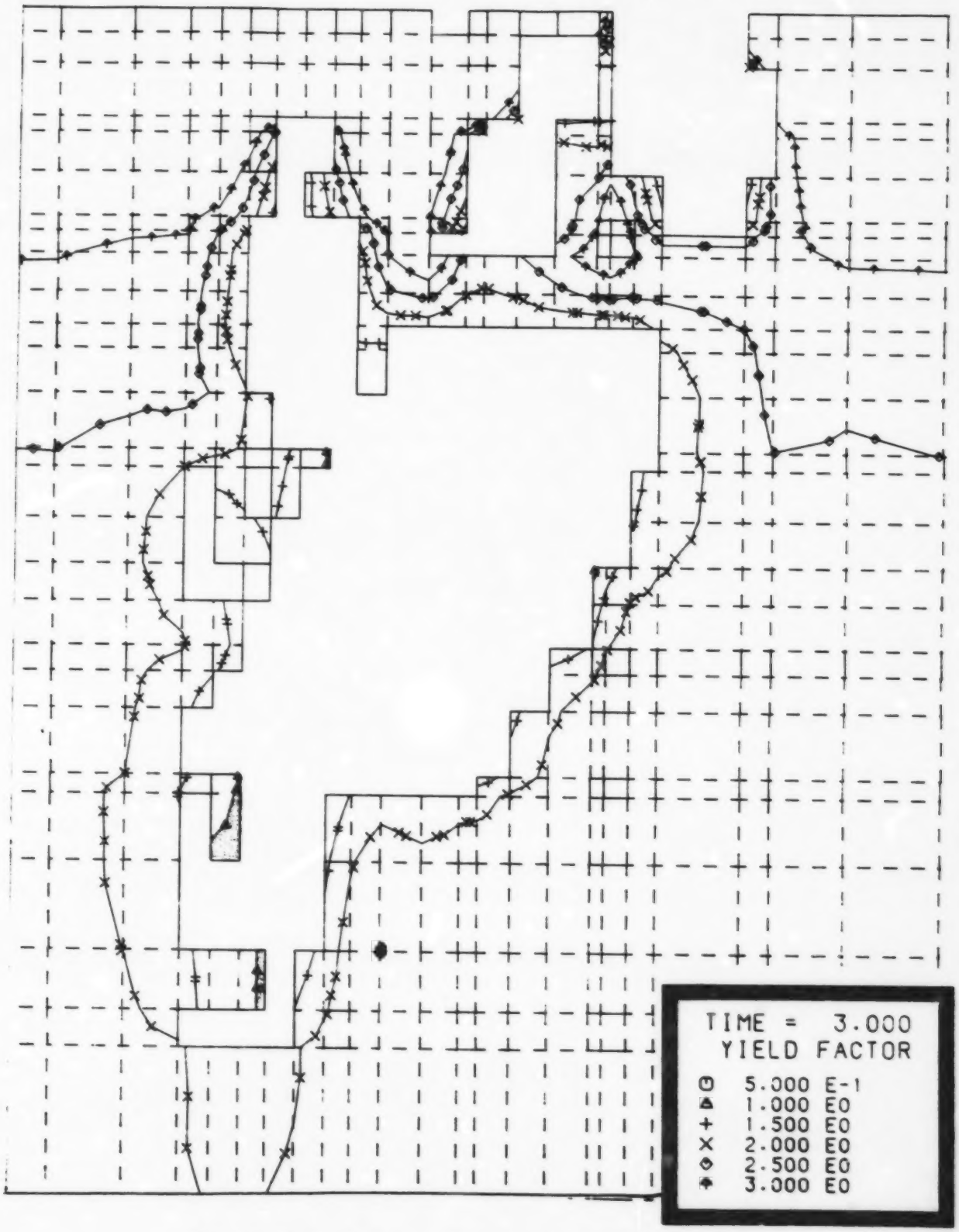

Fig. 31 Strength/stress ratio - Drucker & Prager Yield Criterion
(Mining Stage 3, ore zone (H/W), section z = 1045.7m)

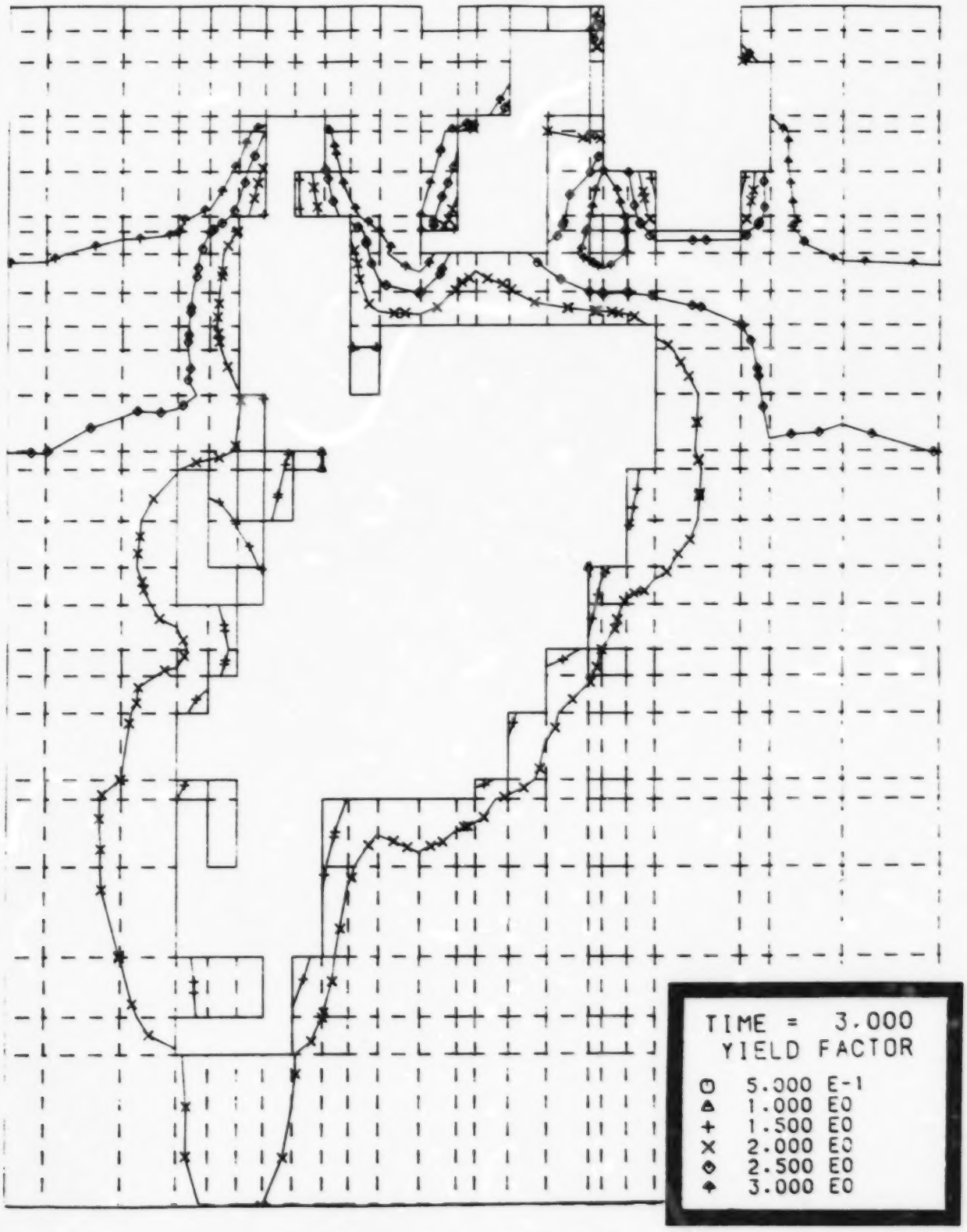

Fig. 32 Strength/stress ratio - Drucker & Prager Yield Criterion
(Mining Stage 3, ore zone (F/W), section z = 1039.2m)

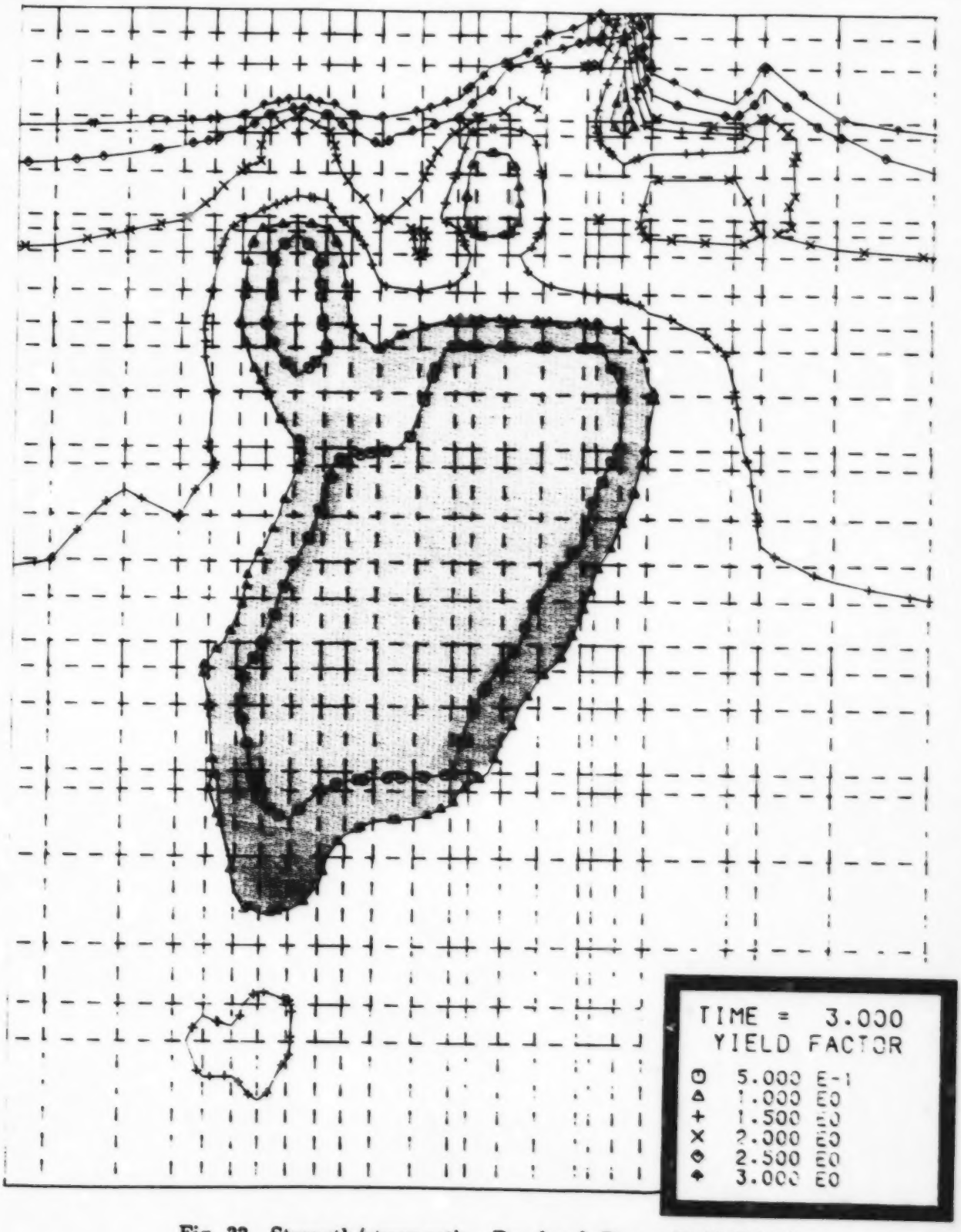

Fig. 33 Strength/stress ratio - Drucker & Prager Yield Criterion
(Mining Stage 3, Footwall, section z = 1032.5m)

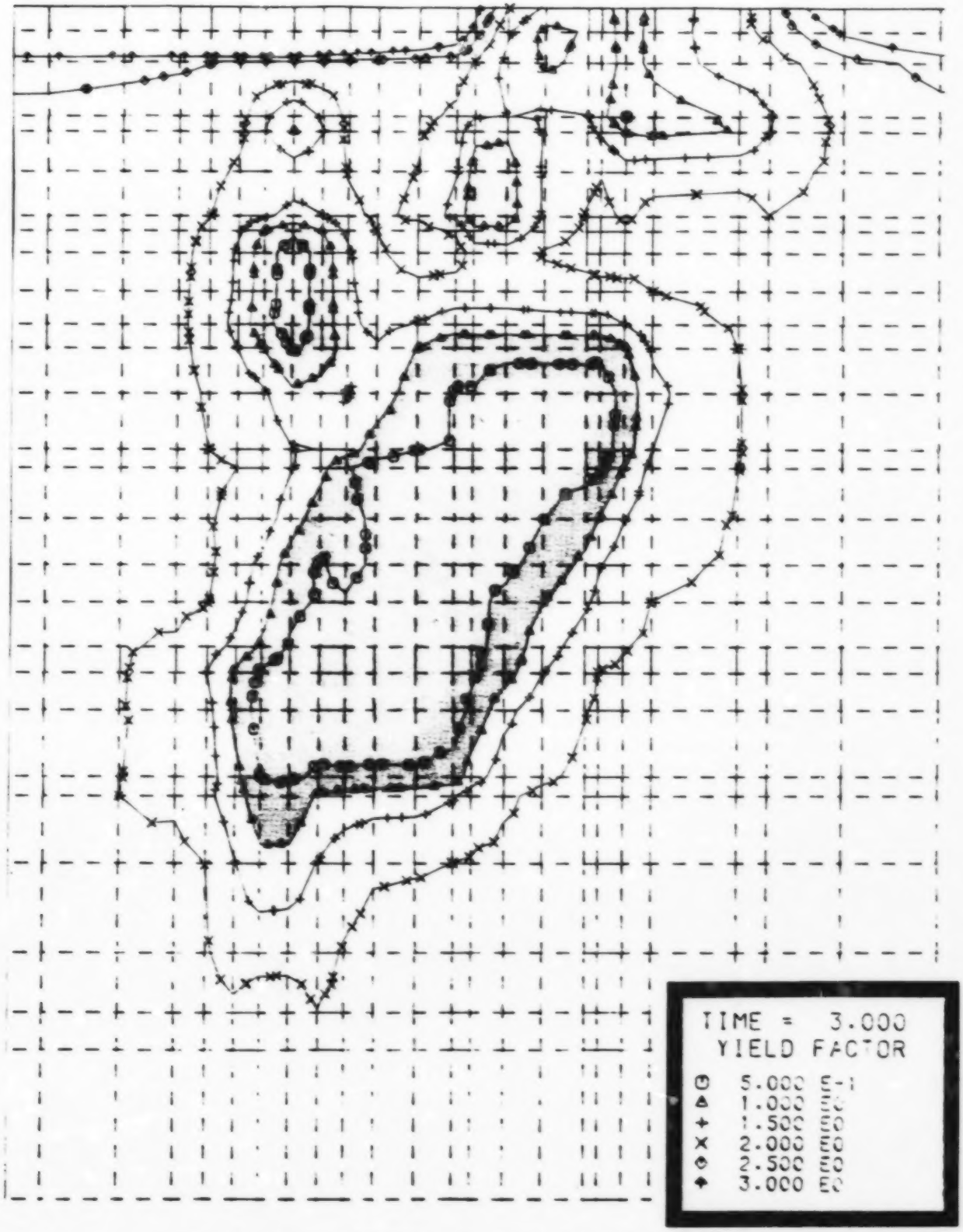

Fig. 34 Strength/stress ratio - Drucker & Prager Yield Criterion
(Mining Stage 3, Hanging wall, section z = 1052.5m)

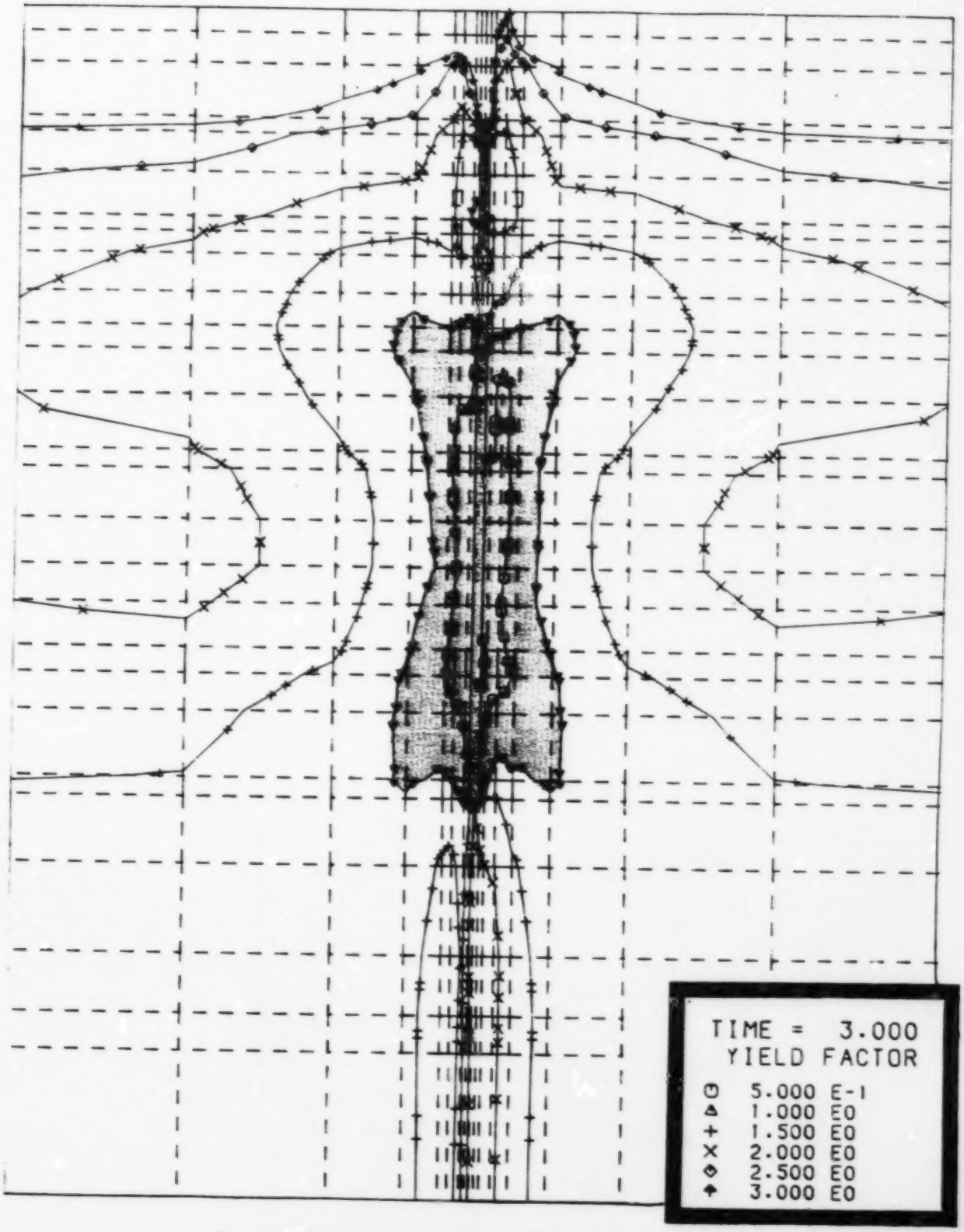

Fig. 35 Strength/stress ratio - Drucker & Prager Yield Criterion
(Mining Stage 3, N-S section x = 1762.5m)

5.0 Acknowledgements

The authors wish to thank MRL management for their encouragement and support in this project. The excellent cooperation received from the management of Dumagami Mine Ltd., is also much appreciated.

6.0 References

1. Charette, F., Wan, R., Dufresne, S. and Bétournay, M. 1991. Modélisation numérique des chantiers à la mine D.J Laronde. Division Report MRL 91-119(TR), Mining Research Laboratories, CANMET, Energy, Mines and Resources Canada.

2. Van Dillen, D.E., Fellner, R.W. and Ewing, R.D. 1981. Modernization of the BMINES Computer Code. Vol 1: User's Guide (BMINES Computer Program for Analytical Modelling of Rock/Structure Reaction). A mineral research contract report U-7910-5117, U.S. Bureau of Mines.

3. Gorski, B. and Folta, J., 1991. Strength determination of Dumagami mine rocks. Division Report MRL 91-093(TR), Mining Research Laboratories, CANMET, Energy, Mines and Resources Canada.

4. Arjang, B., 1987. Ground stress at la mine Bousquet, Quebec. Division Report MRL 87-147(TR), Mining Research Laboratories, CANMET, Energy, Mines and Resources Canada.

5. Arjang, B., 1988. Pre-mining ground stress at the Bousquet/Dumagami mines, Cadillac, Quebec. Division Report MRL 88-132(TR), Mining Research Laboratories, CANMET, Energy, Mines and Resources Canada.

6. Hoek, E., and Brown, E.T.; "Underground Excavations in Rock"; Stephen Austin and Sons Ltd., Hertfort, England; 1980.